An Integrated Geophysical Study of the Central Appalachians of Western Virginia and Eastern West Virginia

Samuel Thomas Peavy

Dissertation submitted to the Faculty of the
Virginia Polytechnic Institute and State University
in partial fulfillment of the requirements for the degree of

Doctor of Philosophy
in
Geophysics

C. Çoruh, co-chairman
J. K. Costain, co-chairman
E. S. Robinson
L. Glover, III
R. D. Law

July 18, 1997
Blacksburg, Virginia

Key Words: Geophysics, Reflection Seismology, Gravity, Central Appalachians

An Integrated Geophysical Study of the Central Appalachians of Western Virginia and Eastern West Virginia

Samuel Thomas Peavy

(ABSTRACT)

Over 700 km of industry seismic reflection data in the central Appalachians were reprocessed using both conventional and newly developed processing schemes. A new processing sequence, called *dip projection*, is introduced. The technique projects crooked-line processed CMPs onto a straight line oriented in the general dip direction for the area. The new stacked sections more closely approximate a dip line and hence are more migration-friendly and interpretable than the crooked-line stacks. Methods of determining the lateral continuity of subsurface density contrasts were also applied to gravity data from the study area. Known collectively as *potential field attributes*, the analytic signal, the tilt angle, and the gradient of the tilt angle (the *potential field wavenumber*) proved valuable in the analysis of the gravity data.

Comparison of reflection seismic data from the southern and central Appalachians revealed a dichotomy of seismic reflectivity from east to west. A highly reflective crust beneath the Piedmont in both the central and southern Appalachians contrasts with a general lack of reflectivity beneath the Blue Ridge and Valley and Ridge provinces where coherent reflections are restricted to the upper 3-4 seconds of the data. This difference in reflectivity is interpreted as a fundamental difference in the location and orientation of preexisting zones of weakness between the different crustal regions with respect to the tectonic events affecting the Appalachians since the early Paleozoic.

The combination of the results of new methods of seismic and potential fields processing with deep well and geologic information allowed the lateral continuity of two major structures in the central Appalachians to be examined. The Blue Ridge in Virginia was found to overly a duplex of Cambrian-Ordovician carbonates formed in response to stresses during the Alleghanian Orogeny. A large thrust sheet of similar carbonate rocks was interpreted beneath the Nittany Anticlinorium in West Virginia. To the south in Virginia, this thrust sheet is replaced by imbrication of the carbonate package. The change in structural style may be related to the existence of a lateral ramp or it may reflect the overall change in structural style from the central to southern Appalachians.

Dedication

To my parents,
James Thomas and Beverly Peavy,
whose love, patience and understanding make all things possible.

Acknowledgments

I would like to thank Dr. Cahit Çoruh and Dr. John K. Costain for serving as co-chairmen of my committee. Their knowledge and experience in the realm of reflection seismology have contributed greatly in the successful completion of my degree. I would like to thank Dr. Edwin S. Robinson, Dr. Lynn Glover, III, and Dr. Richard D. Law for serving on my committee and answering my sometimes obtuse questions. I would also like to thank Dr. Gil Bollinger for serving on my committee before his retirement, and for his continued support since that time. Thanks also to the other faculty here in the department, especially Drs. Snoke, Read, and Hole, for providing timely discussions and answers to my questions, and to Dr. Ron Kriz of ESM.

I would like to thank the following foundation and corporations for providing monetary support during the pursuit of this degree: The Society of Exploration Geophysicists Foundation, Amoco, Chevron, Mobil and Texaco. I would also like to thank the Department of Geological Sciences for providing support in the form of graduate teaching assistantships, and for providing me the opportunity to teach some wonderful students over the past six years. Thanks to Halliburton (now a subsidiary of Western Geophysical) for providing the seismic data that was reprocessed as a part of this work.

For academic support, I would like to thank William S. Henika of the Virginia Division of Mineral Resources and his wife Mary Jane for his geologic expertise and their good home cookin'. Lee Avary and Pat Jones of the West Virginia Geologic and Economic Survey for providing well logs and other pertinent information vital to my research. Dave Dator of the National Geophysical Data Center was helpful in providing programs and other assistance early in my studies. The computer support personnel in geophysics deserve special thanks, especially Mildred Memitt, Bob Montgomery, and John Wonderly, without whom no reflection seismology student would *ever* finish.

I would also like to thank the Linda, Carolyn, Mary, Connie, Ellen, Mark, Eric, Hal, Dan, Mark, Karen, Ron, Hersha, Cathy, Dean, and Belinda for all their help over the past six years. Thanks to all my friends at Graduate Student Assembly over the years – especially Paula Williams. Many thanks to my fellow graduate students then and now, without whom many an intellectual discussion would never have been started and many a beer would have been left untasted. I can't possibly thank you all individually, but I appreciate each and every one of you. I would especially like to thank my fellow graduate students in geophysics, most of whom have gone before me: Mr. Bill, Debbie, Suzanne, Phil, Laura, Mu, Shaosong, Edmundo, Heather, Sara, Jen, Derek, Leslie, and Tina, and the 'new guys' Kai, Lee, Dapeng and Dong-Sheng. Most special thanks to Wil, Zenah, TJ, and Naomi for helping me keep my sanity (most of the time), and to Dave Valentino and his family for similar measures. More special thanks to my friends down south: the Baltzells, the DeGonzagues, the Mehaffeys, the Williams', and C. Abbott. A special thanks to 'Mr. Baseball', Jim Dixon, for putting up with me over this past year. And finally, thanks to my parents and my sister and her family for their love and support.

Table of Contents

List of Figures

List of Tables

Chapter 1: Introduction

Much progress has been made in recent years on understanding the structural and geologic history of the Appalachians. A major contributor to this progress has been the utilization of geophysical data sets, in particular reflection seismic data, in combination with more traditional structural and stratigraphic analyses. The availability of regional-scale reflection data sets from industry – such as the data recorded by Petty Ray Geophysical utilized in this study – has greatly enhanced this effort. Regional reflection data recorded for academic purposes in Georgia (Cook et al., 1979, 1981; Peterson et al., 1984; Nelson et al., 1985), South Carolina (Behrendt, 1986; Williams et al., 1987; Hubbard et al., 1991) and Virginia (Harris et al., 1982; Pratt et al., 1988; Lampshire et al., 1994) in conjunction with detailed geologic mapping have aided in the understanding of the tectonic processes that formed the complex geology that we observe today in the southern and central Appalachians.

In addition to reflection seismic data, large amounts of gravity data have been made available through the efforts of the National Geophysical Data Center (NGDC) in Boulder, Colorado. Over 2,000,000 gravity stations have been collected by the NGDC on the ***Gravity*** CD-ROM (Hittleman et al., 1994). Approximately 17,000 gravity stations from the central Appalachians of Virginia and West Virginia were used in conjunction with the seismic data and well data provided by the West Virginia Geologic and Economic Survey in the analysis of geologic structures in the region.

This study was designed to be an integrated study of subsurface structures in the central Appalachians utilizing over 700 km of reprocessed seismic reflection data and gravity, well, and geologic information within the region. As a consequence of this study, new techniques for processing both reflection seismic and gravity data were developed and four interrelated papers were produced as described in the following paragraphs.

Chapter 2 introduces a new processing sequence for seismic reflection data to better accommodate seismic migration processing and offer improved structural/stratigraphic interpretation. The method projects pre-processed common midpoint (CMP) data from a crooked-line geometry to a straight line oriented along a user selected dip direction. Results from three-dimensional ray trace modeling processed using this technique show the ability of the method to properly orient structures for interpretation and the ability to separate and enhance structures at different structural levels that have conflicting strikes. An application of the method to seismic reflection data from the central Appalachians highlights improvements in seismic migration and interpretation.

Chapter 3 discusses various potential field gradient techniques and introduces a new method of analysis that can successfully delineate density and susceptibility contrasts within the subsurface. The mathematical analogy between certain gradient techniques and seismic attribute analysis are demonstrated, and the concept of *potential field attributes* (PFA) introduced. The accuracy of the various PFA techniques is compared to another gradient technique in a series of

model studies, and then applied to gravity data from the central Appalachians to define the lateral extent of a large duplex structure identified on seismic reflection data.

Chapter 4 contains a general discussion of reflectivity in the southern and central Appalachians. The mid- to deep crust shows a dichotomy of reflectivity as seen from east to west along regional lines in the southern and central Appalachians, with more apparent reflectivity evident in the crust beneath the Piedmont. To the west the reflectivity is restricted to the uppermost 3-4 seconds within the allochthonous and autochthonous crystalline Blue Ridge and the sedimentary Valley and Ridge and Plateau provinces. A review of possible origins of deep crustal reflections and the tectonic history of the central and southern Appalachians have led to a better understanding of the reflectivity seen in the region. Seismic evidence for structures associated with each major tectonic event affecting the southern and central Appalachians is presented, and the implications of this are discussed.

Chapter 5 integrates PFA analysis of gravity data, well information, and geologic data with dip-projected seismic data to examine the along-strike continuity of major subsurface structures in the central Appalachians. The extent of a duplex composed of Cambrian-Ordovician carbonates beneath the Blue Ridge in central Virginia and the structure of the Nittany Anticlinorium in Virginia and West Virginia are the primary targets of the analysis.

Finally, **Chapter 6** restates and summarizes the major contributions of this study and makes suggestions for future research.

Chapter 2: Dip Projection of Crooked-line Reflection Profiles

Abstract

Reflection seismic data acquired in mountainous areas are often plagued with a number of problems that can directly affect the quality of the stack and its interpretation. Among the more serious of the problems is the crooked-line nature of recording, which results in stacks with highly variable fold and a mixture of dip, strike, and oblique sections because of variations in recording line geometry. This not only causes difficulty in interpretation, but also can adversely affect the migration of the data, as 2-D migration algorithms assume the data are in the dip plane.

A new method of crooked-line seismic data processing called *dip projection* is introduced herein, in which pre-processed common mid-point gathers are re-projected from their original crooked-line orientation to a straight line in the general dip direction. The projected line has three advantages over the conventionally processed line: 1) introduction of the geology to the processing stream at an early stage through the choice of dip direction; 2) accommodating the dip assumptions of 2-D migration algorithms; and 3) being more interpretable, as the line now mimics a line recorded in the dip-direction and hence is more closely related to conventional geologic cross-sections. The utility of the new methodology is shown with both synthetic and real data examples.

2.1 Introduction

Reflection seismic data acquired in mountainous areas are often plagued with a number of problems that can directly affect the quality of a stack and its interpretation. Some of these problems include datum statics corrections and highly variable CMP fold caused by crooked-line acquisition geometry. Rugged topography can have an effect on the location of a proper datum, with a change in datum affecting stacking velocities and ultimately the migration through those velocities. Variable fold can reduce stack quality in portions of the line, and even the best fit 'slalom' line geometry may still display the effects of variable fold. Another problem is that the final stack will often have a mixture of both strike and dip sections, causing difficulty in the migration and interpretation of the seismic section.

Lynn and Deregowski (1981) briefly discussed the problem of migrating data from a crooked-line. Data recorded in directions other than parallel to dip violates the assumptions made by 2-D migration algorithms; i.e. that the recorded events be within the plane of section in order to be migrated properly. Their suggestion of migrating the 'dip' sections of a crooked-line separately is not practical, particularly when you consider the severe dip limitation imposed by the restricted length of these sections. Figure 2.1a is a block diagram illustrating a series of straight seismic lines over a single dipping interface overlain by a constant velocity overburden. The three lines, A, B, and C, are oriented along dip, strike, and oblique to dip, respectively. If the three lines are migrated using the correct migration velocity, only the reflection recorded along the dip line (A) will be positioned properly in the subsurface (Figures 2.1b and 2.1c). The reflection as recorded along any other direction will be positioned improperly by the 2-D migration algorithm (Figures 2.1b and 2.1c).

Renick (1974) and Levin (1983) discussed the effects of recording in a direction non-parallel to true dip or strike by analyzing the feathering of a marine cable. Renick analyzed the effects of marine cable feathering and concluded that it degraded the final stack significantly, and that shortening the cable length would improve results. Levin showed through a detailed mathematical analysis that as the streamer moves farther from the line of dip, the hyperbolic reflector shape changes significantly leading to inaccurate velocity estimates. Figure 2.2 shows the geometry of the situation described by Levin. From this geometry he was able to derive a time-distance equation for normal incidence reflections from the planar interface, and show that the stacking velocity and apex of the hyperbola are affected not only by the dip of the interface, but also by the angle between the dip- and line-direction. The travel time as a function of source-to-geophone separation for a 20° dipping interface at different orientations of the seismic line with respect to the dip direction (0°) is shown in Figure 2.3. The figure illustrates directly the problems associated with recording reflection data in a direction significantly different from true dip, as the shape of the travel time curve will directly affect both the stacking velocities obtained and the quality of the final stack. Figure 2.4 is a plot of seismic line direction with respect to dip direction versus dip-corrected stacking velocities. Stacking velocities are corrected for dip by multiplying by the cosine of the true dip angle under the assumption that the line was recorded in

the dip-direction.. The set of curves show that velocities obtained from normal moveout (NMO) analysis result in large variation; NMO velocities are best for profiles within 15° of the dip direction.

Levin (1984) also analyzed the effects of the traditional practice of CMP binning perpendicular to the line of section. He concluded that binning in a direction other than perpendicular to dip causes a degradation of the stack produced by the binning of arrivals from the same reflector having different zero-offset arrival times. The application of residual statics corrections can reduce the effects of the distortion of the arrival times, but this does not correct for the overall problem of data acquisition in a non-dip direction.

Levin's analysis is important in the consideration of crooked-line processing, as a typical line recorded in mountainous areas changes directions many times during acquisition, with each change affecting the final product. The gathering of traces with different zero-offset arrival times into traditional bins along a slalom line will often produce poor results in spite of a careful conventional processing flow because problems with stacking velocities, statics solutions, and migration become magnified. One way of reducing the problem is to bin the data in the strike direction as suggested by Costain and others (1991, 1992). The process of *strike-binning* forms CMP gathers by collecting traces in the direction of strike and therefore reduces the problems discussed above. After strike-binning, processing proceeds in a normal manner through a final stacked section. The result, though an improvement over conventionally processed sections, takes an amount of time equal to the original processing to produce a stack. The collapse of strike-dominated portions of the seismic line into narrow zones on the new projected line leads to enormous values of fold often juxtaposed with zones of much smaller fold. The highly variable fold distribution can cause a variation of the signal-to-noise ratio between the lower- and higher-fold zones and may lead to possible interpretation and migration problems.

Wu and others (1995) and Wu (1996) suggested a combination of binning along a straight line, crossdip corrections, and editing of CMPs as a solution to the crooked-line processing problem. By selective editing of CMPs to remove traces of nearly equal offset from the gathers and the application of crossdip corrections, Wu and his co-workers effectively reduced the distortions introduced by binning in a non-strike direction as described by Levin (1984). These steps combined with careful reprocessing of the original data from the Sudbury area in Ontario led Wu and others (1995) to a better understanding of a complex geologic problem.

A new method of processing crooked reflection seismic lines called *dip projection* is introduced herein. Dip projection is different from the approaches of either Costain and others (1991, 1992) or Wu and others (1995) as it takes advantage of prior processing steps such as editing, filtering, deconvolution, and statics solutions derived for the conventional CMP gathers. Because some of the more labor- and time-intensive steps of the conventional processing stream have been completed, the addition of the dip projection processing sequence takes minimal time to implement and perform. The original stack section is then used as a quality control check on the dip-projected stack. Synthetic data from a three-dimensional seismic model and actual reflection data collected along the crooked roads of the Appalachian mountains is introduced to

illustrate the ability of the technique to produce a more interpretable and migration-friendly stack.

2.2 The Dip Projection Method

Figure 2.5 is a flowchart for dip-projection processing. The dip projection method introduces the geology into the processing sequence by projecting conventionally processed CMPs onto a straight line in the general dip direction. ***Dip projection*** sorts the CMP data into new, smaller CMP bins that are perpendicular to dip (along strike). The use of preprocessed CMPs as input to this processing step allows the steps of editing, deconvolution, and residual statics calculations – all very time intensive – to be eliminated from the subsequent processing.

As discussed above, as long as the bins are oriented within 15° of the true dip-direction, the arrival time of reflections on the CMP gathers should form hyperbolic curves that are close to those of a true dip line, thereby producing accurate stacking velocities for the appropriate zero-offset times. The size of the bin along the dip-projected line was determined empirically to be 1/10th the station separation, or 1/5th the nominal CMP separation. For example, a line with stations 100 m apart should have a nominal CMP-spacing of 50 m. The dip-projection method would therefore have a CMP-spacing of 10 m. The smaller bin sizes allow better control over the fold coverage over the entire length of the seismic section, particularly in areas formerly oriented parallel to strike. The initial CMP gather produced after the dip-projection and resorting step displays highly variable fold, and in fact the fold may be zero for a number of the newly formed CMP gathers.

The process of ***gathering*** is used to smooth the variation in fold. This step groups the smaller dip-projected CMPs into new CMPs using the following criteria:

a) The fold must transition smoothly along the line; i.e. no isolated areas of abnormally low or high fold are allowed, and transitions from lower to higher fold and vice versa are made as smooth as possible;
b) The maximum fold throughout most of the line be limited to the nominal fold for the data based on the number of channels in the recording system (e.g. a fold of 24 for a 48-channel system);
c) All traces within a new CMP gather must come from within the same distance range along the line; and
d) No more than 5 consecutive small-bin CMPs can be grouped, thereby maintaining a maximum CMP spacing equivalent to the nominal CMP spacing.

Following these criteria, a FORTRAN program was used to generate a list of prospective gathers that are checked and adjusted for quality control as necessary before the gathering process. CMP gathers are generated and then edited to limit the number of traces with similar offsets. This step is necessary as explained by Levin (1984) and Wu and others (1995) to remove traces originating

from areas along strike wherein the zero-offset time could be significantly different from the zero-offset time of a dip line, thereby causing a degradation of the stack. Another way of dealing with this problem would be through the application of cross-dip corrections (Wu et al., 1995).

After the above steps have been performed, velocities are calculated along the new projected line and then the CMP gathers are stacked. This stack is a dip-projected version of the original and has the dual advantages of being a straight line and of having relatively even fold coverage. Unfortunately, the stacked traces are *not* a constant distance apart; the distance between traces in the stack will ordinarily vary between 1/5th and one full nominal CMP interval. The greater distances are caused by a lack of data that can mostly be attributed to skips in seismic coverage along the line. This variation in CMP interval is addressed in the final steps of the dip-projection process − calculation of CMP distance along the line, resorting by that distance, trace interpolation, gathering and summation – producing a final stack that has a constant CMP interval equivalent to the nominal CMP spacing as dictated by the original recording geometry. The final stack, as shown below, has all the properties of a true dip section, and hence is more suitable for interpretation and responds to 2-D migration algorithms better than the original crooked-line stack.

2.3 Synthetic Data Example

Figure 2.6 displays the multi-layer test model created using GX Technology's 3D AIMS modeling system. Table 2.1 summarizes the properties of the input model. Note that the lowermost interface (Interface 6) has a strike that is diffrent from the overlying interfaces.

Table 2.1: Physical dimensions and properties for 100x100x30 km synthetic model. Densities are calculated via Gardner's equation.

Layer Name	Strike	Dip	Velocity (km/s)	Depth Range(km)
Layer 1	------	0°	4.0	0
Layer 2	N	2°E	5.0	2 - 5.5
Layer 3	N	------	6.2	4 - 6.8
Layer 4	------	0°	6.0	6.8-7.0
Layer 5	------	0°	6.1 & 6.2*	7.0
Layer 6	N35°W	15°NE	6.1	7 - 27.85

* Velocity below Layer 5 is higher when over Layer 6.

A plan view of the crooked line shot directly over the model is shown in Figure 2.7. Data recording was simulated with 48 channels and a symmetric, split-spread geometry to match with available seismic reflection data. Station spacing was made larger than desired (500 m) during modeling due to computer system limitations and time constraints. The results, however, are illustrative of the ability of the method to separate and properly stack conflicting dips in the subsurface.

The crooked-line stack obtained using conventional processing techniques is shown in Figure 2.8. All the interfaces show distortions and undulations produced by line bends in the slalom line used for processing. The lowermost interface shows a flattening at approximately 6.6 seconds (labeled 'A' in Figure 2.8) caused by the line turning strike parallel for this interface between stations 146 and 191 (see Figures 2.6 and 2.7).

The result of the application of the dip-projection method, with the direction of dip taken to be directly perpendicular to the strike of the upper interfaces, is shown in Figure 2.9. A comparison with Figure 2.8 shows several areas of improvement, in particular the flattening of the upper horizons. A calculation of the dip of the upper interface using the overlying material velocity of 4 km/s gives the correct dip of approximately 2° for that interface. Interface 3 is also in its correct location and not stretched out as in the conventional crooked-line stack. In addition, the overall length of the dip-projected line is shorter than the original line as expected. This should always be the case, as the process of projecting the oblique and strike-parallel portions of the line onto the dip line will shorten the lengths of those segments while leaving the dip-parallel sections in their proper location. Distortion is still present in the deepest reflector, but that is expected because the projected line is still oblique to the deeper structure.

The result after projecting the data onto a seismic line down-dip for the deepest horizon, or in a direction of N55°E, is shown in Figure 2.10. While the upper part of the section is poorly imaged, the deeper reflector has had the distortion caused by the crooked-line geometry removed from it. The only distortion now seen on that deeper reflector is some velocity pull-up caused by the higher velocities associated with Interface 3. The kinking seen on the upper reflectors below CMP 265 is caused by the collapsing of the section between stations 146 and 191 into the dip line for the deeper layer. This juxtaposes portions of those layers that have different zero-offset times, hence the kinked appearance. This result illustrates the importance of understanding which structural level that one is looking at when analyzing the field data. In this example, the upper sections *should* appear distorted as the data have not been properly projected for their dip. With real data, it is critical to have *a priori* information about the general orientation of structures in an area before applying this method, and to realize that in regions with zones of conflicting dip, those dips that are not dip-parallel to the projected line *will be distorted in the final stack*.

As noted above, the dip-projected stacks will be shorter than the original crooked-line stacks. The original stack (Figure 2.8) has a length of 102.5 km, whereas the dip-projected stack for the upper interfaces (Figures 2.9) has a length of 90 km and the dip-projected stack for the

deeper interface (Figures 2.10) has a length of only 76 km. The trace interval for each stack display are the same along a given line; the process of dip projection has reduced the line length by compressing the non-dip parallel sections.

2.4 Real Data Example

The dip projection method described above was applied to seismic reflection data from the central Appalachians. Figure 2.11 is a map view of Line WV1 used in this study. The line is typical of many 'dip lines' recorded in the Appalachian mountains where crooked roads cross major structures of the Appalachian Plateau, Valley and Ridge, and Blue Ridge provinces. The structures are oriented at a strike of approximately N35°E. In addition to the obvious problems associated with processing a crooked line, the changing near surface geology produced statics and multiple problems of differing levels that were minimized during processing by the application of overlapping surface-consistent residual statics solutions and deconvolution operators along the entire length of the line. The resulting final stack is shown in Figure 2.12.

This stack (Figure 2.12) and the following stacks are displayed as *automatic line drawings* (ALD). Conventional line drawing presentations of large-scale seismic sections are subjective representations of those reflections judged to be significant by the interpreter. The ALD technique is a more objective process that produces unconventional line drawings in which *the seismic waveform and relative amplitude information are preserved*. The processing is based upon the Fresnel zone concept that requires the reflections from a subsurface reflecting "point" be on several traces on seismic sections in the space-time domain. The ALD process converts the seismic amplitudes into two-dimensional coherency estimates using a moving window in which a scanning procedure searches for the angular direction with the highest correlation. The results are then subjected to an exponential amplitude adjustment that forces the background noise outside of the dynamic range of the plotter. The result is a section *of relative seismic reflectivity*. The ALD process is especially useful for crustal seismic data because of the larger Fresnel zone size at depth. Excellent results have been obtained from reprocessed seismic reflection data using the ALD technique (e.g. Çoruh et al., 1987; Çoruh et al., 1988; Hubbard et al., 1991; Lampshire et al., 1994). Similar methods are also used to enhance noisy seismic record sections (e.g. Kong et al., 1985).

The stack (Figure 2.12) displays several important features, including the manifestation of the Blue Ridge front (CMP 2800), the Massanutten Synclinorium (CMP 2600), the Allegheny structural front (CMP 1200), and the broad open folds of the Appalachian Plateau (CMP's 4 - 1200). Proper interpretation of these and other structural features is important in understanding the deformation history of the central Appalachians and the oil and gas potential of the region. Before a proper interpretation can be made, however, the stacked sections of the line not oriented in the dip direction need to be examined along true dip (see Figures 2.11 and 2.12).

The dip projected stack of the same line after ~58 km of shortening is shown in Figure 2.13. The length of the dip-projected line is ~199 km; the original line was ~257 km long. A

comparison of the fold between the original and dip-projected line over a particularly crooked section across the Blue Ridge is shown in Figure 2.14. This comparison shows that while the fold along the dip-projected line shows some variability, the transitions are much smoother than those in the original crooked-line processing. The highest fold on the original line, between stations 2900 and 2925, is associated with a long and sharp line bend, where a very few CMPs absorb a large number of traces in this area (see Figure 2.14b). The highest fold area on the dip-projected line is between stations 2840 and 2925. An examination of the line geometry (Figure 2.14a) shows this to be the section most oblique to strike, hence concentrating the fold in this region. The highest fold areas, near stations 2850 and 2890, are associated with the dip projection of seismic data from several sections of the line onto the dip line (see Figure 2.14c).

Figures 2.15 – 2.17 are close-up views of several of the structural features and their equivalent regions on the original stack. Dip projection has removed some of the ambiguity from the interpretation by putting several of the features in a more proper structural context. Figure 2.15 shows the result for the region near the Allegheny structural front. Both seismic sections clearly show the transition from the gently folded Plateau province to the west to the more complexly folded strata of the Valley and Ridge to the east. Reflection A is along a section of the line oriented roughly down-dip, and so there is little difference in the continuity of this reflector or of the reflectors above or below it. Reflection B has a relatively steep dip and is located in a short section of the line between two along strike sections. These reflections are also similar in appearance with the only difference being the slight flattening of the reflection on the original stack (Figure 2.15a). Reflection C is distinctly different on the two stacks. The original stack shows an undulatory shape to the reflection package, while the dip-projected version shows a simpler upward curvature below reflection B and a relatively flat profile to the east. The upwarping of this reflection package is most likely a velocity pull-up caused by an increased thickness of high velocity Cambrian-Ordovician carbonates. Referring back to Figures 2.12 or 2.13, a large ramp bringing up the high velocity carbonates can be seen near station 1600, implying large-scale thrusting of these units towards the structural front. This thrust block is responsible for the velocity pull-up seen in both sections.

Figure 2.16 shows a close-up of the area near the Massanutten Synclinorium. The original line cuts obliquely across the structure at an angle of ~30-60° degrees to regional strike. Reflection D is slightly steeper in the dip-projected version of the seismic line (Figure 2.16b). Reflections E represent a series of reflectors in the section that is oriented the most obliquely to dip. The upper part of the section above reflection package E in Figure 2.16a shows some reflections dipping to the west also. In Figure 2.16b, the section above E has been collapsed into a short interval and the dipping reflections in the upper part have all but disappeared. The removal of the dipping reflections is a consequence of the method, as those reflections were not oriented within 15° of regional dip.

Figure 2.17 is a section over the Blue Ridge to the east of the Massanutten Synclinorium. Dip projection has cleaned up the section considerably, allowing a clearer view of what appears to be an imbricate stack duplex from 1-4 s beneath the crystalline Blue Ridge basement complex

that crops out at the surface. The very bright reflection ('F' in Figure 2.17) between stations 2800 and 2900 is beneath the surface exposure of the high velocity Catoctin metavolcanics.

Application of Kirchhoff migration at 90% stacking velocities to the conventionally stacked data makes some difference (Figure 2.18), but the interpretive problems in the original stack have not been solved by the 2-D migration algorithm. In addition, a large amount of migration noise is readily evident in the section, as both edges and the section below 6 s are completely smeared. The upper part of the section also appears to have a large amount of migration operator smearing. The most logical explanation for this is the crooked nature of the originally processed line, with the juxtaposition of dip, near dip, and oblique sections and changes in the signal-to-noise ratio caused by highly variable fold leading to the poor migration result. Application of the same migration algorithm at 90% of stacking velocities to the dip-projected line shows some remarkable differences (Figure 2.19). The migration smear near the edges and deeper in the section have been reduced substantially, with migration effects only destroying the data below ~ 8 seconds. In addition, even these large sections show more clearly the reflections throughout the entire upper section.

Figures 2.20-2.22 provide close-up views of the same areas discussed earlier in a comparison of the stacked sections (see Figures 2.15-2.17). Letters identifying different reflections are primed to indicate migration.

Data from both lines near the structural front are shown in Figure 2.20. Reflection A' has changed little from the original stacks (Figure 2.15), and there are small differences between the two sections even after migration. This result is expected as the section is essentially a dip line in this region. Reflection B' has completely disappeared in the original stack after migration, while the same reflection has been migrated successfully in the dip-projected stack. The explanation for this is most likely poor velocity definition in the oblique and strike-parallel sections on either side of the dipping reflector. The NMO stacking velocities, as noted earlier, could be substantially different from the correct velocities, causing the migration algorithm to misposition or even destroy events in and surrounding those areas (see Figure 2.4). Reflection C' has changed little after migration, with only a slight migration smile evident below station 1450 on the migrated crooked-line section (Figure 2.20a). The dip-projected section shows better continuity of this and other reflections above it.

The section over the Massanutten Synclinorium has undergone substantial changes (Figure 2.21). A comparison of the results before (Figure 2.16) and after migration (Figure 2.21) show that the dip projection method has oriented the reflections properly for migration in this region. Reflection D' has become buried in a large amount of migration noise on the crooked-line section (Figure 2.21a). The dip-projected section, however, shows the same reflection more clearly (Figure 2.21b). Flat-lying reflection package E' has remained mostly unchanged by the migration process in both sections, but reflection D' shows some migration smearing in both cases.

The region near the Blue Ridge structural front after migration is shown if Figure 2.22. The section processed using conventional methods (Figure 2.22a) is even more difficult to

interpret than the original stack (Figure 2.17a). Migration has not significantly improved the results of the dip-projected stack either (compare Figure 2.17b with Figure 2.22b). The reason for this is probably related to the velocity function used during migration, as some of the traces from different sections of the line were projected to the dip line. Even after the editing step, if there is any substantial crossdip, the reflection hyperbolae will not be as well defined and consequently produce a relatively poor stacking velocity and hence final migrated section; however, it should be noted that the dip-projected section *is* substantially better than the original stack in either stacked or migrated form.

2.5 Conclusions

A new method of dealing with crooked-line data, called *dip projection*, has been introduced. The new technique produces a true dip section that is more readily interpretable and it migrates better than the conventional stack. The keys to the technique are the processes of *dip projection* and *gathering*. These two processes produce a shorter straight line stack that is perpendicular to local tectonic strike. Once produced, the final stacks are the equivalent of true dip lines, and hence are comparable to geologic cross-sections and honor more of the assumptions implicit in 2-D migration algorithms; i.e. that the data be on a vertical plane in the dip direction. Of course, the determination of velocities, as with all migrations, is a crucial step in the process. The new dip-projected CMP gathers generated by the technique in most cases will produce better stacking velocities (Levin , 1983).

Model studies and real data results presented here show that remarkable improvements in interpretation and migration of crooked-line seismic data can be made if dip-projection is applied as an interpretive processing sequence. However, there are still issues that will have to be addressed in the future. For example, the application of crossdip corrections in an iterative scheme may help with some of the problems noted for the real data. In addition, the assumption of one general regional strike direction for an area may not be valid for all regions, and a series of sections could be produced for all the possible dip directions. By scanning the data for differing dip directions, regions of crossdip may be separated, but at the cost of distorting the rest of the section. The distortion beyond the focused horizon is an unavoidable side-effect of the method, but the improvements in both interpretation and migration in this interpretive processing sequence outweigh this potential pitfall.

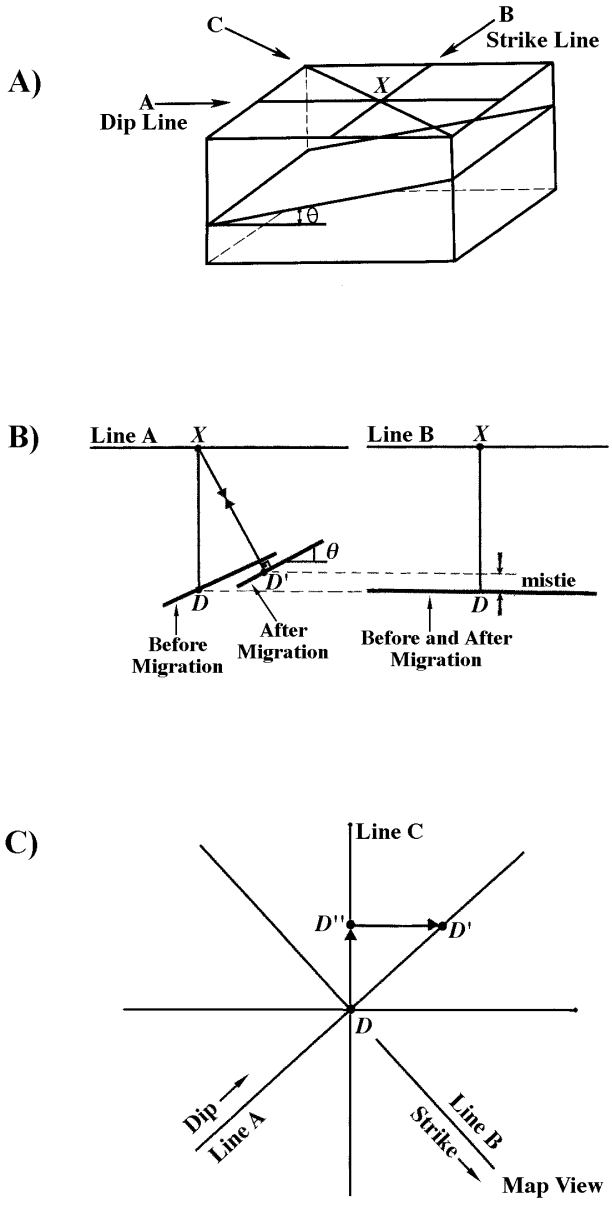

Figure 2.1: Migration of 2-D seismic data recorded in different orientations with respect to subsurface structure. A) Block diagram showing three seismic lines over a single dipping interface. Vertical slices (B) and a plan view (C) show correct (line A) and incorrect (lines B and C) positioning of a reflection (*D*) after migration. Only the line recorded in the dip direction migrates properly (after Yilmaz, 1987).

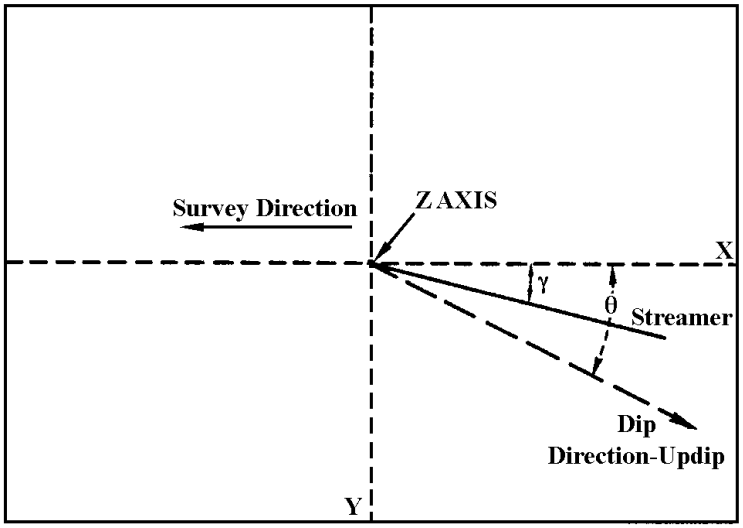

Figure 2.2: Map view of geometry used by Levin (1983) to derive a time-distance equation for feathering of a marine cable over a single dipping interface. θ is the angle between the dip and profile directions. γ is the angle between the streamer and the profile direction.

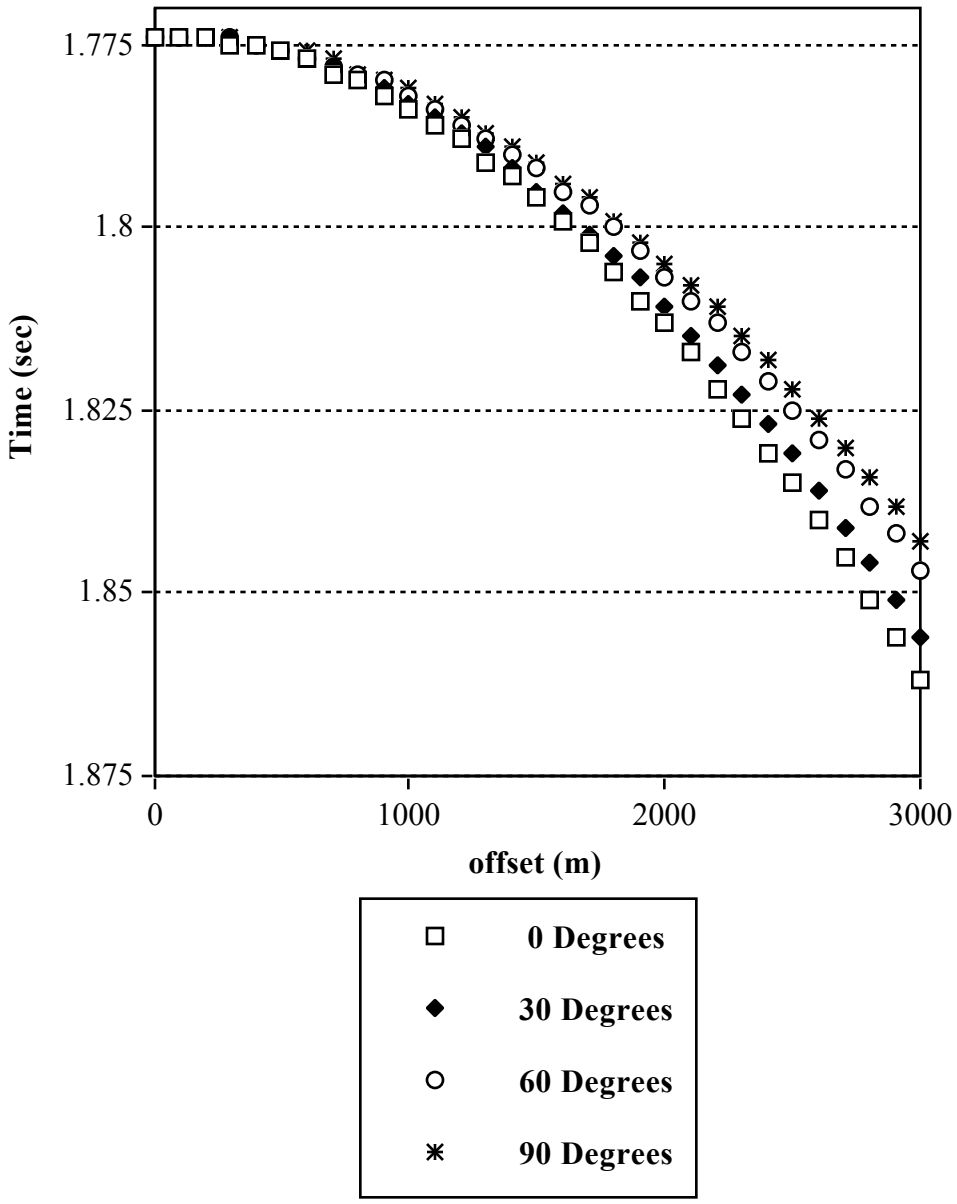

Figure 2.3: Traveltime curves over a single, 20° -dipping reflector at various angles with respect to the dip direction (dip = 0°).

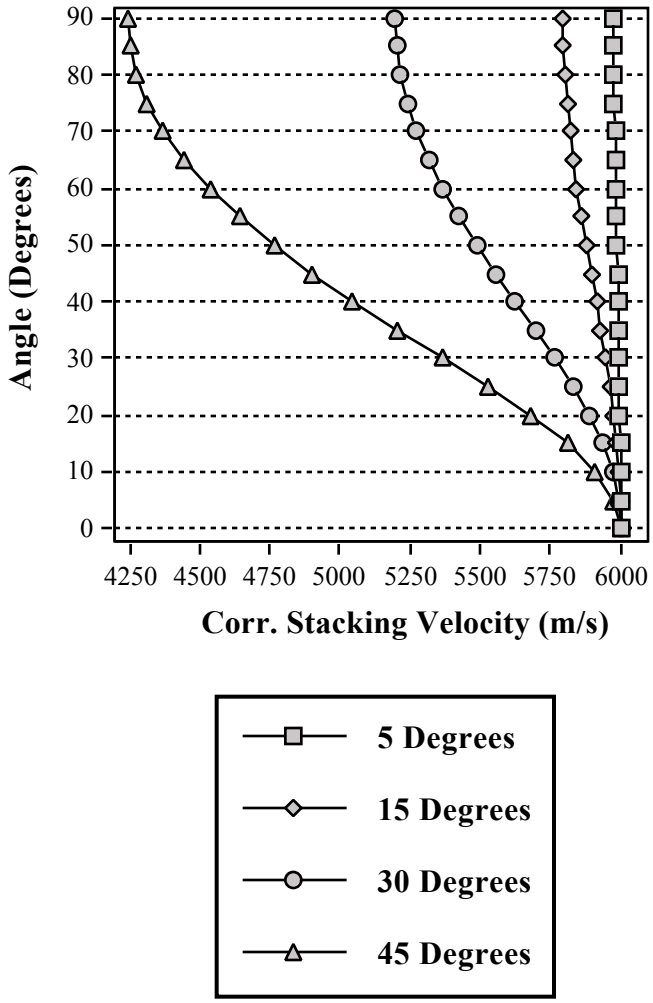

Figure 2.4: Plot of angle with respect to dip direction (dip = 0°) versus dip-corrected NMO stacking velocities for a range of reflector dip angles. For dips up to 45°, corrected velocities are within 5% of the actual velocity for profiles recorded less than 15° from the true dip direction.

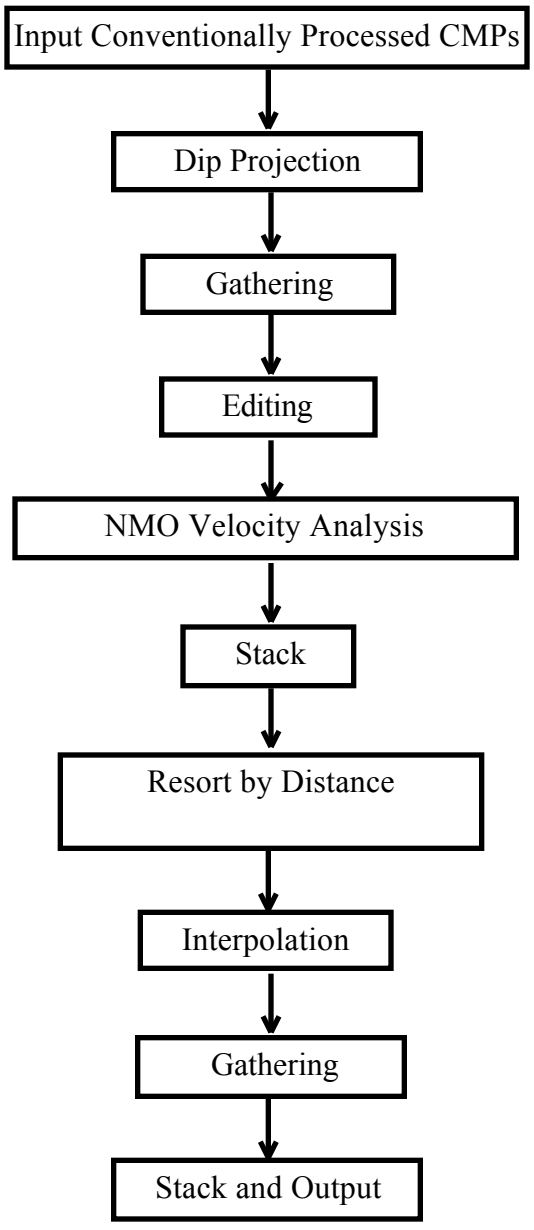

Figure 2.5: Flowchart for Dip Projection. See text for details.

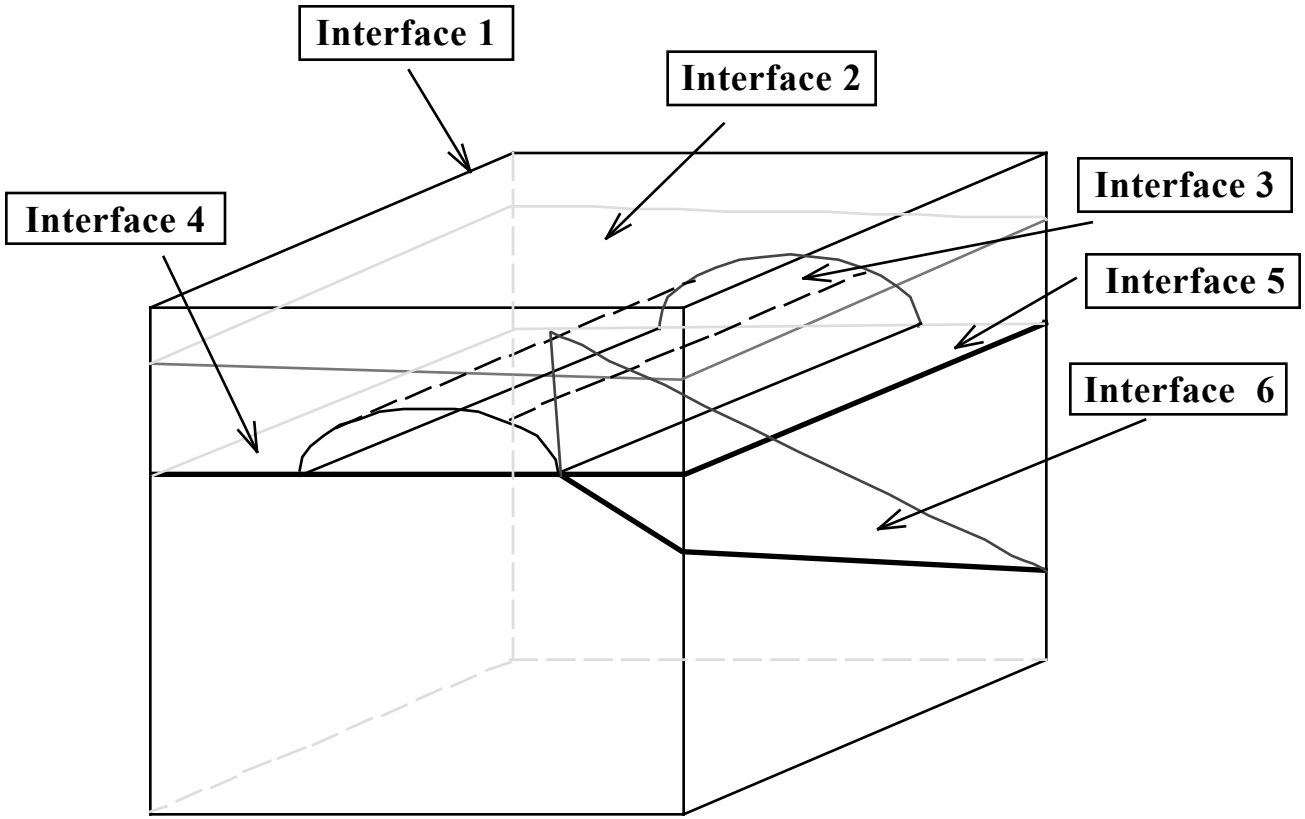

Figure 2.6: Model used to generate synthetic seismic data using GX Technology's 3D AIMS seismic modeling software. Table 2.1 summarizes the input model properties.

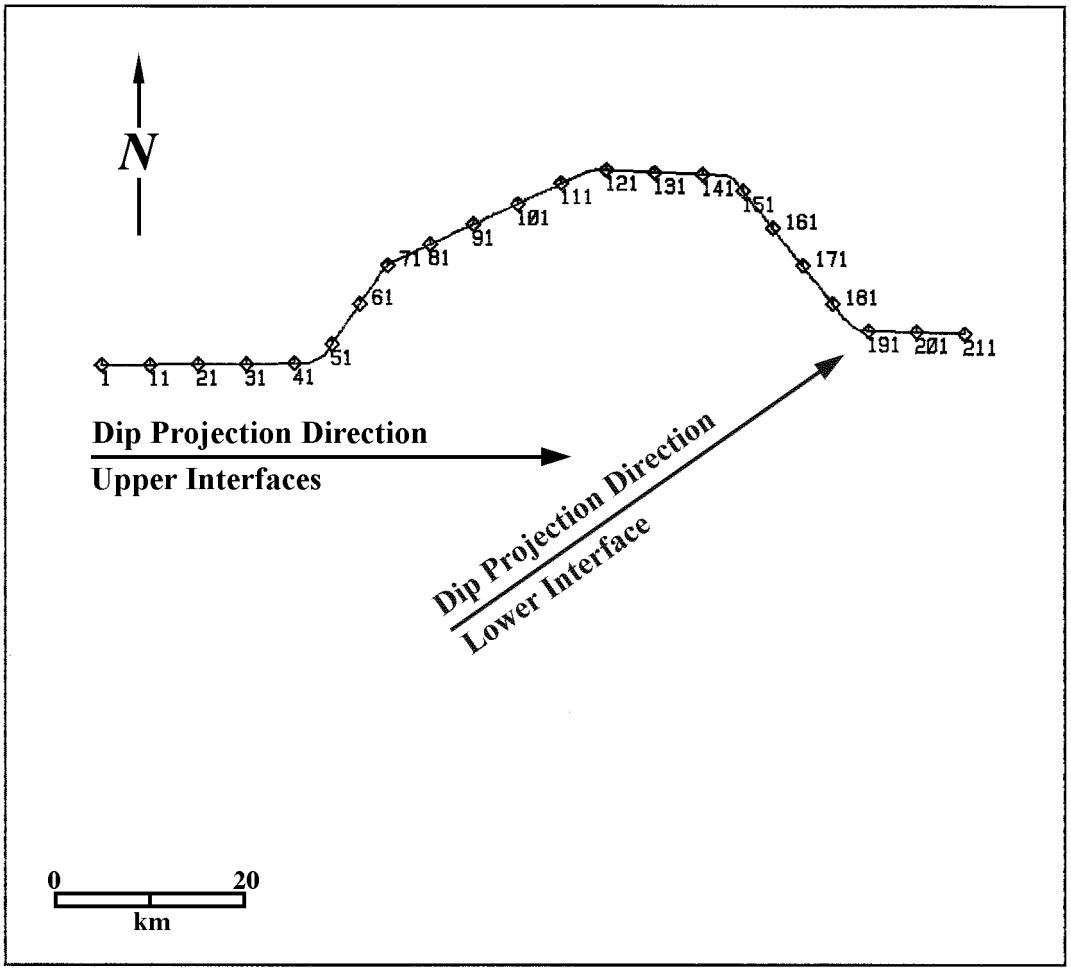

Figure 2.7: Crooked seismic line simulated over the model shown in Figure 2.6. Map area is 100x100 km.

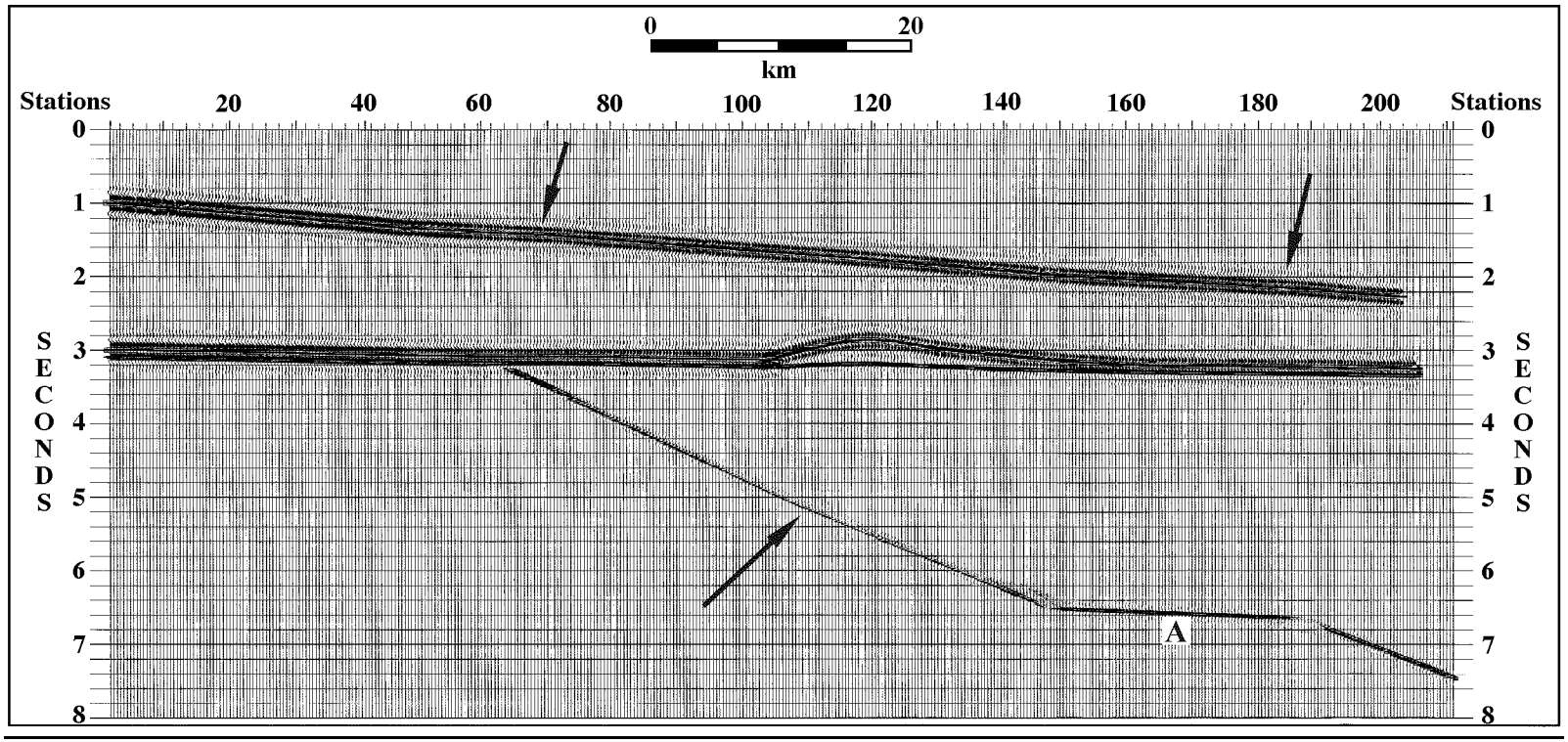

Figure 2.8: Conventionally processed stack using the data generated from the subsurface model shown in Figure 2.6. Note the undulatory nature of the dipping events, and the flattening of the lowermost reflection event ('A') due to the line bend (see Figure 2.7). Arrows point to some of the undulations on the various reflections.

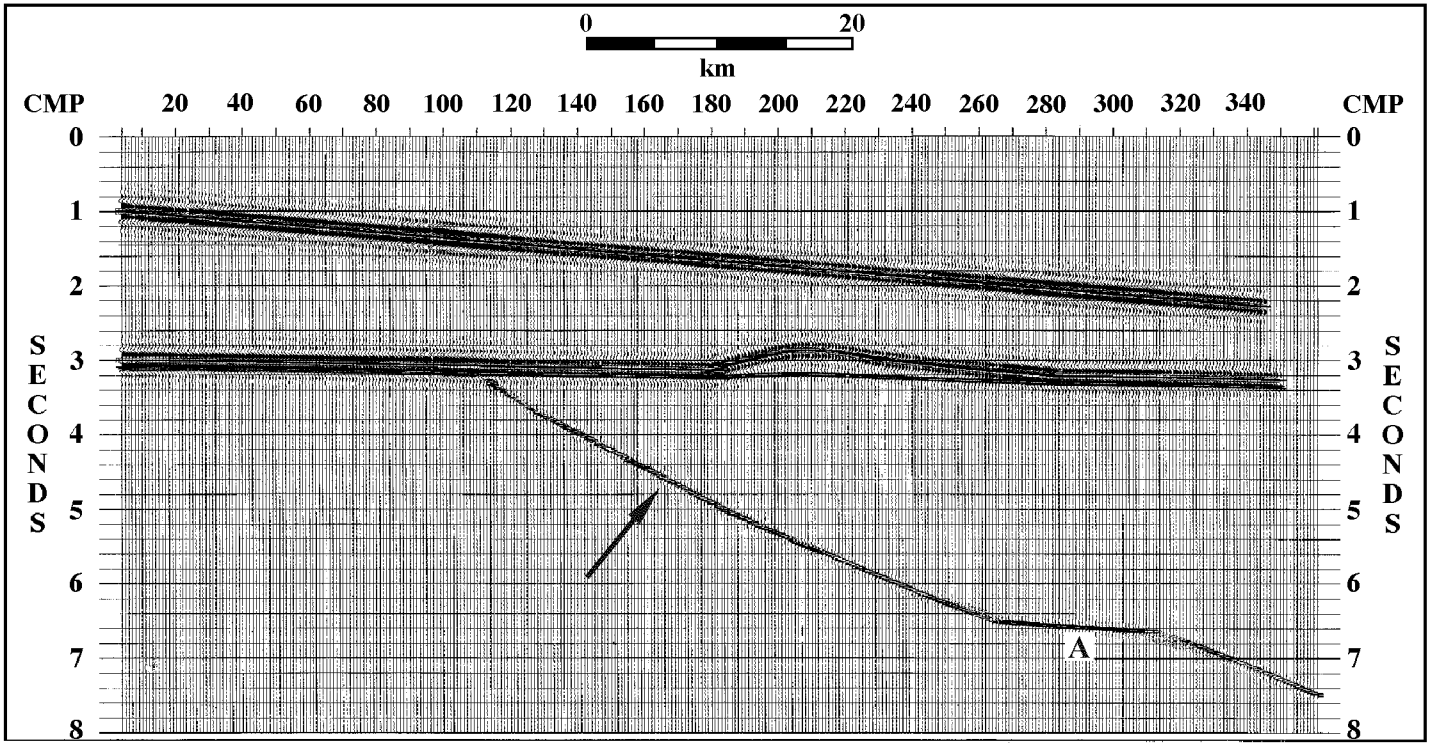

Figure 2.9: Stack after dip projection along an east-west line (see Figure 2.7). Note the improvement on the upper level reflections and the continued poor result (e.g. apparent flattening 'A') for the lower portion because the line is not down-dip for the lowermost interface (compare with Figure 2.8). Arrow points to downward warping on lowermost reflection caused by the incorrect projection.

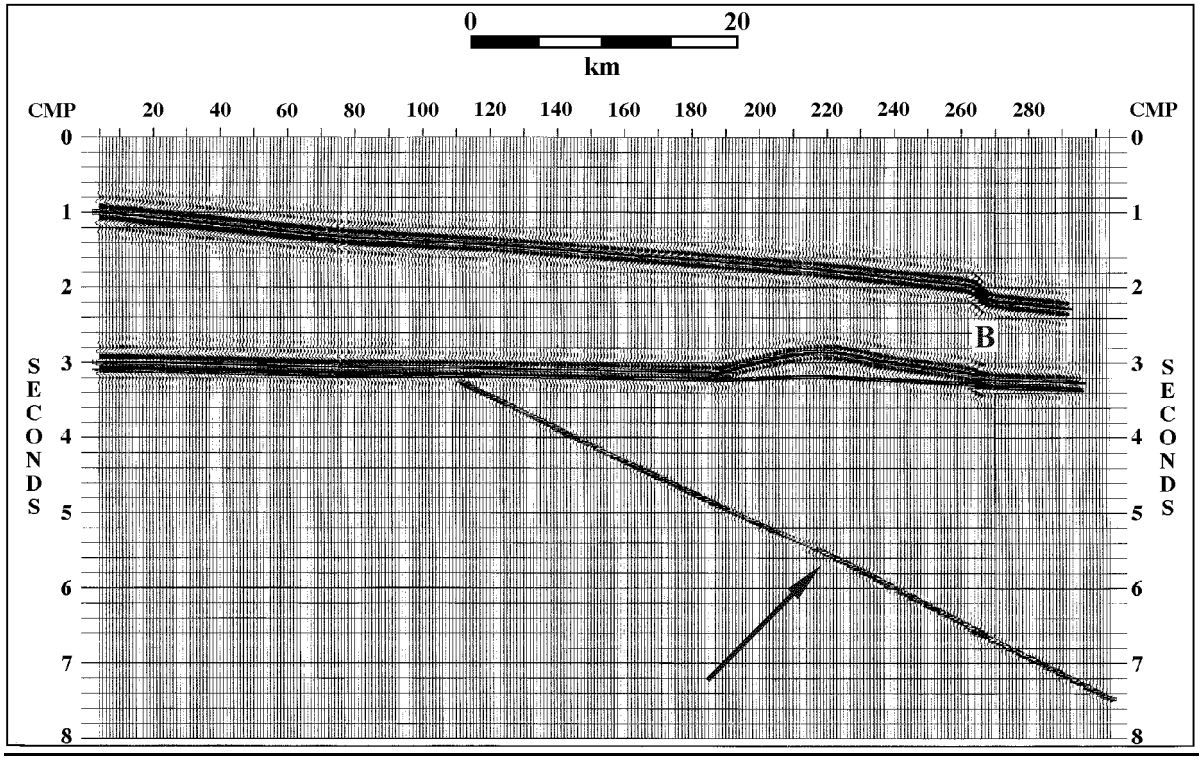

Figure 2.10: Stack after dip projection along a line oriented down-dip for the lowermost interface in the model (N55°E; see Figure 2.6). Comparison of this stack with the prior two stacks (Figures 2.8 and 2.9) shows that dip projection has worked for the lowermost reflection while distorting the upper section ('B'). Arrow points to veloctiy pull-up on the lowermost reflection.

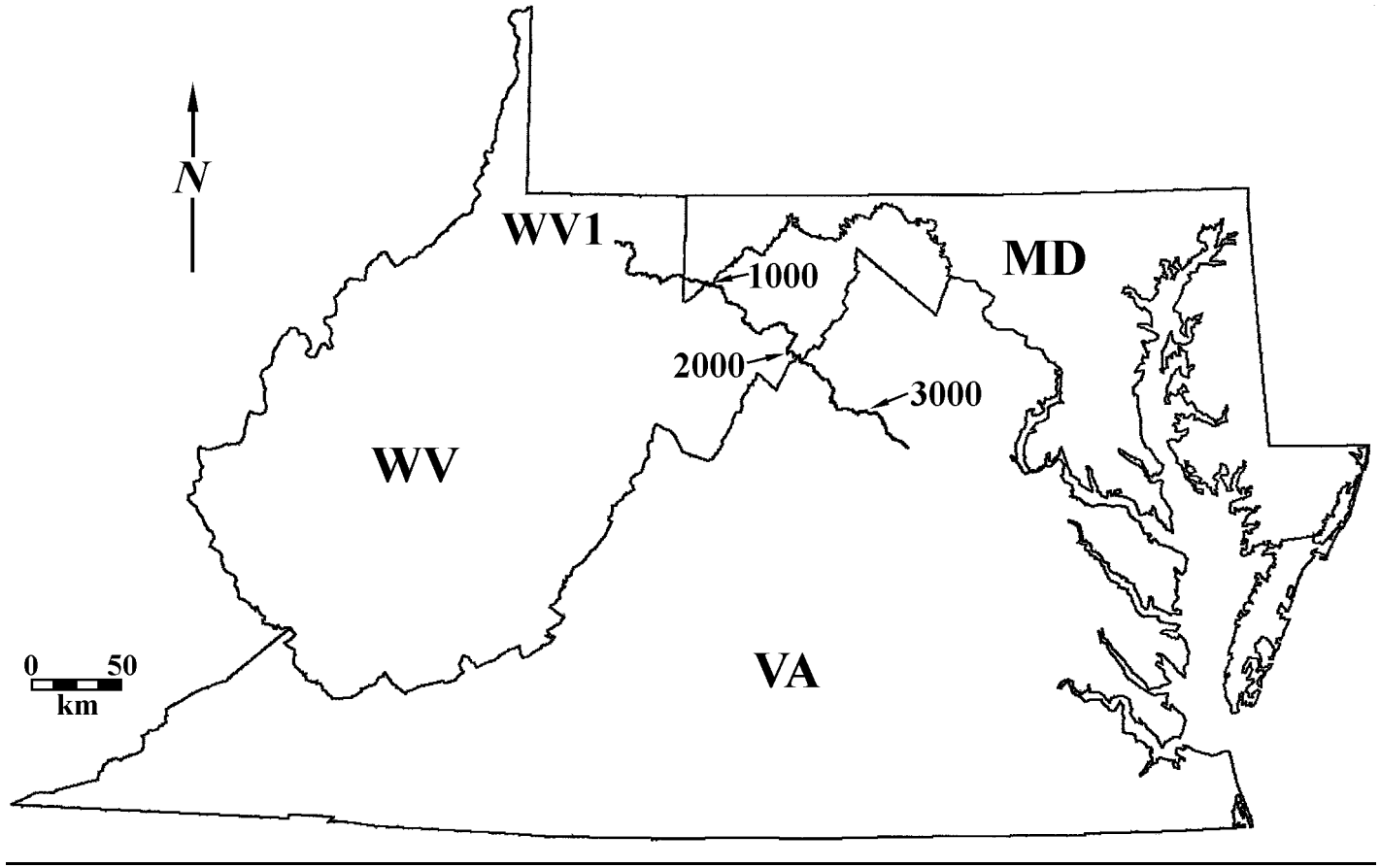

Figure 2.11: Map showing location of seismic line WV1. Map scale is 1:4000000. Projection in Virginia North state plane coordinates.

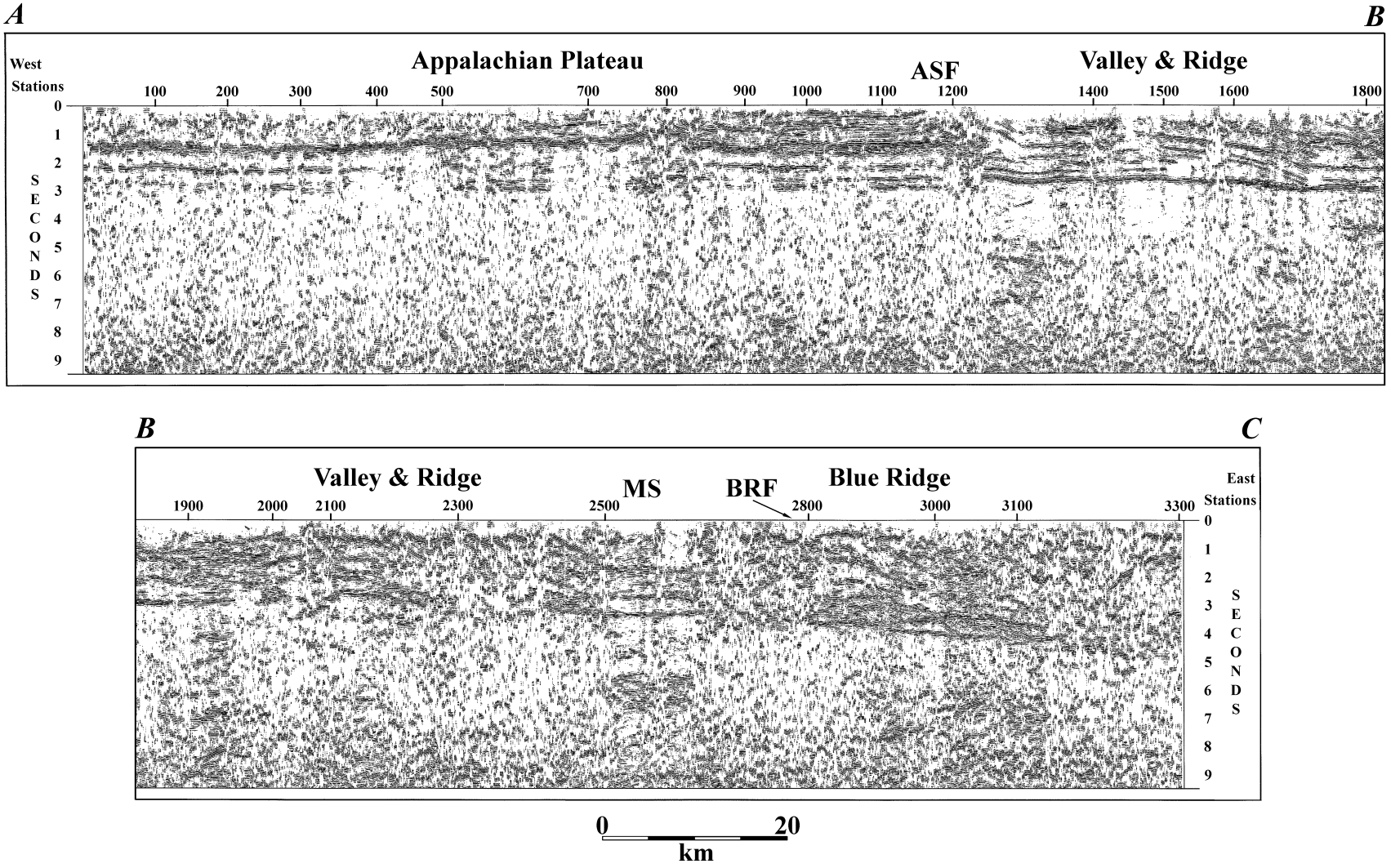

Figure 2.12: Display of WV1 stack after conventional crooked-line processing. Scale for this and all succeeding seismic sections is ~1:1 for 6 km/sec. ASF = Alleghany Structural front; BRF = Blue Ridge Front; MS = Massanutten Synclinorium. (Large PDF can be viewed by clicking on the figure.)

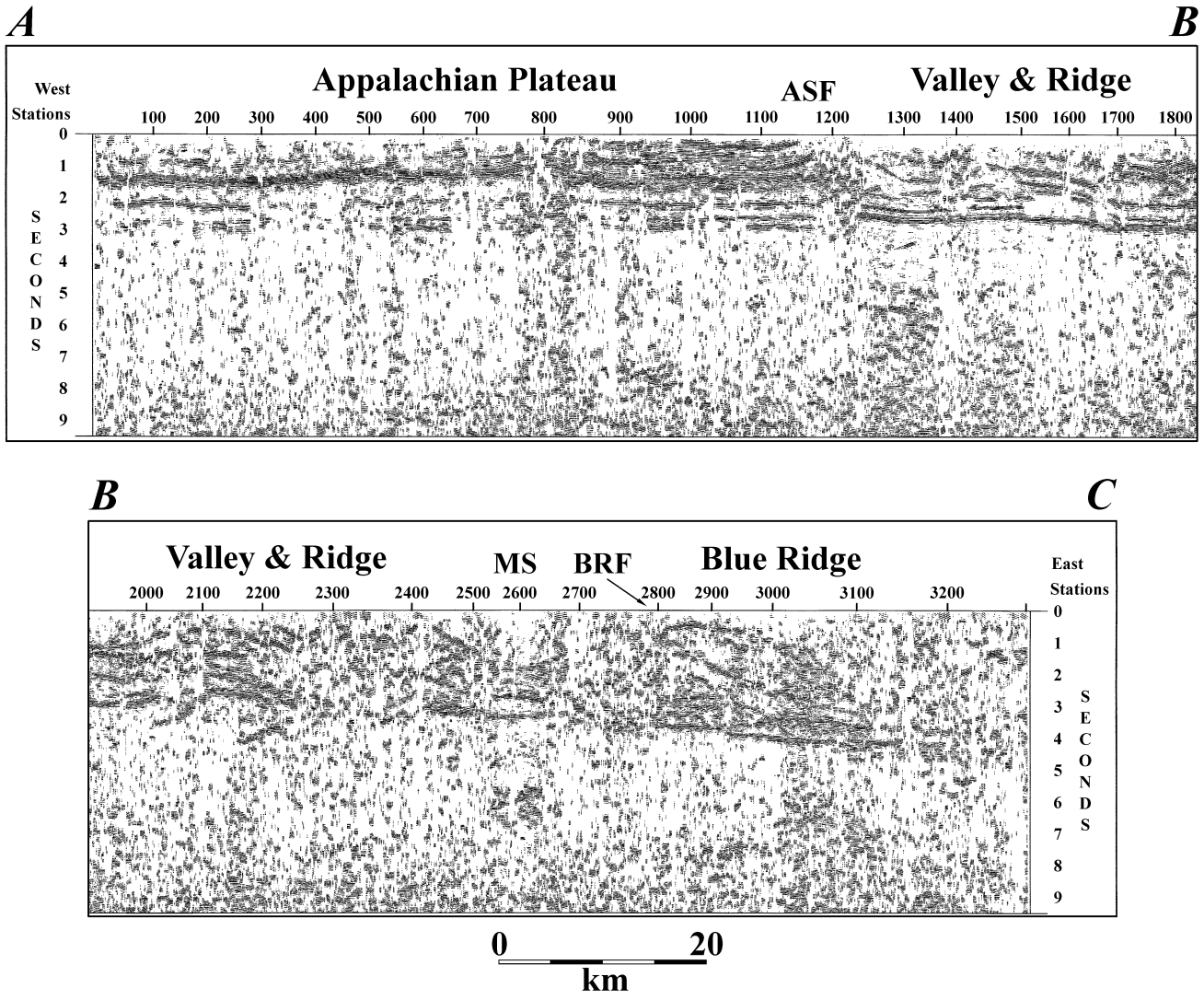

Figure 2.13: Dip projected version of seismic line WV1. Station numbers for this and subsequent dip-projection displays are approximate. ASF = Alleghany Structural front; BRF = Blue Ridge Front; MS = Massanutten Synclinorium. (Large PDF can be viewed by clicking on the figure.)

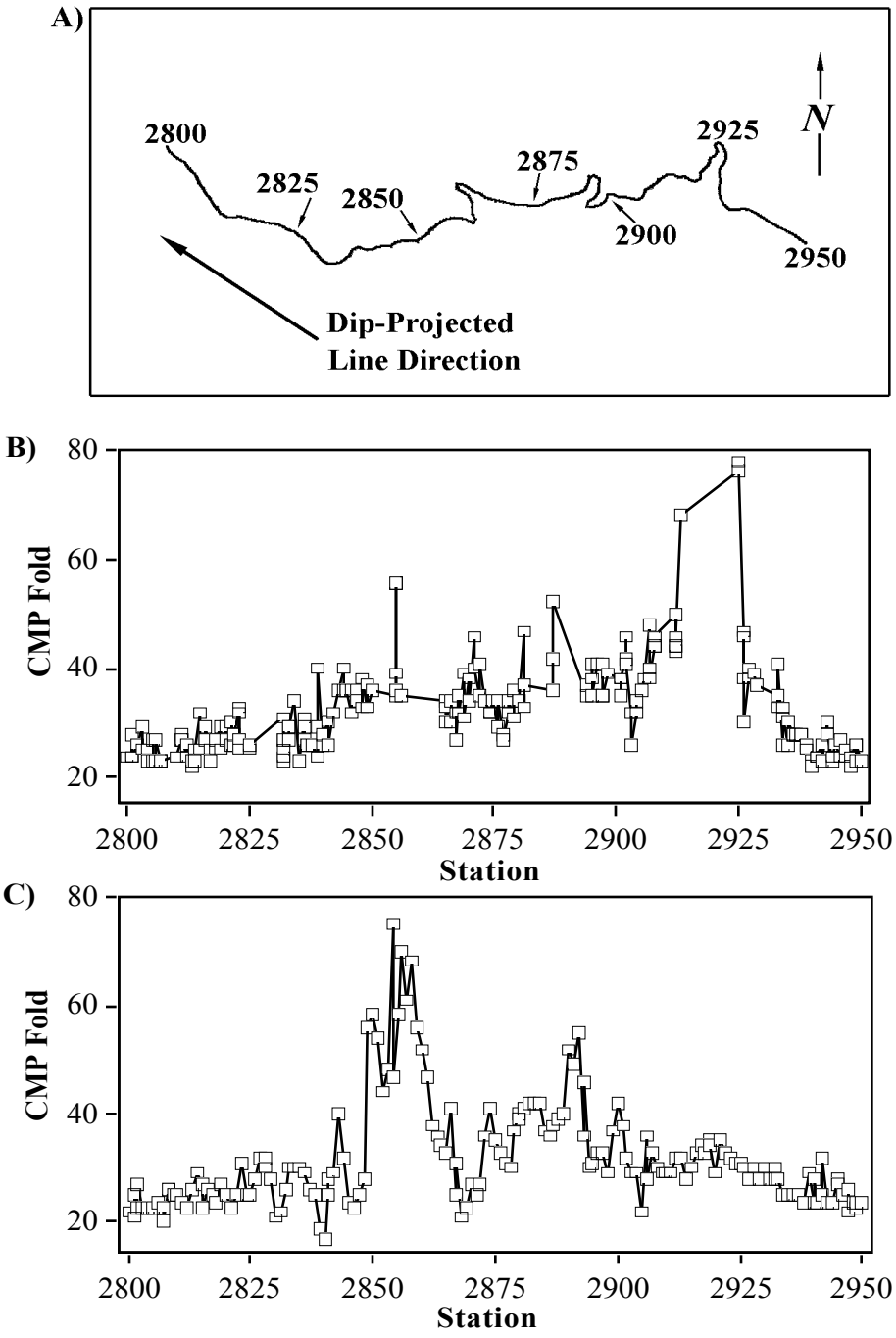

Figure 2.14: Fold variation between the two stacks of WV1 over a portion of the Blue Ridge. A) Station location map. Scale is 1:100000. B) Fold variation along conventionally processed WV1. C) Fold variation along dip-projected WV1.

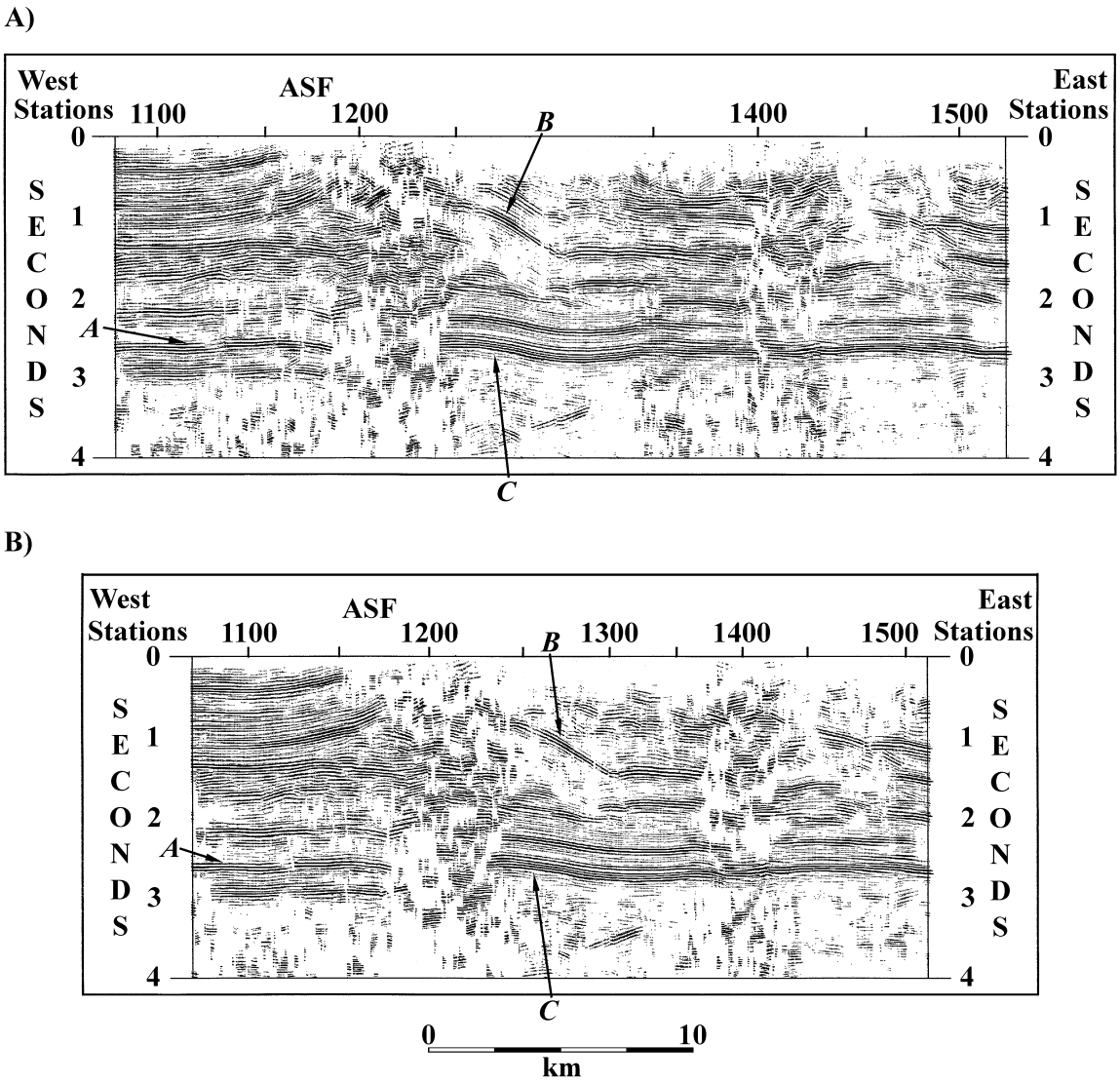

Figure 2.15: Close-up view of the Alleghany Structural Front (ASF) in West Virginia, showing the results of A) conventional and B) dip projection processing. Labeled reflections discussed in text. Tick marks along top of section are 50 stations apart.

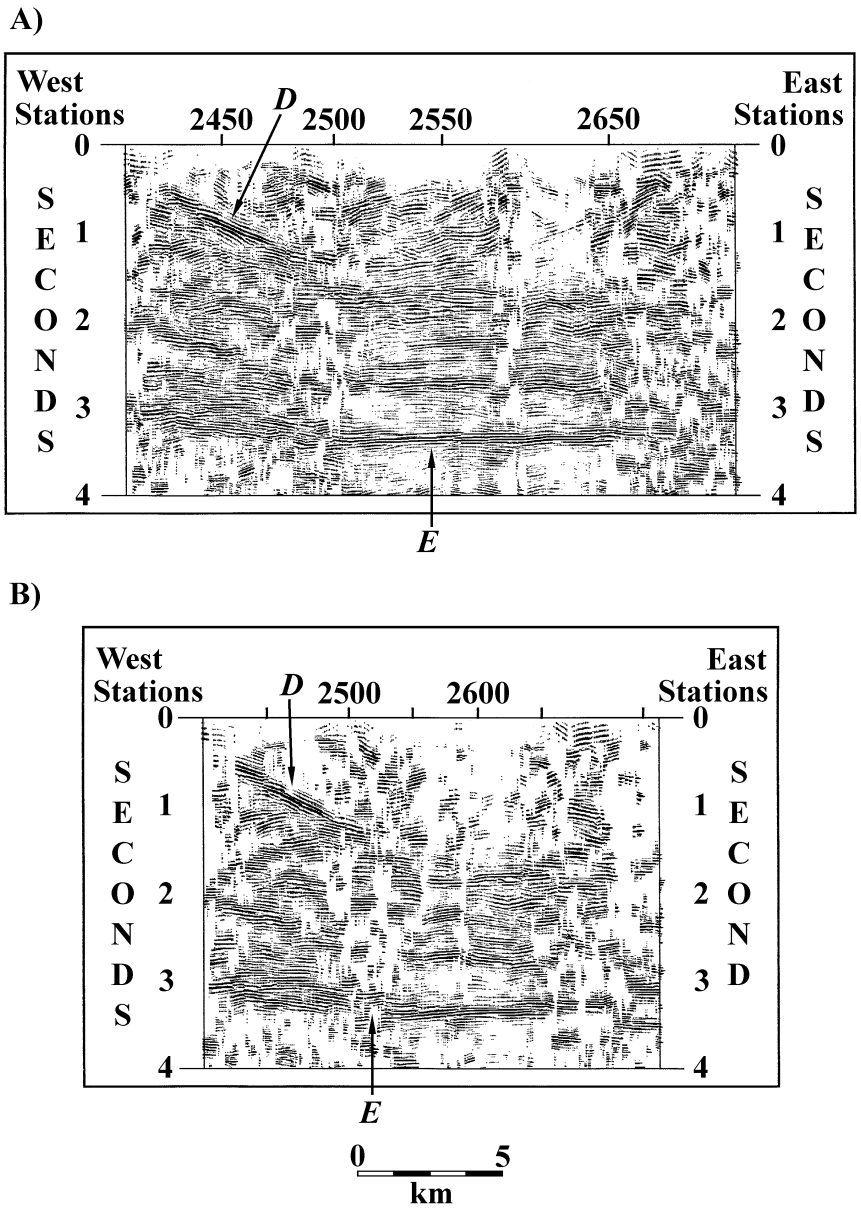

Figure 2.16: Close-up view of the Massanutten Synclinorium in Virginia showing the results of A) conventional and B) dip projection processing. Labeled reflections discussed in text. Tick marks along top of section are 50 stations apart.

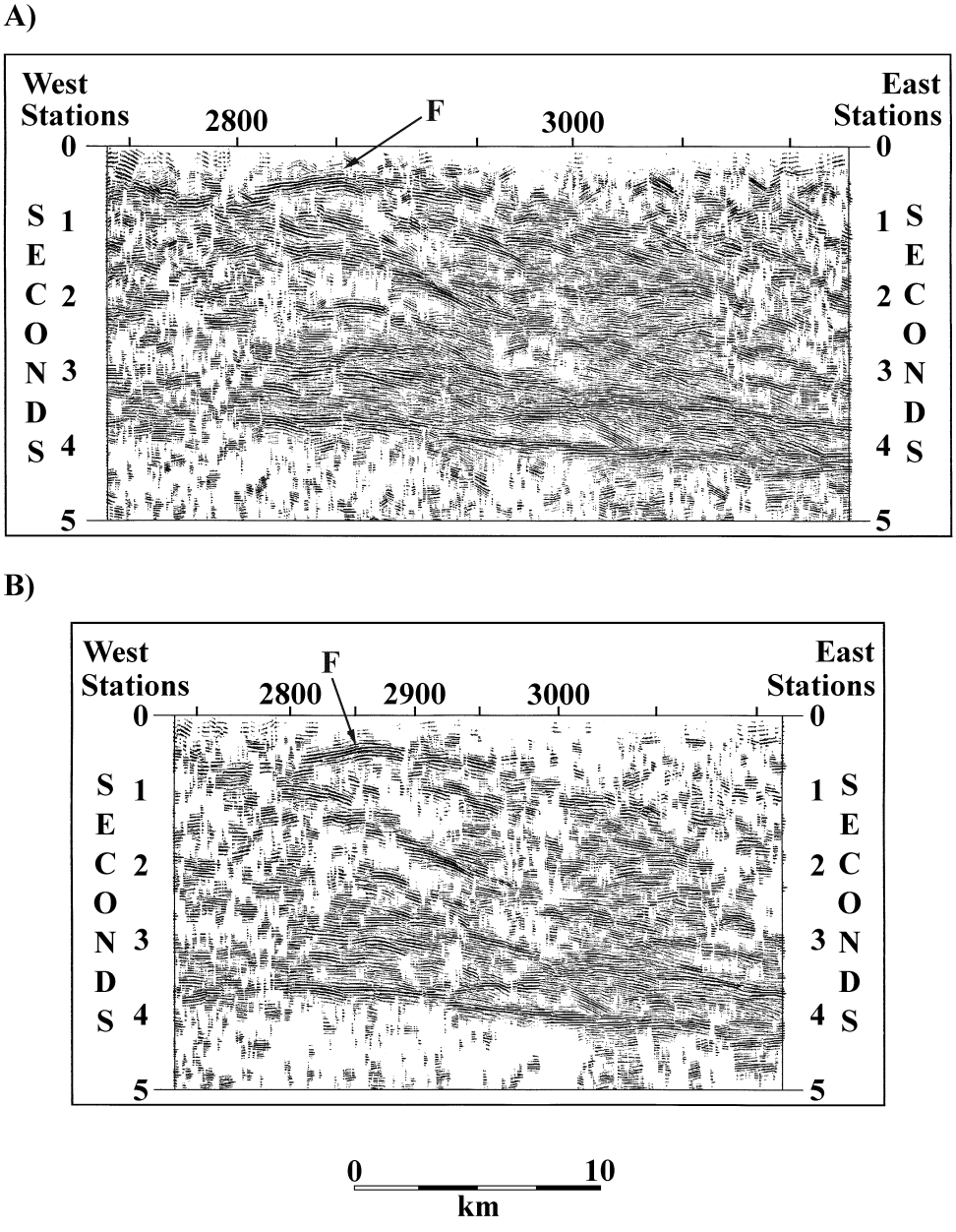

Figure 2.17: Close-up view of the Blue Ridge front in Virginia showing the results of A) conventional and B) dip projection processing. Labeled reflection discussed in text. Tick marks along top of section are 50 stations apart.

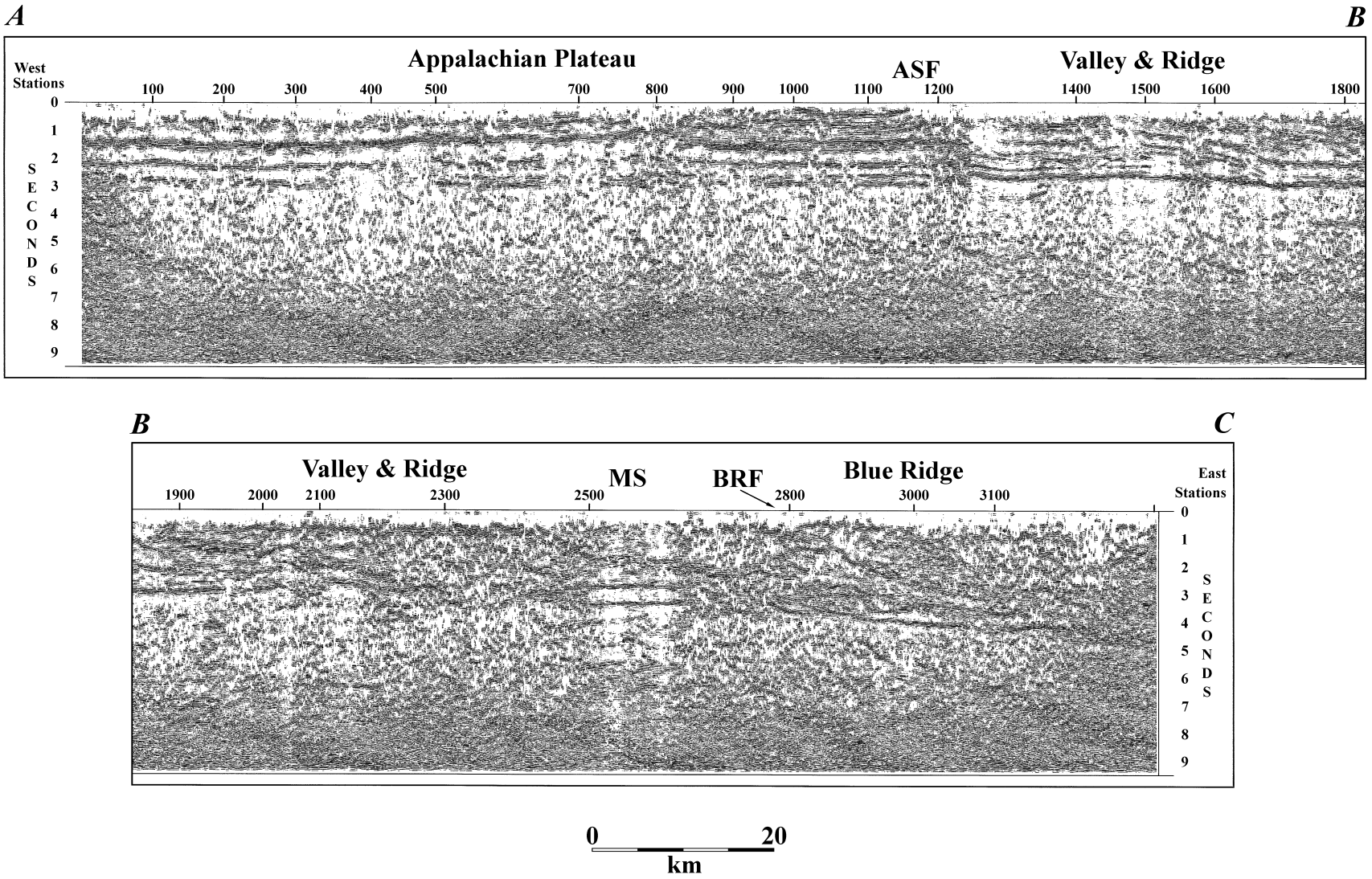

Figure 2.18: Kirchhoff migrated version of conventional stack from Figure 2.12. Migration velocities are 90% of stacking velocities. Migration noise can be seen in the deeper part of the section up to a time of 6 seconds. ASF = Alleghany Structural front; BRF = Blue Ridge Front; MS = Massanutten Synclinorium.

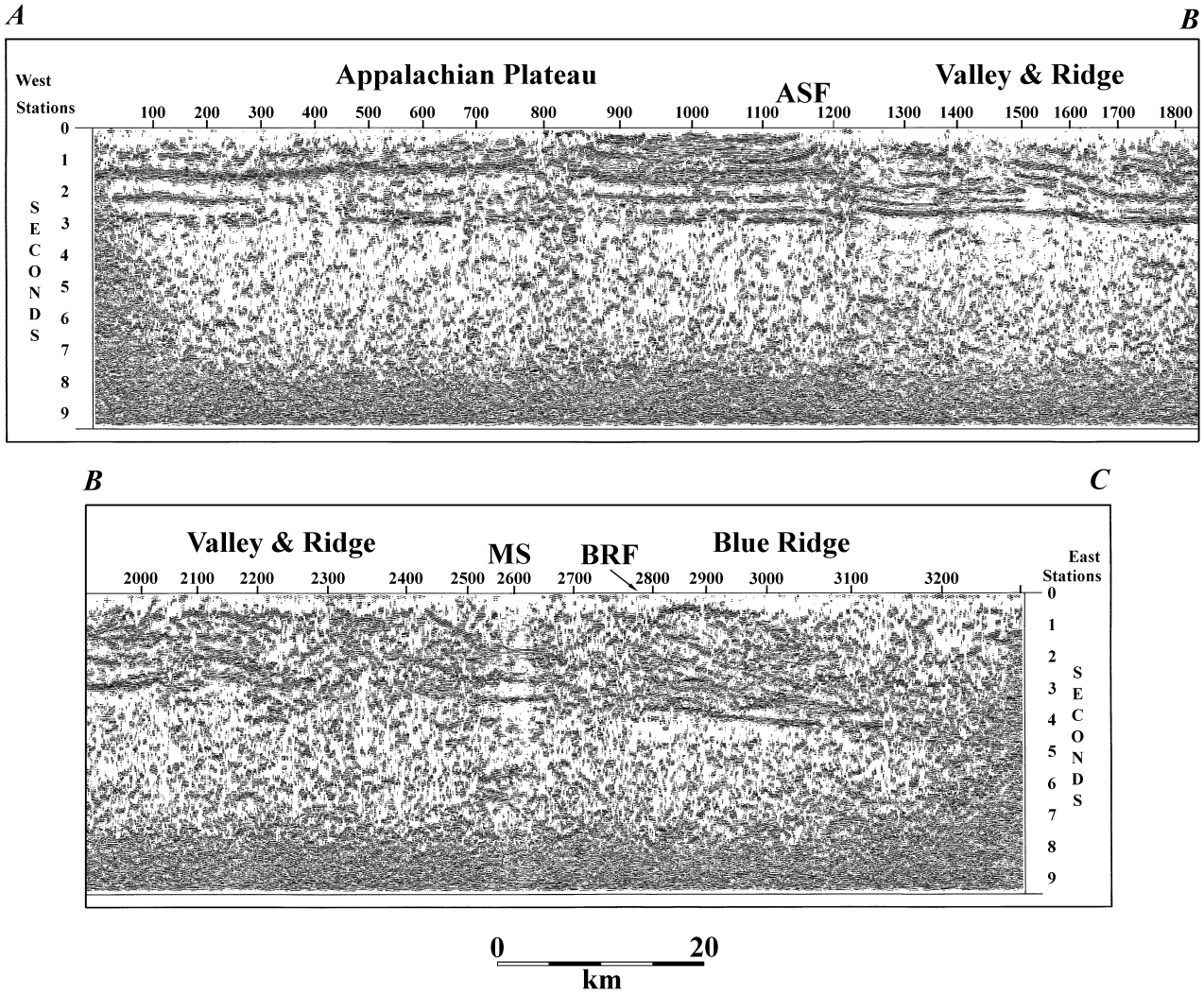

Figure 2.19: Kirchhoff migrated version of dip-projected stack from Figure 2.13. Migration velocities are 90% of stacking velocities. Migration noise is reduced significantly, and reflector continuity is improved in comparison to the migration result shown in Figure 2.18. ASF = Alleghany Structural front; BRF = Blue Ridge Front; MS = Massanutten Synclinorium. (Large PDF can be viewed by clicking on the figure.)

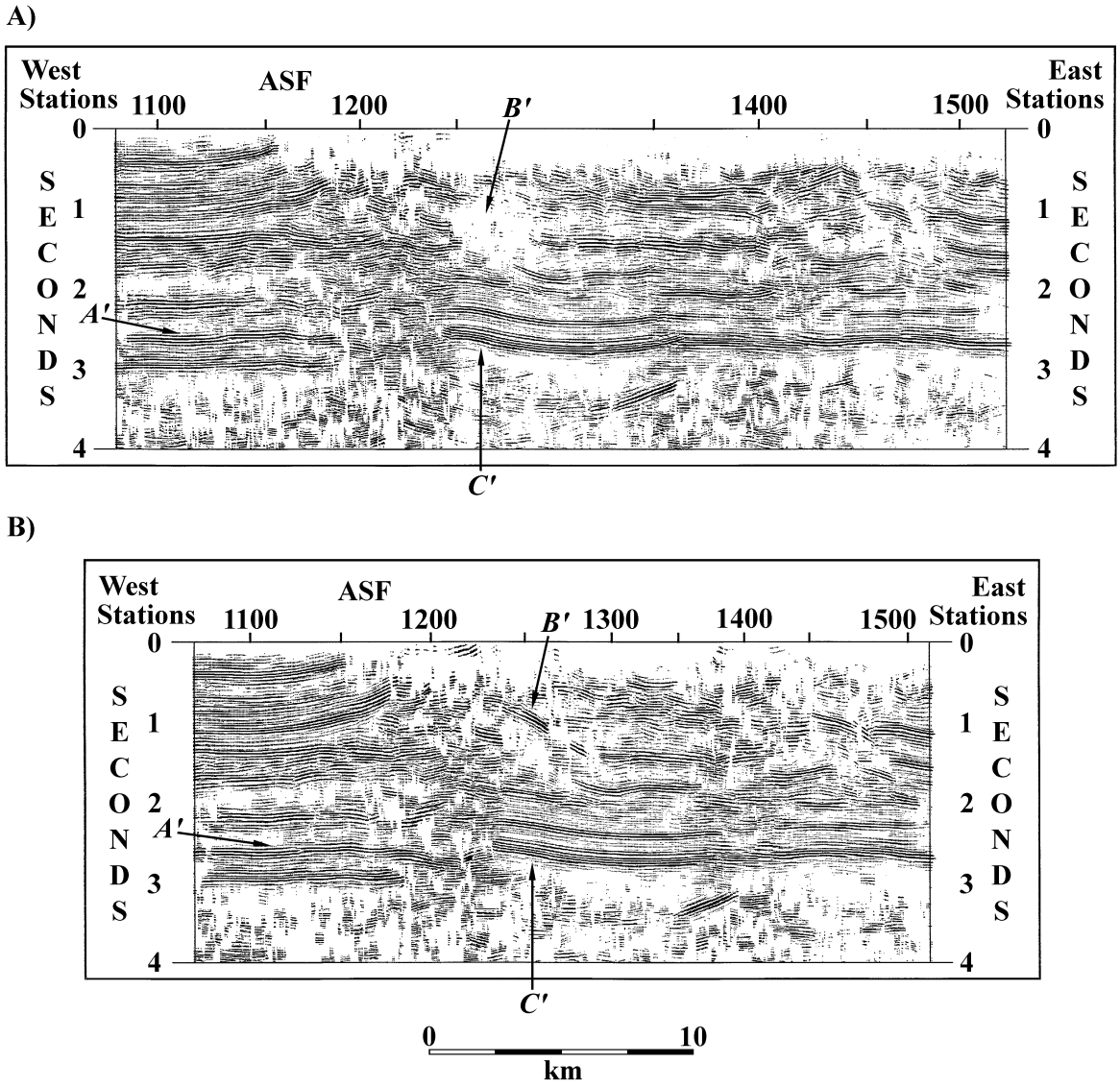

Figure 2.20: Close-up view of the Alleghany Structural Front (ASF) in West Virginia showing the migrated results from A) conventional and B) dip projection processing. Labeled reflections discussed in text. Tick marks along top of section are 50 stations apart.

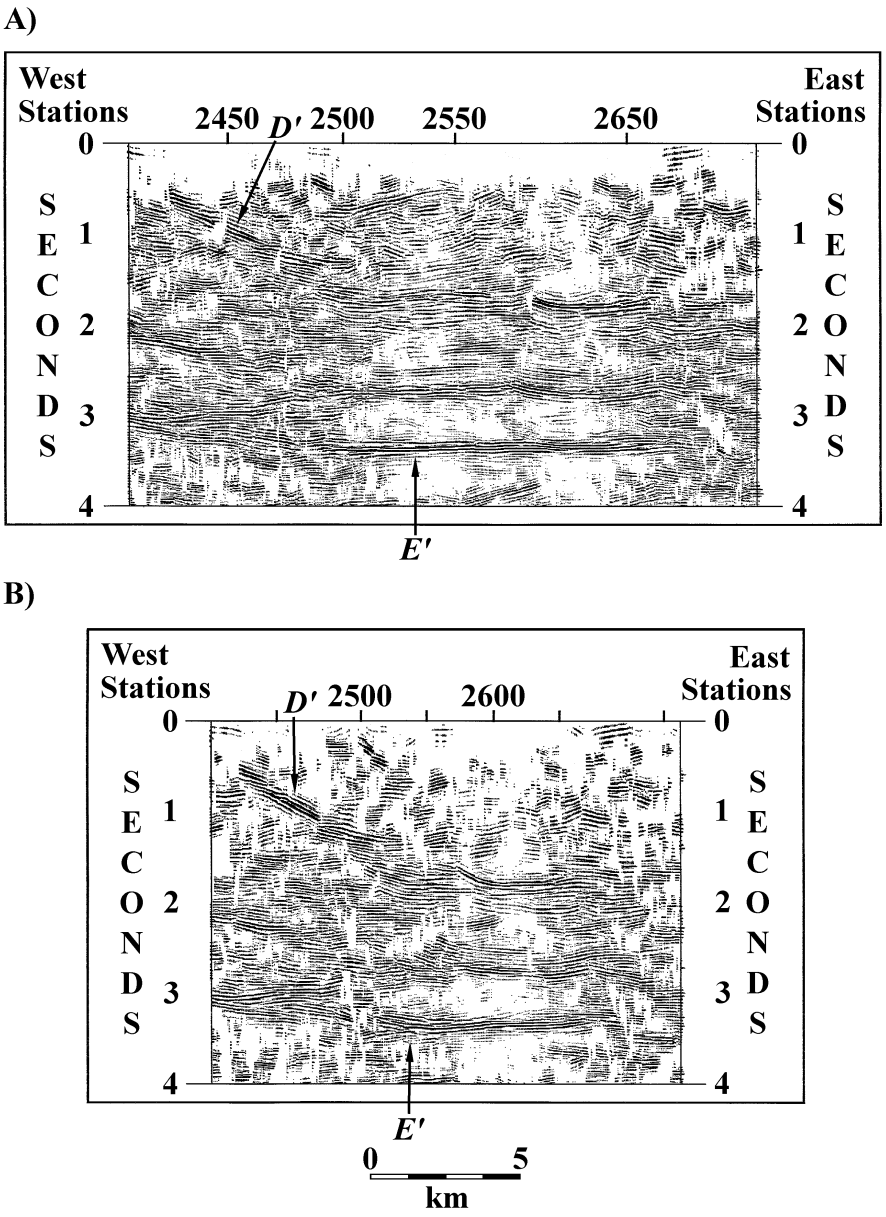

Figure 2.21: Close-up view of the Massanutten Synclinorium in Virginia showing the migrated results from A) conventional and B) dip projection processing. Labeled reflections discussed in text. Tick marks along top of section are 50 stations apart.

A)

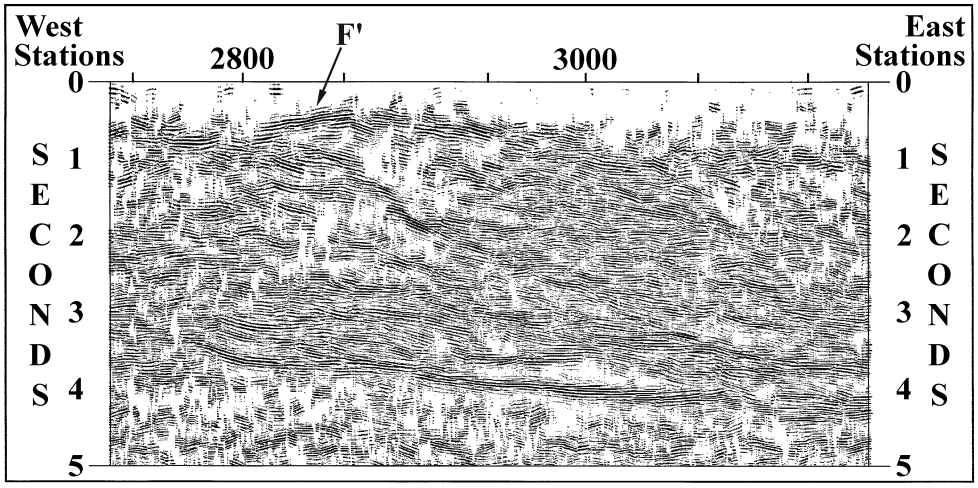

B)

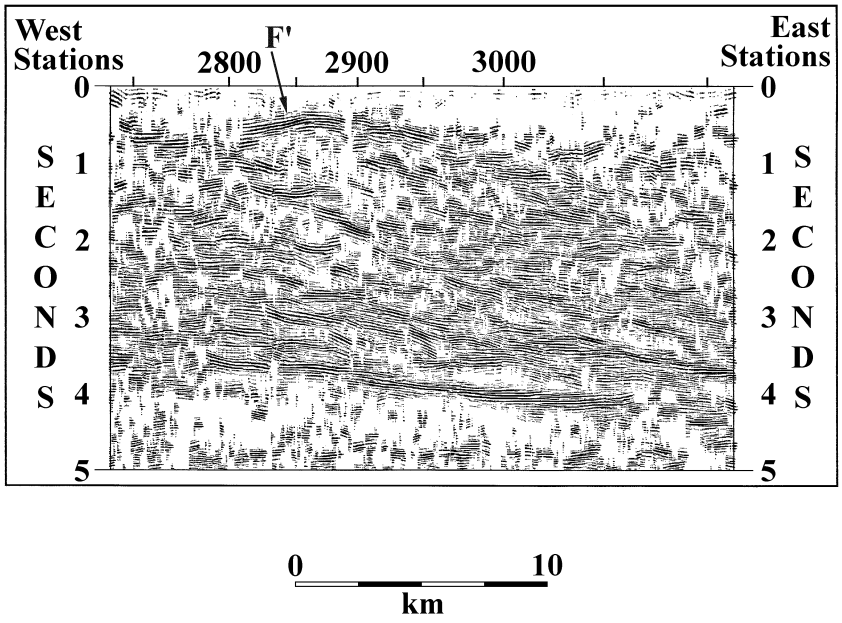

Figure 2.22: Close-up view of the Blue Ridge front in Virginia showing the migrated results from A) conventional and B) dip projection processing. Tick marks along top of section are 50 stations apart. F ' = Migrated version of reflection F in Figure 2.17.

Chapter 3: Potential Field Attributes Analysis

Abstract

Horizontal and vertical derivatives of gravity and magnetic data have long been used in the interpretation of geologic structures and subsurface density and susceptibility boundaries. In recent years, new techniques that use horizontal and vertical derivatives, such as the *analytic signal* and *potential field tilt angle* methods, have been used preferentially over more traditional gradient methods. In particular, the analytic signal in its original and various modified forms has been used by a number of authors to ascertain the locations of subsurface structures.

The mathematical relationship between the above potential field analysis methods and seismic attribute analysis is demonstrated herein, and by direct analogy, a new measure -- the *potential field wavenumber* -- is introduced. The utility of these attributes in the identification and location of subsurface density contrasts are examined using both model and real data.

3.1 Introduction

Horizontal derivatives of gravity and magnetic data have been used in the interpretation of geologic structures (e.g. Nettleton, 1940; Vacquier et al., 1953), and to ascertain subsurface density boundaries for use in modeling and inversion. The direct measurement of horizontal gradient and curvature of gravity using a torsion balance was an important method used to locate salt domes and other geologic structures along the Gulf Coast during the 1930's (Nettleton, 1940). Horizontal gradient and curvature vectors were plotted and interpreted with the aid of charts and nomographs. With the advent of highly portable, accurate, and faster vertical gravimeters however, the use of true gradient and curvature data has been reduced in spite of it's proven ability to discriminate density contrasts in the subsurface.

It wasn't until the 1960's and the use of the digital computer that interest in horizontal derivatives of the gravity field was rekindled. Most methods to compute the derivatives have either used 2-D linear filter theory (e.g. Gunn, 1975; Mesko, 1984), or finite differences (Cordell and Grauch, 1985; Blakley and Simpson, 1986) to obtain the necessary derivatives. In general, these horizontal derivative maps are plotted as contours of the magnitude of the horizontal derivative vector. The resulting scalar magnitude map is then interpreted. The plotting and interpretation of horizontal gradient vectors themselves is not often attempted, although good results for a regional survey in southern Alberta were recently reported (Edwards et al., 1996).

Nabighian (1972) introduced the concept of the *analytic signal* of a potential field by showing that the horizontal and vertical gradients of a potential field represent an analytic signal; i.e. they constitute a Hilbert transform pair. It was soon discovered that the analytic signal has properties similar to the horizontal gradient in that it peaks over the edges of bodies with differing density or susceptibility contrasts in the near surface. Since then, the analytic signal in various forms has been used in the interpretation of potential field maps by many investigators (e.g. Hsu et al., 1996; Debiglia and Corpel, 1997).

Miller and Singh (1994) introduced the concept of a *potential field tilt angle*. The tilt angle is detemined from the ratio of the vertical to horizontal derivatives. Larger values of the tilt angle are obtained when the ratio of the vertical to horizontal derivatives is at its largest, which for both gravity and magnetic data occurs over the center of bodies with differing density or susceptibility. As pointed out by Miller and Singh (1994), the tilt angle reacts in a similar manner to both shallow and deep bodies, as the ratio of the vertical to horizontal derivatives is insensitive to depth of burial (Figure 3.1). In addition, there is a change in sign for the tilt angle near the edges of the body, so that the zero contour approximates the edges of the causative bodies.

In this paper, the mathematical analogy between the analytic signal and tilt angle of potential field analysis and seismic attribute analysis is demonstrated, and through that analogy a new method is developed called the *potential field wavenumber*. These *potential field attributes* are compared to other gradient techniques in a model study, and then applied to gravity data from

the central Appalachians to define the lateral extent of a large duplex structure identified on seismic reflection data.

3.2 Mathematical Analogy Between Potential Field Attributes and Complex Trace Analysis

The *analytic signal*, A, of a potential field is defined by Roest and others (1992) as:

$$A(x,y) = \sqrt{[H(x,y)]^2 + [Z(x,y)]^2} \qquad (1)$$

where H and Z are the horizontal and vertical derivatives given by:

$$H(x,y) = \sqrt{\left(\frac{\partial M(x,y)}{\partial x}\right)^2 + \left(\frac{\partial M(x,y)}{\partial y}\right)^2} \qquad (2)$$

$$Z(x,y) = \frac{\partial M(x,y)}{\partial z} \qquad (3)$$

respectively, and M is the potential field in question. Nabighian (1972; 1984) demonstrated that the horizontal and vertical derivatives of a potential field are Hilbert transform pairs and that peak values of the analytic signal indicate density or susceptibility boundaries in the subsurface.

The *potential field tilt angle* (Miller and Singh, 1994) is defined as

$$\Theta(x,y) = \tan^{-1}\left(\frac{Z(x,y)}{H(x,y)}\right) \qquad (4)$$

Peak values of the tilt angle are located over the center of mass of bodies in the subsurface, and the zero contour of tilt angle values approximates the edges of these bodies (see Figure 3.1).

The above *potential field attributes* have mathematically analogous counterparts in reflection seismology called *seismic attributes*. The seismic attributes, as defined by Tanner and others (1979), are reflection strength (RS), instantaneous phase (θ), and instantaneous frequency (f). Reflection strength is defined as follows:

$$RS(t) = \sqrt{[Re(t)]^2 + [Q(t)]^2} \qquad (5)$$

where Re(t) and Q(t) are the real and quadrature (imaginary) parts of the seismic trace. Reflection strength is used to indicate local changes in lithology or fluid content, which is utilized as a hydrocarbon indicator.

Equations (1) and (5) are mathematically similar in two ways: a) both are an expression of the magnitude of a vector (A represents the magnitude of the total gradient vector; RS the magnitude of a rotating phasor in the complex plane), and b) the values within the square root are related through the Hilbert transform. In the case of potential fields, the horizontal derivatives (H) are used to obtain the vertical derivative (Z). For a seismic trace, the recorded seismic trace (Re) is used to obtain the quadrature trace (Q). In both cases the Hilbert transform mathematically converts data from one plane to another, perpendicular plane.

Instantaneous phase is an angle defined by the arctangent of the ratio of the magnitudes of the quadrature to the real trace, and represents the angle of a phasor in the complex plane at any point in time relative to an arbitrary starting point (Taner et al., 1979). It is defined as

$$\theta(t) = \tan^{-1}\left(\frac{Q(t)}{\mathrm{Re}(t)}\right) \qquad (6)$$

A mathematical analogy exists between equations (4) and (6), as both equations represent the angle between two halves of a Hilbert transform pair. In addition, instantaneous phase emphasizes the continuity of events in the subsurface (Taner et al., 1979), as does the potential field tilt angle.

The instantaneous frequency, f(t), is defined as the time derivative of the instantaneous phase, or

$$f(t) = \frac{\partial\,\theta(t)}{\partial\,t} \qquad (7)$$

Instantaneous frequency emphasizes local changes in the instantaneous phase and can aid the seismic interpreter in the location of pitch outs and hydrocarbon-water interfaces (Taner et al., 1979).

By mathematical analogy to the instantaneous frequency, the horizontal gradient of the tilt angle is defined in this study as the *potential field wavenumber*:

$$\Lambda(x,y) = \sqrt{\left(\frac{\partial\,\Theta(x,y)}{\partial\,x}\right)^2 + \left(\frac{\partial\,\Theta(x,y)}{\partial\,y}\right)^2} \qquad (8)$$

where Θ is the tilt angle as defined in equation 4, and Λ is the potential field wavenumber. The units for wavenumber are degrees per unit length as the tilt angle is defined in degrees. For this study, the units will be degrees per kilometer (deg./km). The wavenumber is a *local* measure (Bracewell, 1965) that peaks over the edges of density or susceptibility contrasts in a similar manner to the analytic signal (Figure 3.2), and its properties are investigated in a later section.

The mathematical relationship between the potential field wavenumber and the instantaneous frequency is not as clear as those between the other seismic and potential field attributes. A seismic trace exhibits amplitude versus time information for propagating seismic waves. As such, the concept of 'frequency' and 'wavelength' have an exact and mathematical definition and meaning. In potential field data, on the other hand, there is a spatial variation of amplitude information that relates the potential field response (anomaly) to its source(s). It is this relationship that can be highlighted through the calculation of a horizontal gradient. In particular, the spatial relationships described earlier between the tilt angle and its causative body can be enhanced by using the gradient, just as the complex phase relationships revealed by the instantaneous phase in seismic data are emphasized via by the calculation of the instantaneous frequency. The wavenumber, as a spatial gradient of a two-dimensional distribution, requires derivatives in both X and Y. Instantaneous frequency, as a time derivative (gradient) along the instantaneous phase trace, requires only a single derivative in time. Therefore, the calculation of a potential field wavenumber is mathematically analogous to the calculation of the instantaneous frequency, and will highlight abrupt lateral changes in density and susceptibility much as the instantaneous frequency enhances differences in acoustic impedance. Table 3.1 summarizes the relationships discussed above for potential and seismic wave fields.

3.3 Calculation of Potential Field Attributes

Potential field attributes were calculated from the horizontal and vertical derivatives of the original gravity data from a 1x1 km grid using two-dimensional discrete Fourier transform techniques to obtain the necessary derivatives. The original gridded gravity values were centered in a new grid of size $(2^N)^2$, where 2^N is larger than the size of the original grid matrix. The values are then extended to the edges of the new grid matrix using a tapered cosine-bell window to suppress edge effects generated during the filtering process. This modified grid was then transformed into the frequency domain, where the horizontal derivative was calculated using the filter described by Gunn (1975). Gunn expressed the derivative of a function, M, in the frequency domain as

$$F\left[\frac{\partial M}{\partial x}\right] = (ik_x)^n \, \mathrm{M}(k_x, k_y) \qquad (9a)$$

in X, and

$$F\left[\frac{\partial M}{\partial y}\right] = (ik_y)^n \, \mathrm{M}(k_x, k_y) \qquad (9b)$$

in Y, where F [ ] represents the Fourier transform of the bracketed item, k_x and k_y are the frequency domain wavenumbers in the X- and Y-directions, respectively, and n is the order of the

Table 3.1: Comparison of seismic wave and potential field attribute analysis, demonstrating the mathematical analogy between types of analysis. *H* represents the Hilbert transform.

Seismic	**Potential Fields**
Hilbert Transform: $Q(t) = H\{Re(t)\}$	Hilbert Transform: $Z(x,y) = H\{H(x,y)\}$
Reflection Strength (RS): $RS(t) = \sqrt{[Re(t)]^2 + [Q(t)]^2}$	Analytic Signal: $A(x,y) = \sqrt{[H(x,y)]^2 + [Z(x,y)]^2}$
Instantaneous Phase: $\theta(t) = \tan^{-1}\left(\frac{Q(t)}{Re(t)}\right)$	Potential Field Tilt Angle: $\Theta(x,y) = \tan^{-1}\left(\frac{Z(x,y)}{H(x,y)}\right)$
Instantaneous Frequency: $f(t) = \frac{\partial\,\theta(t)}{\partial\,t}$	Potential Field Wavenumber: $\Lambda(x,y) = \sqrt{\left(\frac{\partial\,\Theta(x,y)}{\partial\,x}\right)^2 + \left(\frac{\partial\,\Theta(x,y)}{\partial\,y}\right)^2}$

derivative. For a first derivative or gradient calculation, n is set to 1. The resultant grid was then filtered using a frequency domain equivalent of the Hilbert transform (Nabighian, 1984) to produce a second grid containing the vertical derivative. The freqency domain expression for the vertical derivative is

$$F\left[\frac{\partial M}{\partial z}\right] = H_1 F\left[\frac{\partial M}{\partial x}\right] + H_2 F\left[\frac{\partial M}{\partial y}\right] \qquad (10)$$

where *M* is the potential field being transformed, *F* [ ] represents the Fourier transform of the bracketed item, and H_1 and H_2 are frequency domain Hilbert transform operators such that

$$H_1 = \frac{-ik_x}{\sqrt{(k_x)^2 + (k_y)^2}} \qquad (11a)$$

and

$$H_2 = \frac{-ik_y}{\sqrt{(k_x)^2 + (k_y)^2}} \qquad (11b)$$

for the X- and Y-directions, respectively. The application of equation 10 in the frequency domain and the subsequent inverse Fourier transform yields the vertical derivative from the horizontal derivatives calculated using equation 9. Once the horizontal and vertical derivatives are determined, the analytic signal and tilt angle are calculated using equations (1) and (4). The tilt angle grid is then transformed into the frequency domain, and the horizontal derivative filter (equation 9) applied again. Inverse Fourier transformation returns the local potential field wavenumber.

During initial tests of the program, it was noted that the local wavenumber results were plagued by high frequency jitter, possibly caused by the sensitivity of the Gunn's horizontal derivative filter to small changes in the potential field tilt angle. The option of calculating the final horizontal derivative using the three-point finite-difference method of Cordell and Grauch (1985) was added to the algorithm, as was an unweighted 3x3 grid-point smoothing filter. The smoothing method gave satisfactory results when applied to the noise-free model data, but the finite difference method was also retained as an option. Output from the algorithm includes the horizontal and vertical derivative of the gravity field, and the three potential field attributes; i.e. the analytic signal, the tilt angle, and the local wavenumber.

3.4 Properties of the Potential Field Attributes

As an initial test of the effectiveness of the algorithm, a 20x20x2 km block with a density contrast of 0.1 g/cm^3 was placed at the center of a grid. The depth of the body's center of mass was allowed to vary as a test of the various attribute's ability to discriminate the edges of the body as the depth was increased. In addition, the attributes were compared with results obtained for the same models using the enhanced analytic signal of Hsu and others (1996). Error was determined by finding the difference between the peak values (for the analytic signal and local wavenumber) and the location of the zero crossover (for the tilt angle) and the known edges of the body. The results of this test indicate that the new wavenumber method was better at determining the edges of the body, as it was accurate to within the grid spacing of 1 km up to at least a 10 km depth of burial for the center of mass, with an error of only 1 km at a depth of 15 km (Figure 3.3). The analytic signal had a 1 km error at 3 km depth. However, the maximum error was limited by the fact that unlike the other methods, the analytic signal's error actually

reduces the body's size with increasing depth; all the other methods show the spreading of the anomaly by locating the body edges farther to the outside of the body as the depth increases. The enhanced analytic signal (Hsu et al., 1996) performed better than the analytic signal, with the first errors showing up at 7 km depth, whereas the tilt angle had steadily increasing error beyond a depth of 4 km. These results indicate that the local wavenumber is a better tool than other currently utilized methods in accurately locating the lateral extent of subsurface density contrasts.

The results of application of the attribute analysis algorithm to the gravity field from a three-dimensional distribution of bodies at varying depths in the subsurface are shown in Figure 3.4. The results from the enhanced analytic signal technique of Hsu and others (1996) are shown also for comparison. The zero degree contour of the tilt angle and local maximum values of the wavenumber locate the source body edges well, whereas the enhanced analytic signal gives a poor result for the deeper bodies. Although the enhanced analytic signal locates the body edges with relatively small error (see Figure 3.3), the magnitude of the values decreases rapidly for deeper bodies. This is expected because the method relies on higher-order derivatives to sharpen the boundaries revealed using the analytic signal technique, and therefore would preferentially enhance the nearer surface features over those at greater depths (Hsu et al., 1996). The absolute magnitude of the local wavenumber is much larger than that of either analytic signal technique and decays less rapidly with depth. A comparison of absolute signal strength vs. depth to center of mass for each of the techniques is shown in Figure 3.5.

A model containing four bodies of varying shapes including a dipping body was constructed as a final model test for the potential field attribute techniques. The results of this test are shown in Figure 3.6. As before, the attribute results were compared to the enhanced analytic signal method of Hsu and others (1996). The results show that the three vertical-sided bodies are well-resolved spatially by the zero-degree contour of the tilt angle. The edges of the more deeply buried triangular body are not well-resolved by the other techniques, perhaps due to the depth of burial and its size. All of the methods display an asymmetry with respect to the left-dipping body, with the enhanced analytic signal technique providing the best overall location for the upper-most surface. The asymmetry is such that the steeper slopes are located on the updip side of the body in question (to the right in Figure 3.6). The location provided by the tilt angle is not only asymmetric, it is also shifted to the left by several kilometers. The shifting of gravity gradient peaks by the dip of a subsurface density contact was discussed by Grauch and Cordell (1987). In the case of a horizontal derivative, the shift was directly related to the angle of dip and the depth of burial. Model studies indicate that for the potential field attributes, the effect is most notable for bodies dipping shallower than 60°, but the shift in edge location is also related to the thickness of the dipping body, with thicker bodies having more pronounced shifts. The analytic signal and wavenumber methods also display some interference effects from the proximity of the two largest bodies, as their gravity fields overlap at the near points. The overlapping gravity anomalies tend to shift the location of the edges of both bodies at that location. Grauch and Cordell (1987) discussed this effect also, but as yet no studies have been

undertaken to study in detail the results of interference on any of the potential field attributes. The results from this more complex model indicate the necessity of using all the attributes and including the enhanced analytic signal in the proper location of anomaly sources.

The model studies indicate that the various potential field attribute techniques are accurate to differing degrees in their ability to locate the lateral distribution of potential field anomaly sources. The level of accuracy is determined by depth of burial, dip of the body edges, and the effects of interference between anomalies, with the accuracy deteriorating for greater depths of burial, shallower dips, and the proximity of the anomaly sources. The tilt angle and related wavenumber provided the best results overall, with the analytic signal technique performing best for bodies in the near surface. A complete interpretation of a complex situation would require the joint use of all of the attributes.

3.5 Real Data Example

The central Appalachians of western Virginia and eastern West Virginia consist of Paleozoic sedimentary rocks of the folded Valley and Ridge and Plateau provinces underlain by basement assumed to be of Grenville age (Wilson and Shumaker, 1992). Surface geologic mapping indicates a series of anticlines and synclines with a northeasterly strike that formed during the late Paleozoic Alleghanian orogeny (Wilson and Shumaker, 1992; Figure 3.7). There are few mapped faults at the surface, and the complexity and amplitude of the folding increases as the structural front is approached. The folding is a result of thin-skinned tectonic processes above a master decollement in the lower Cambrian Waynesboro Formation (e.g. Kulander and Dean, 1986; Wilson and Shumaker, 1992). Additional detachments in the middle Ordovician Martinsburg and Devonian shales are also interpreted to have played a major part in the formation structures within the Valley and Ridge and the broader structures of the Appalachian Plateau (Wilson and Shumaker, 1992). This portion of the central Appalachians of Virginia and West Virginia was chosen for study because of the existence of co-located reflection seismic profiles that have been reprocessed by the author and a colleague (see Lampshire et al., 1994).

Over 17,000 gravity stations provided by the Defense Mapping Agency (DMA) for the region of interest were taken from a CD-ROM published by the National Geophysical Data Center (Hittleman et al., 1994). Terrain corrected data from the National Geodetic Survey (NGS) was not used due to insufficient data coverage in the region. the error associated with using the DMA data was estimatied by computing differences between the data sets at the same stations. The differences were less than 0.2 mgal which is smaller than the maximum station error of ~0.5 mgal in either data set, therefore the DMA data set was used for its superior coverage.

The original data distribution for the DMA data set is shown in Figure 3.8. The DMA point data were gridded at an initial spacing of 4 km and missing grid values filled by linear interpolation. The final grid of 56x61 points was interpolated onto a 1x1 km grid for calculation of the potential field attributes.

The Bouguer gravity field in the region and the location of the seismic lines is shown in Figure 3.9. The gravity field is dominated by a large regional low attributed to the thickness of the crust in the region (Kulander and Dean, 1978). Removal of the regional gravity field was accomplished by the removal of a 3rd-order trend surface from the original data grid. The resulting residual gravity field is shown in Figure 3.10. The residual gravity anomaly map shows a local high near the Virginia-West Virginia border in the northern part of the study area ('X' in Figure 3.9); this is the region examined in detail using the attribute maps.

The results of the attribute analysis within the study area are shown in Figure 3.11. The analytic signal map (Figure 3.11a) shows a mixed character, most likely due to the narrow range of density values for the Silurian and Devonian strata in the near surface (Kulander and Dean, 1978). The tilt angle map shows a prominent, northeasterly trending high that extends from the northern edge of the map to just across the Virginia/West Virginia border to the southwest (Figure 3.11b). This anomaly is along the general strike of the Appalachian fold and thrust belt.

The wavenumber map (Figure 3.11c) was calculated using the three-point finite difference scheme of Cordell and Grauch (1985) after it was determined that the method of Gunn (1975; equation 9) was giving inconsistent results. A combination of noise, interference effects and a grid interval (1 km) that was too large for the steeper gradients in the tilt angle map to be resolved properly using the frequency domain method were probably responsible. The finite difference wavenumber results (Figure 3.11c) also show a northeasterly trending series of highs. The highlighted zone corresponds nicely to the steeper western flank of the northeast trending high on the tilt angle map.

The tilt angle and wavenumber maps are correlated with the seismic data at the location of the tilt angle anomaly. The data for lines WV1 and WV2 are shown in Figures 3.12 and 3.13, respectively. In addition to the seismic data, residual gravity and potential field attribute values projected onto the seismic line are shown. The data indicate that the tilt angle high is associated with a blind thrust sheet of the strata in the lower part of the section. Correlation of the seismic data with subsurface data provided by deep wells in the region indicate that the thrust sheet is composed of high density Cambrian-Ordovician carbonates (Wilson and Shumaker, 1992). The relatively stiff carbonate rocks were transported over a ramp to the northwest for a distance of up to 20 km on a detachment within the Ordovician Martinsburg shale. This large blind thrust is beneath the complex folding associated with the southern extension of the Nittany Anticlinorium (Wilson and Shumaker, 1992; Figure 3.7). The tilt angle high is interpreted as the expression in the gravity field of this large-scale thrust structure. The southern termination of the tilt angle anomaly is interpreted to be the end of this large thrust sheet, with with a change in deformation style to the southwest in Virginia or a lateral ramp at that location. The wavenumber map also shows a low saddle or discontinuity ('S' in Figure 3.11c) near the southern termination of the thrust sheet as interpreted from the tilt angle map. This would also tend to support the existence of a major change in the subsurface along strike.

The possibility of a local basement uplift was interpreted by Kulander and Dean (1978) from gravity data and Lampshire and others (1994) from seismic reflection line WV2. Supporting

the idea that the possible basement structure plunges to the northeast is the reduction in the amount of apparent velocity pull-up at the detachment level to the north (compare Figures 3.12 and 3.13). This can not be explained by a thinner thrust sheet to the north, as the measured time thickness of the thrust sheet is similar on both lines (~750 ms). Quantification of this result awaits combined gravity and seismic modeling.

3.6 Conclusions

The analytic signal and potential field tilt angle have been demonstrated to be mathematically analogous to their counterparts in seismic exploration, reflection strength and instantaneous phase. By extension of this analogy, the gradient of the tilt angle, herein named the *potential field wavenumber*, was defined. The wavenumber is a local measure (Bracewell, 1965) of the spatial change in the tilt angle and it is mathematically analogous to the instantaneous frequency.

Potential field attribute analysis of model data has shown the method to be a useful tool in the interpretation of gravity data. A combination of different attribute maps can be used to not only define the distribution of anomalies, but also the relative depth. The analytic signal and its cousin, the enhanced analytic signal, were shown to react best to steeply dipping bodies in the near surface. The potential field tilt angle was shown to give edge discrimination and to perform well for bodies up to three times deeper than the older analytic signal technique. The wavenumber was also shown to locate the body edges as well, and had the additional property of being diagnostic of relative depth.

Application of the method to gravity data from the central Appalachian Valley and Ridge confirmed the location of a large-scale blind thrust in the subsurface. The utility of the attribute maps, in particular the tilt angle and wavenumber maps, to distinguish lateral changes in density in the subsurface was also confirmed. The combined interpretation of the attribute maps with the seismic reflection data revealed the southern termination of a major thrust sheet beneath the Nittany Anticlinorium that may be associated with a change in deformation style to the southwest in Virginia or a lateral ramp. Major discontinuities in the subsurface located through the use of potential field attribute maps could aid in the location of oil and gas plays around the world.

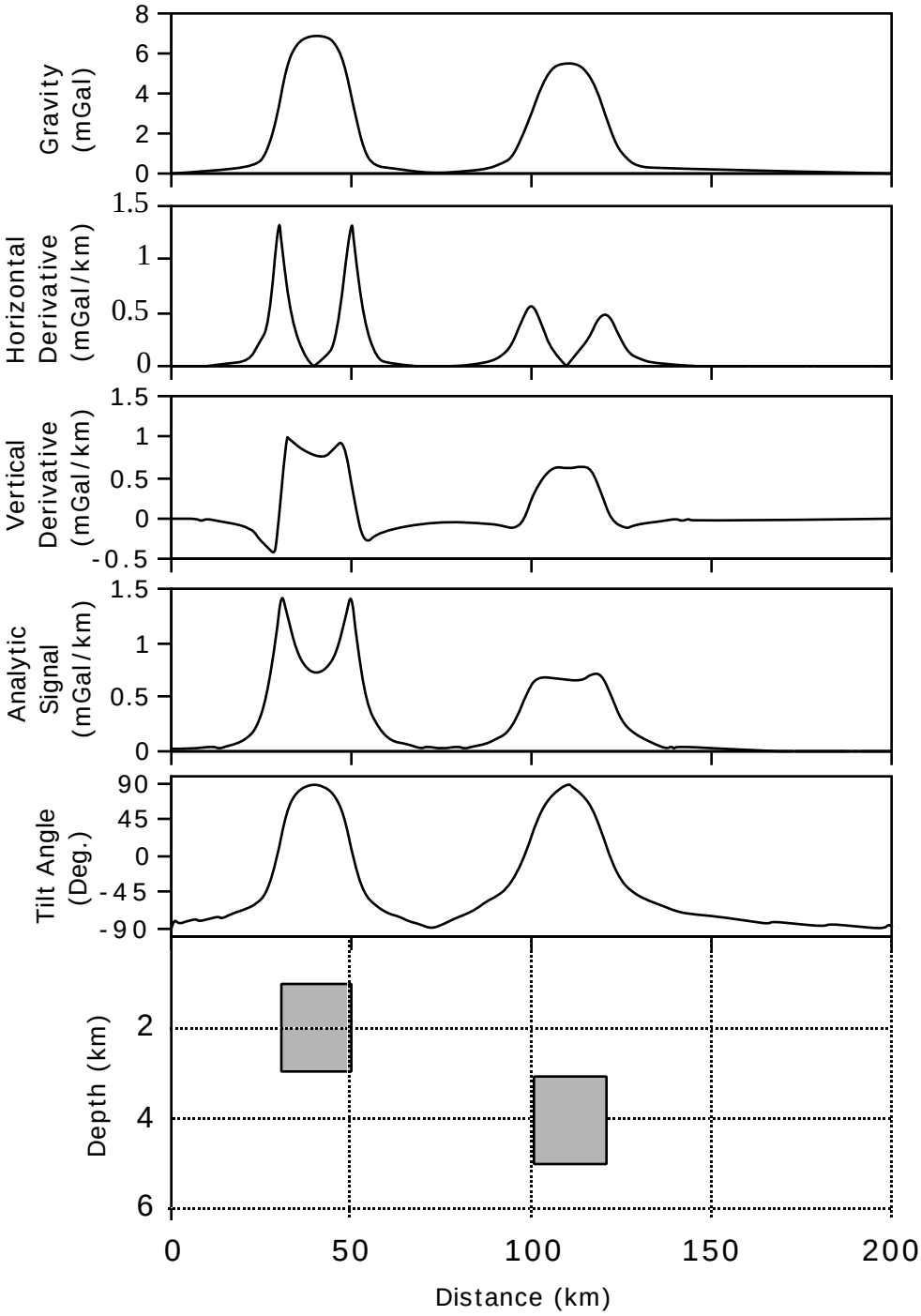

Figure 3.1: Gravity anomaly and derivatives for two bodies buried at 1 and 3 km depth with a +0.1 g/cm^3 density contrast. The calculated tilt angle shows that the *ratio* of the horizontal to vertical derivatives over the two bodies is insensitive to burial depth.

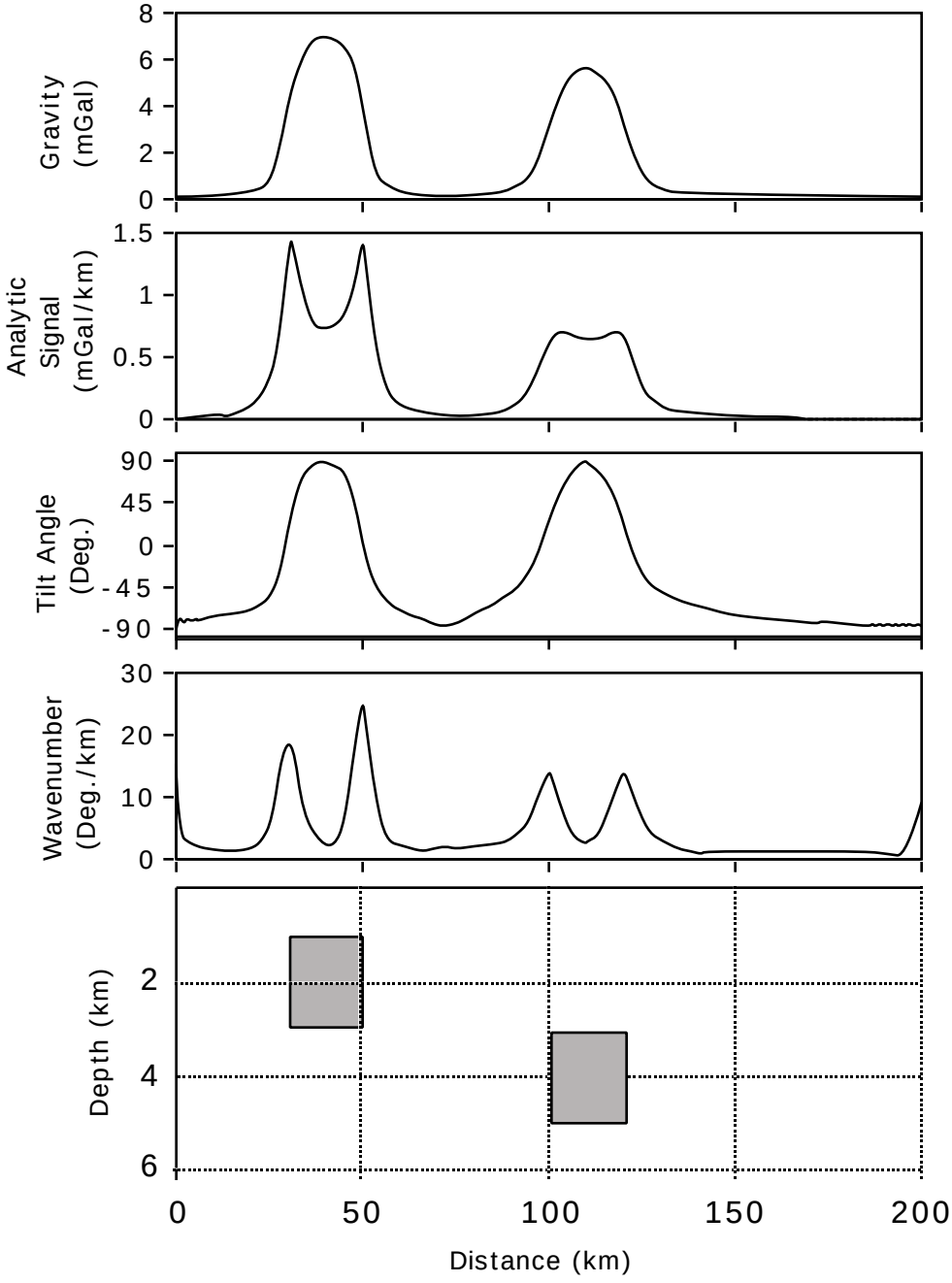

Figure 3.2: Gravity anomaly and potential field attributes for two bodies buried at 1 and 3 km depth with a +0.1 g/cm^3 density contrast. The calculated wavenumber has sharper peaks over the edges of the bodies than the analytic signal.

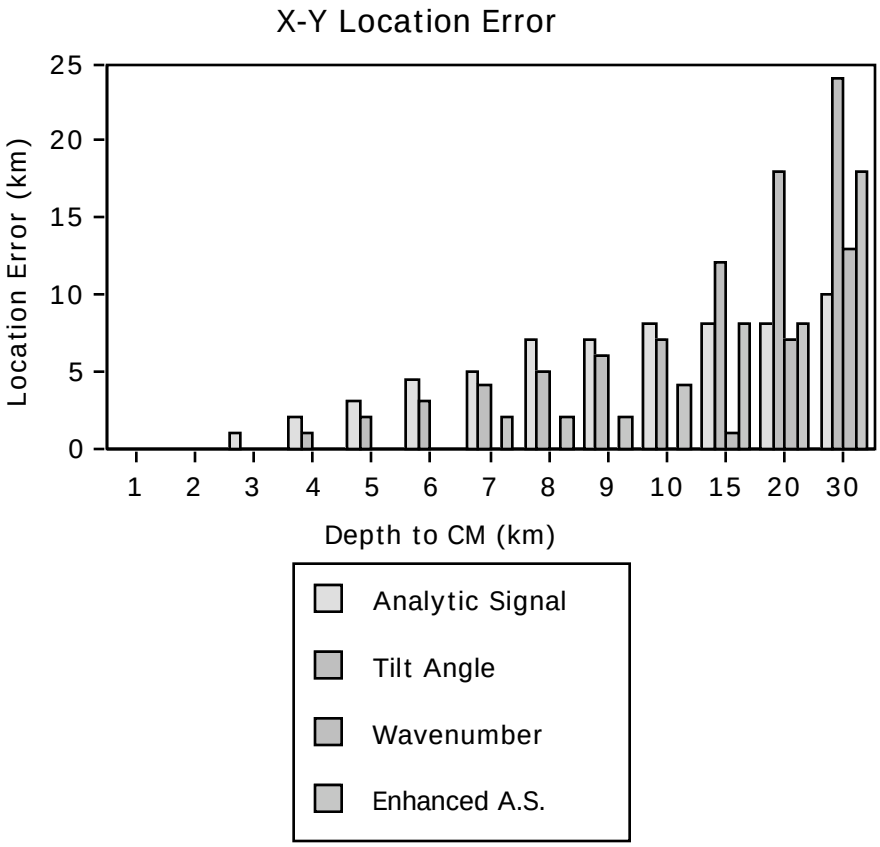

Figure 3.3: Bar graph showing the error above grid spacing in body edge location with respect to the depth of the center of mass of the body.

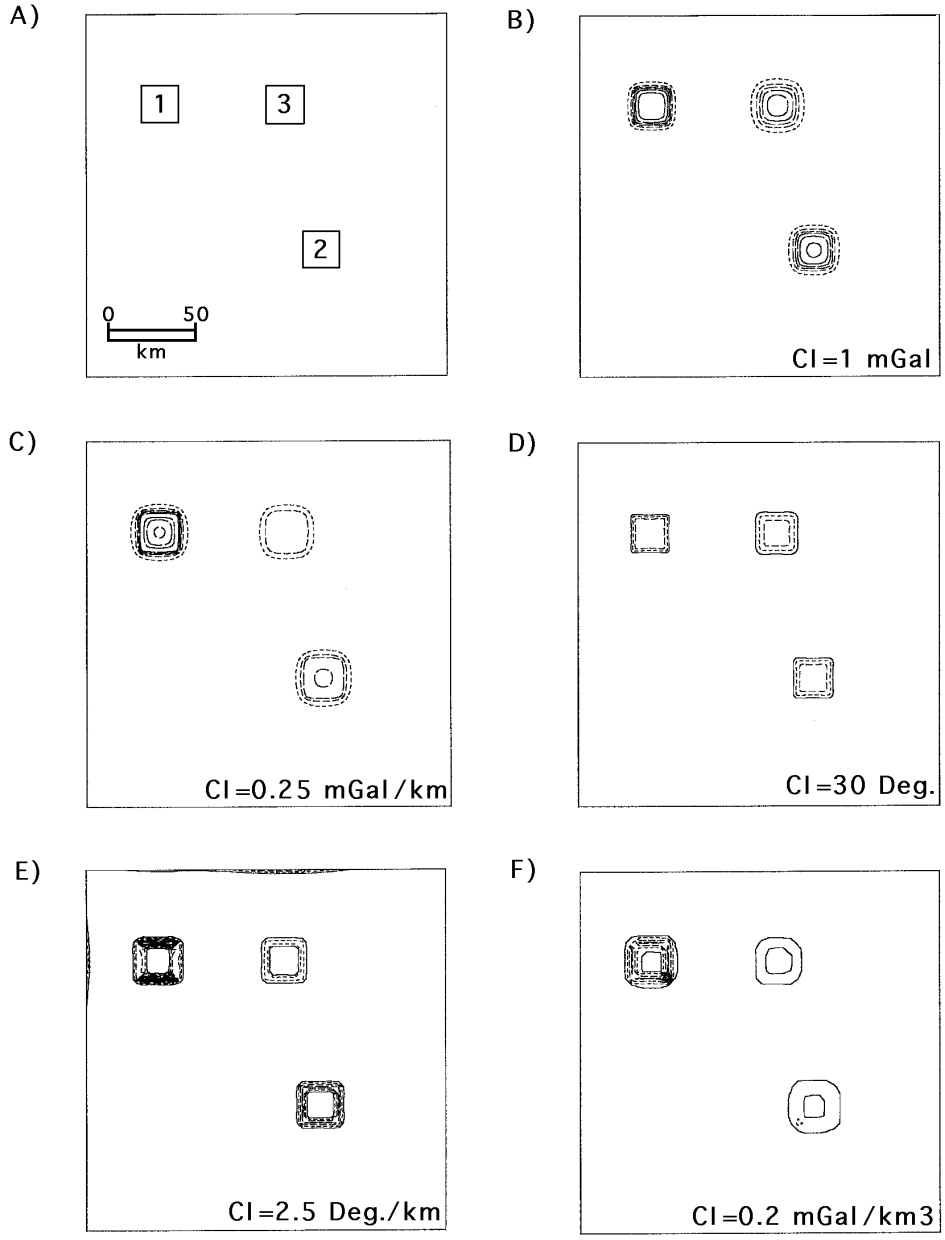

Figure 3.4: Attribute analysis results for three bodies with the same size, shape, and density contrast at different depths of burial. (A) Spatial distribution of the bodies; the numbers indicate the depth to the top surface of each body. (B) Calculated gravitational field. (C) Analytic signal, (D) tilt angle, (E) wavenumber, and (F) enhanced analytic signal results. Contour interval (CI) indicated on each map.

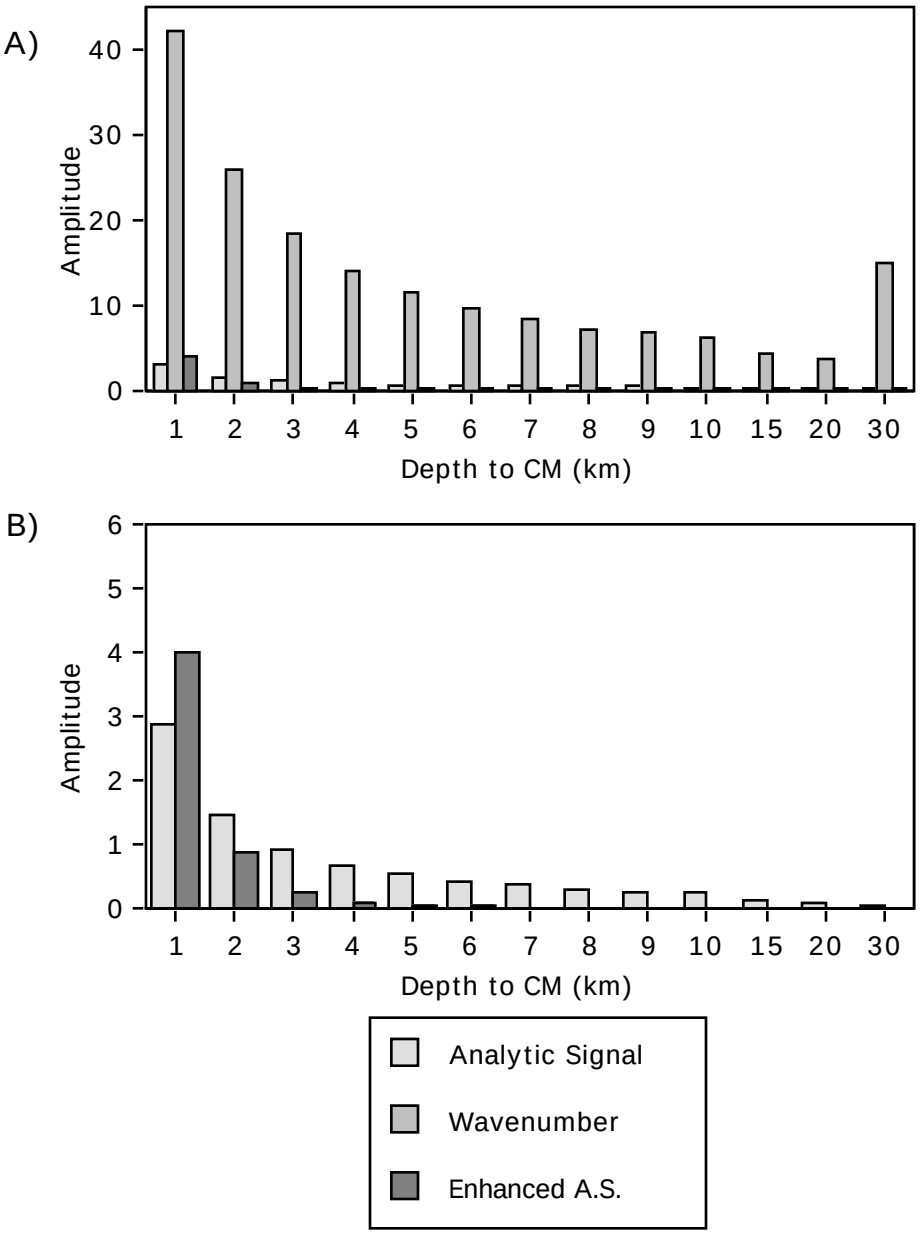

Figure 3.5: Absolute signal strength vs. depth to center of mass at the edges of a body for the analytic signal, enhanced analytic signal and wavenumber techniques. (A) Overall signal strength. Note that the wavenumber method provides much larger absolute values than the other techniques. (B) Plot of signal strength for the analytic signal and enhanced analytic signal. Note that the enhanced analytic signal is larger than the analytic signal but decays more rapidly with increasing depth.

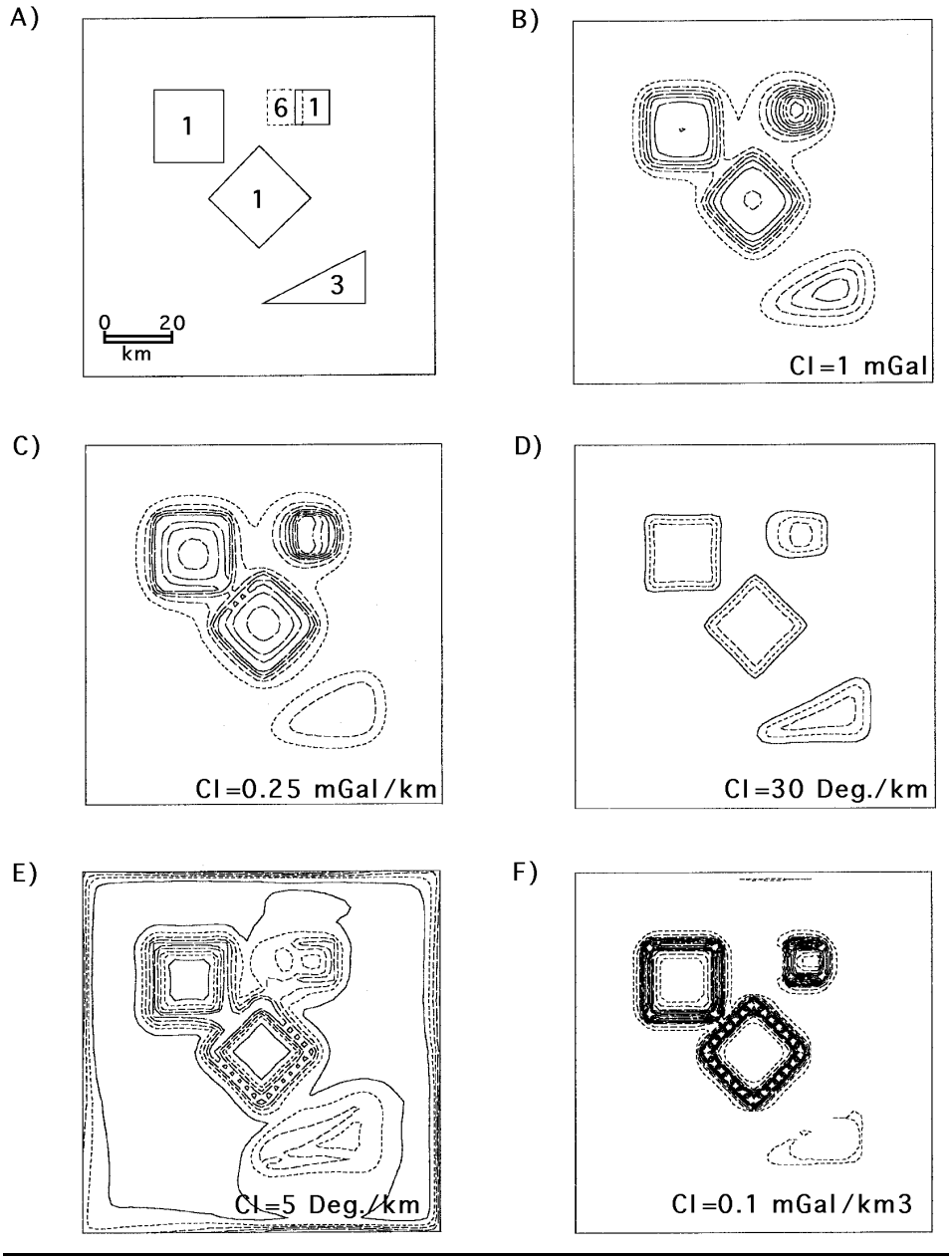

Figure 3.6: Attribute analysis results for four bodies with the same density contrast, but with different sizes and shapes buried at different depths. (A) Spatial distribution of the bodies; the numbers indicate the depth to the top surface of each body. In the case of the dipping body, the two numbers ("1" and "6") indicate the depths to the top and bottom of the body. The dip is 30°. (B) Calculated gravitational field. (C) Analytic signal, (D) tilt angle, (E) wavenumber, and (F) enhanced analytic signal results. Contour interval (CI) indicated on each map.

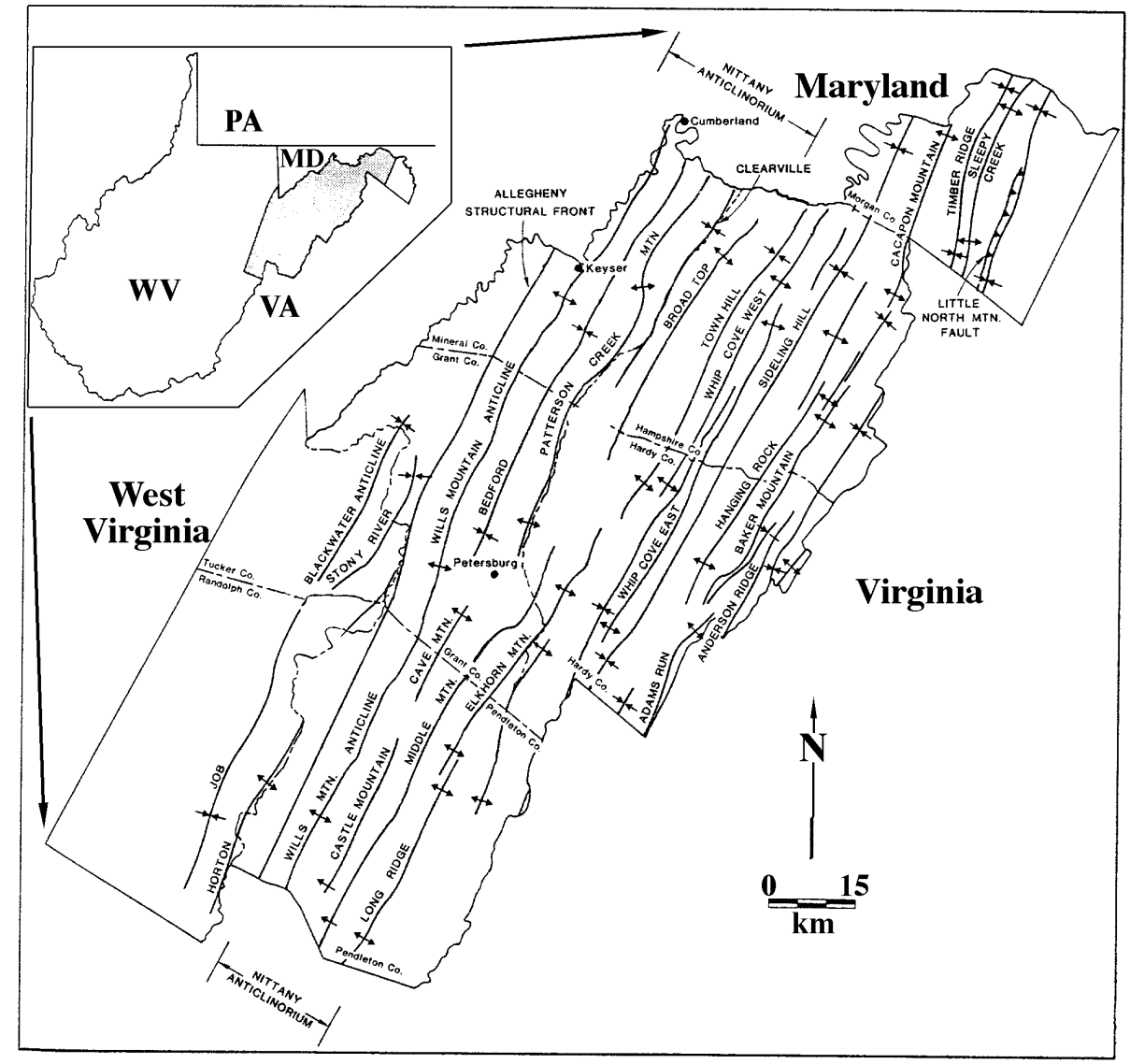

Figure 3.7: Generalized geologic map of the structural front in eastern West Virginia (after Wilson, 1989).

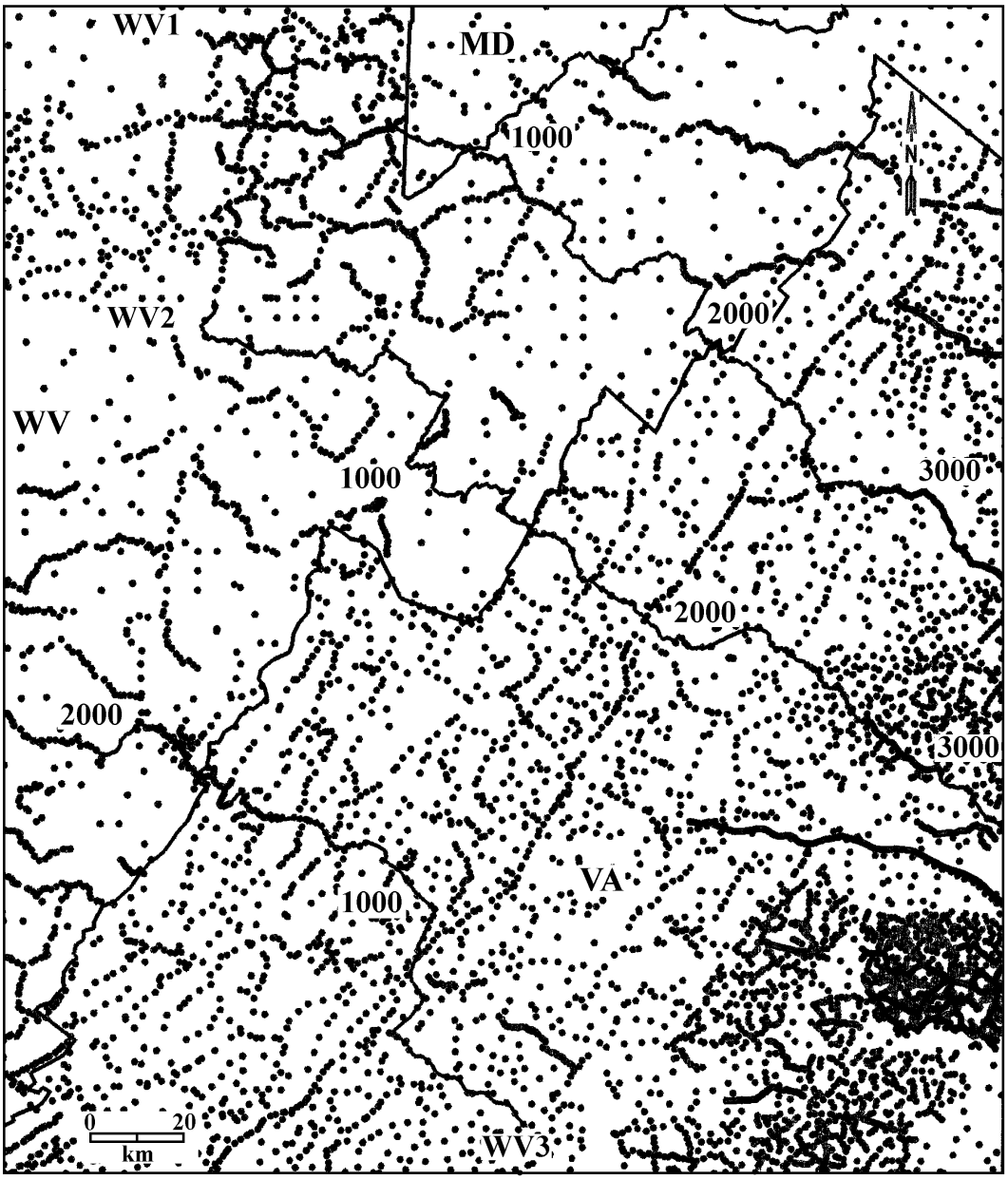

Figure 3.8: Original distribution of gravity stations within the study area before gridding. The gravity station data are from the Defense Mapping Agency (Hittleman et al., 1994). Contour interval 5 mgal. Scale is 1:100000. Projection: Virginia North State Plane.

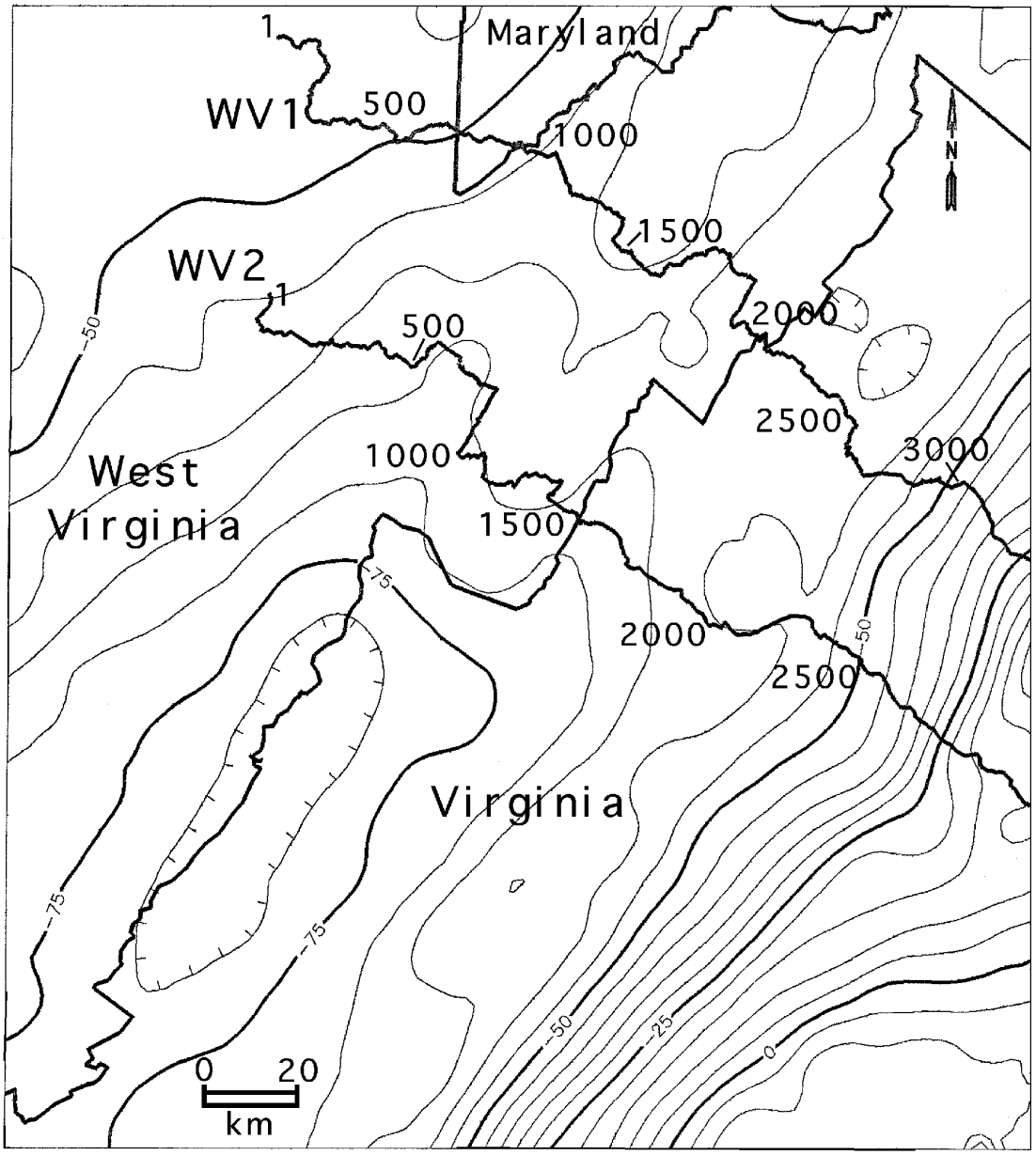

Figure 3.9: Bouguer gravity anomaly map of the study region. The gravity station data are from the Defense Mapping Agency (Hittleman et al., 1994). Contour interval 5 mgal. Scale is 1:100000. Projection: Virginia North State Plane.

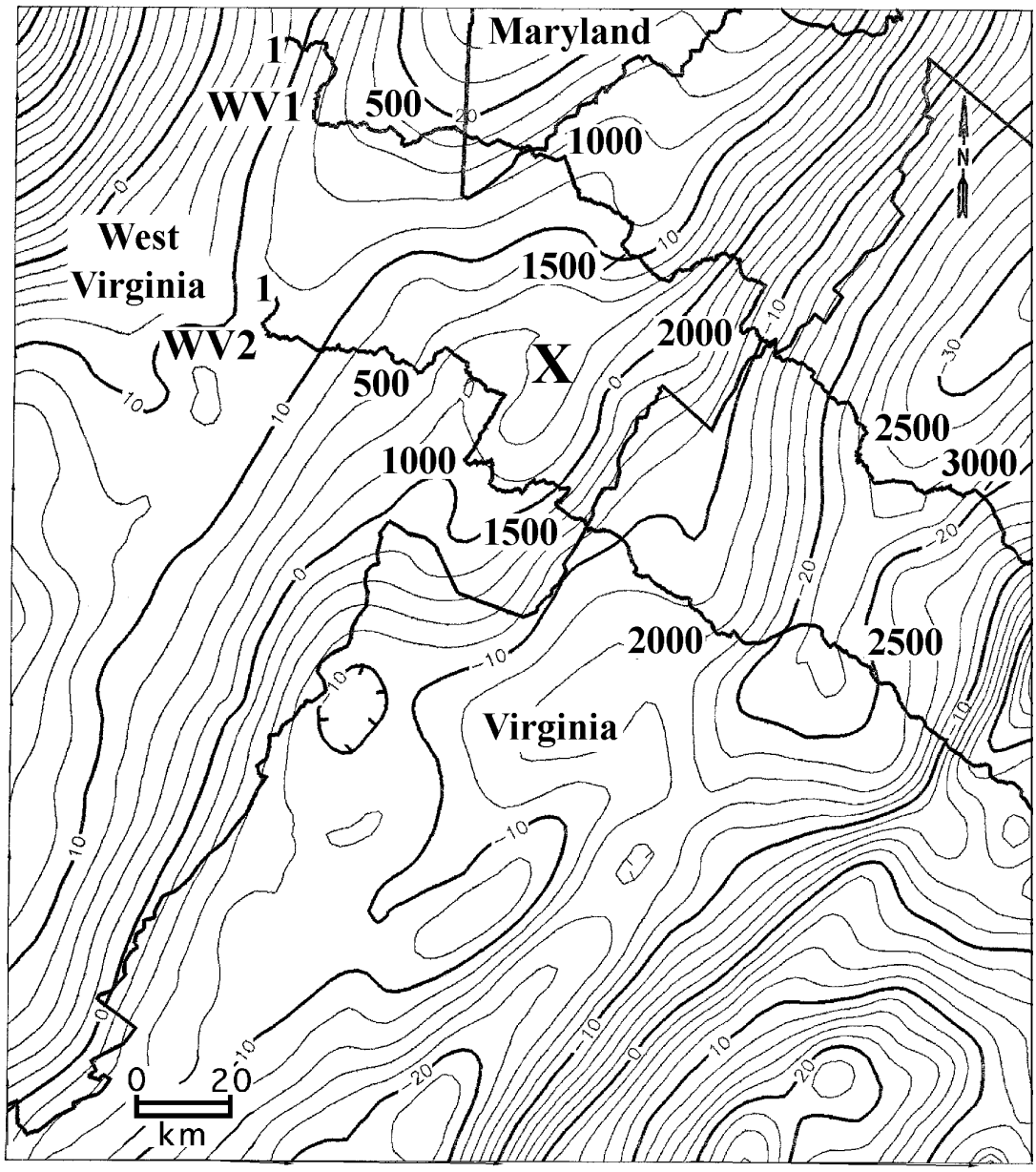

Figure 3.10: Residual gravity anomaly map of the study region generated by the removal of a 3rd-order trend surface. 'X' marks the center of a residual high studied in detail using the potential field attribute maps. The gravity station data are from the Defense Mapping Agency (Hittleman et al., 1994). Contour interval 2 mgal. Scale is 1:100000. Projection: Virginia North State Plane.

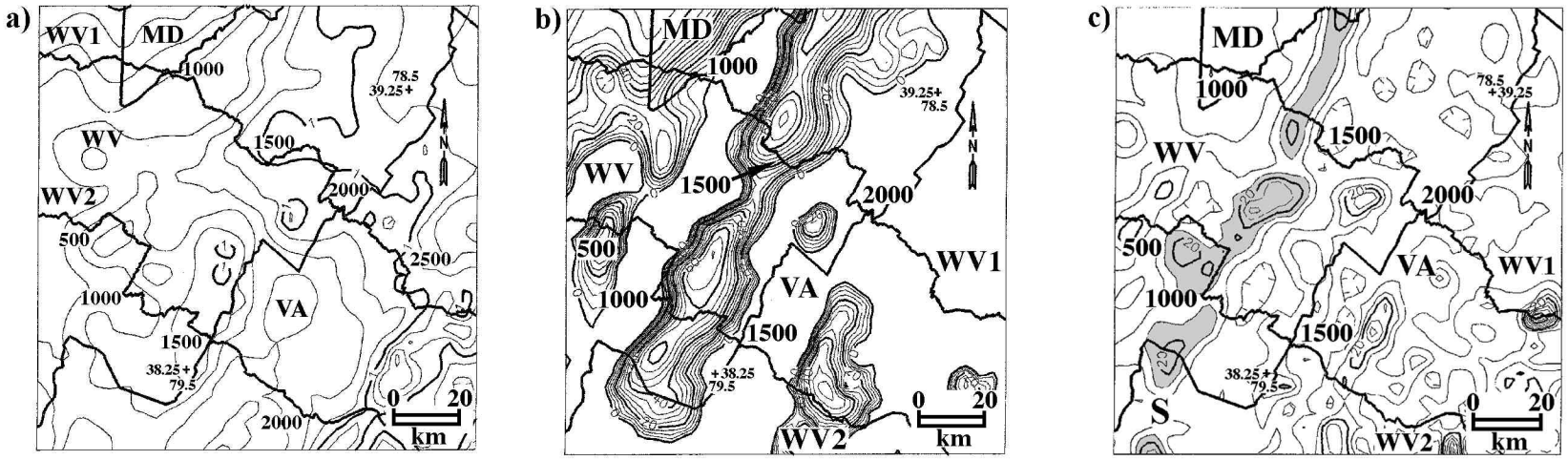

Figure 3.11: Results of attribute analysis near the structural front. (a) Analytic signal (Contour Interval = 0.25 mgal/km), (b) tilt angle (Contour Interval = 5 degrees), and (c) wavenumber (Contour Interval = 5 deg./km). 'S' indicates a saddle point discussed in the text.

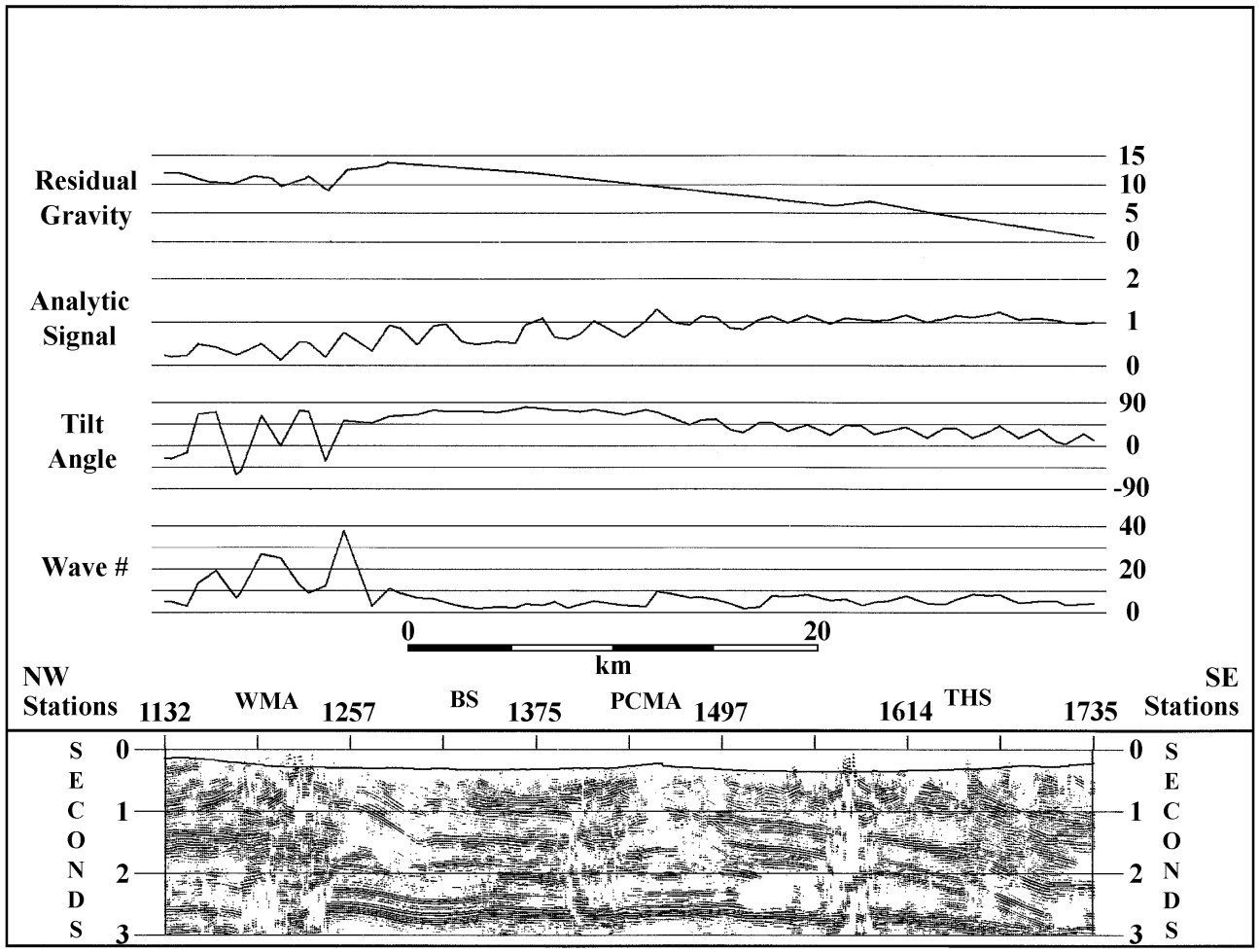

Figure 3.12: Seismic line WV1. Projected residual gravity values and potential field attributes are plotted above the data set. Note the ramp from the basement level decollement on the right side of the line (near station 1614) and the steeper ramp near the structural front (near station 1257). WMA = Wills Mountain Anticline; BS = Bedford Syncline; PCMA = Patterson Creek Mountain Anticline; THS = Town Hill Syncline. Seismic data plotted at 1:1 for 6 km/s.

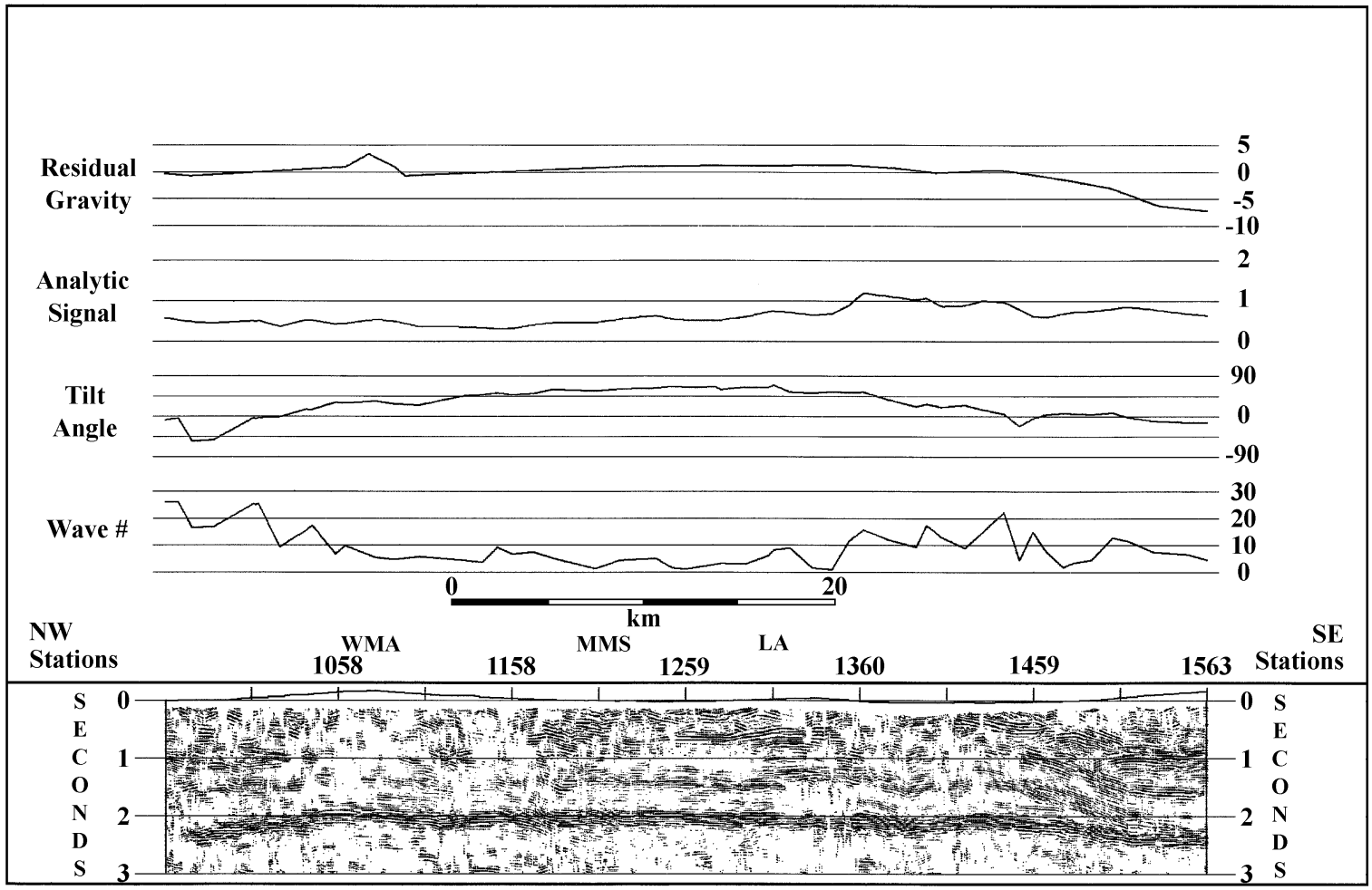

Figure 3.13: Seismic line WV2. Projected residual gravity values and potential field attributes are plotted above the data set. Note the ramp from the basement level decollement on the right side below station 1459. WMA = Wills Mountain Anticline; MMS = Middle Mountain Syncline; LA = Long Anticline. Seismic data plotted at 1:1 for 6 km/s.

Chapter 4: The Architecture of the Appalachian Orogen: Insights from Seismic Reflection Data

Abstract

Reprocessing of seismic reflection data in the southeastern U.S. has revealed a significant contrast in mid- and lower crustal reflectivity from east to west. Data to the east of the Blue Ridge geologic province show a highly reflective crust extending from the near-surface to the Moho. In this region, reflector geometries are complex and suggestive of crustal-scale detachments. Reflection seismic data to the west of the Blue Ridge are characterized by reflector geometries related to deformation above a master decollement, leading to classic 'thin-skinned' structures in the overlying allochthon, and few, if any, apparent structures in the underlying basement.

Understanding the contrast in seismic reflectivity requires an understanding of the timing and effects of the various deformational episodes that have occurred in the Appalachians since the early Paleozoic. Geologic evidence indicates at least three orogenic episodes: the Taconic, the Acadian and the Alleghanian, with the latter event being transpressional. The transpression produced both dextral offset along major faults in the Piedmont and thin-skinned deformation of Paleozoic shelf strata into the Valley and Ridge to the west of the Blue Ridge. The opening of the Atlantic Ocean during the Mesozoic produced the numerous exposed and buried Triassic basins along the east coast of North America, and the mafic dikes and associated intrusions that penetrate the orogen as far west as the Valley and Ridge. It has been suggested that Mesozoic extension was at least in part aided by reactivation of pre-existing compressional and strike-slip structures.

The seismic reflectivity observed in the mid- to lower crust beneath the Piedmont in the southeastern United States is most likely a result of its participation in multiple episodes of deformation from the early Paleozoic through the middle Mesozoic. The preexistence of favorably oriented structures is interpreted to have played a critical role in the distribution of seismic reflector geometries and the observed reflectivity.

4.1 Introduction

Studies of mountain belts have been enhanced over the past 20 years by the utilization of seismic reflection data. The data obtained have provided a means of studying reflection properties and reflector geometries, and initiating debate on the origin and preservation of crustal reflectivity and the tectonic history of these regions. In the southern and central Appalachians, regional reflection data in Georgia (Cook et al., 1979, 1981; Peterson et al., 1984; Nelson et al., 1985), South Carolina (Behrendt, 1986; Williams et al., 1987; Hubbard et al., 1991; Domoracki, 1995) and Virginia (Harris et al., 1982; Pratt et al., 1988; Lampshire et al., 1994) in conjunction with detailed geologic mapping have aided in the understanding of the tectonic processes that formed the complex geology that we observe today.

This paper looks at two reflection seismic transects in the central and southern Appalachians. The transects consist of a combination of COCORP Georgia lines l, 5, and 8 in the southern Appalachians and of reprocessed industry line WV2 and USGS I-64 in the central Appalachians (see Figure 4.1 for approximate locations). Both of these transects are approximately perpendicular to regional strike as defined by exposed structures in the Valley and Ridge, Blue Ridge, and Piedmont geologic provinces, and therefore should approximate dip sections. An analysis of the sections reveals a dichotomy of reflectivity between the eastern and western halves of the transects, with the eastern half being reflective throughout the crust, and the western half having almost all of its reflectivity restricted to the upper 3-4 seconds of the data sets. This change in reflectivity from west to east and its possible origin are discussed below, and the importance of properly oriented mechanically weak zones within the crust in the origin of reflectivity will be emphasized.

4.2 General Geology

The southern and central Appalachians can be divided into five geologic provinces (Figure 4.1). From west to east these are the Appalachian Plateau, Valley and Ridge, Blue Ridge, Piedmont (including the Inner Piedmont and the Charlotte, Kiokee, Pine Mountain, Kings Mountain and Carolina Slate Belts) and the Atlantic Coastal Plain.

The Appalachian Plateau and Valley and Ridge Provinces consist of carbonate shelf strata and foreland basin clastics deposited on Precambrian basement (Colton, 1970). Structurally, the Plateau is characterized by horizontal to relatively gently folded strata whereas the Valley and Ridge consists of a series of anticlinal and synclinal structures interspersed with thrust faults. The southern Appalachian Valley and Ridge is characterized by having more exposed major thrust faults than the central Appalachian Valley and Ridge, which exhibits more folding above zones of blind thrusting. On the basis of geologic mapping, reflection seismic data and well information, the Valley and Ridge province is interpreted to be the result of thin-skinned deformation above a master decollement in the lower Cambrian Rome/Waynesboro formations (Gwinn, 1964; Rodgers, 1970; Jacobeen and Kanes, 1974, 1975; Harris and Milici, 1977; Perry,

1978; Clark et al., 1978; Harris and Bayer 1979; Kulander and Dean 1986; Evans, 1989; Wilson and Shumaker 1992; Lampshire et al., 1994).

The Blue Ridge and Piedmont Provinces consist mostly of crystalline metamorphic and igneous rocks varying in age from Grenvillian (~1.1 billion years) in the Blue Ridge through the late Paleozoic in the Piedmont (Glover, 1992). A regional summary of metamorphic ages in the Blue Ridge and Piedmont is given by Glover and others (1983). The Piedmont province is structurally complex, containing both folds and a number of exposed faults of large strike length which were ductile during the early stages of their evolution. In addition to crystalline rocks, the Piedmont contains a number of exposed Mesozoic basins (Figure 4.2) in the southern and central Appalachians containing 700 to ~9000 m of fluvial and laucustrine sediments and redbeds with intercalated basalt flows, dikes and sills (Olsen et al., 1982).

The sediments of the Atlantic Coastal Plain (ACP) consist of a variety of marine and fluvial/deltaic sediments uncomformably onlapping the rocks of the Piedmont province at its western edge and extending to the Atlantic Ocean on the east (Olsson et al., 1988; Gohn, 1988). The sub-coastal plain basement displays a variety of lithologies ranging from phyllite and biotitic schist, metavolvanics, mafics, possible ultramafics, and Mesozoic basin sediments (Hubbard et al., 1978; Chowns and Williams, 1983; Daniels and Leo, 1985; Hanson and Edwards, 1986; Wilkes et al., 1989). The ACP sediments are part of the passive margin sequence depositied since rifting during the Mesozoic (Grow and Sheridan, 1988).

The juxtaposition of such differing geologic regions suggests a long and varied geologic history. Indeed, at least three separate orogenic episodes during the Paleozoic are recognized in the central and southern Appalachians on the basis of the sedimentary, metamorphic, and structural evidence: the Taconic (~440−480 Ma), the Acadian (~360−385 Ma) and the Alleghanian (~250−324 Ma). These orogenies were preceded and followed by rifting episodes, the first of which formed the Iapetus Ocean during the latest Precambrian, and the latter the present Atlantic Ocean basin during the Mesozoic (Glover, 1992). The combined effect of all of these tectonic episodes influence the interpretation of seismic reflectivity in the southern and central Appalachians that follows.

4.3 Reactivation of Faults in Eastern North America

There are numerous examples in the literature detailing geologic evidence for late Paleozoic dextral transpressive reactivation of faults in the central and southern Appalachian Piedmont (see Figure 4.2 and Bobyarchick and Glover, 1979; Bobyarchick, 1981; Gates et al., 1988; Valentino et al., 1994; Valentino et al., 1995; and references therein). The near pervasive evidence for reactivation leads to a model of transpressional deformation during the Alleghanian orogeny to explain the preponderance of strike-slip faults. These faults have been interpreted as moderately dipping crustal shear zones that penetrate to the Moho (Gates et al., 1988; Glover, 1992; Gates, 1997). Seismic data have been interpreted to include the formation of a transpressive dome involving the Eastern Piedmont fault system (Gates et al., 1988). Many of the faults in the

Eastern Piedmont fault system show an early phase of thrust motion during the Taconic orogeny, and were reactivated later as strike-slip faults (Glover, 1992). Ferrill and Thomas (1988) have proposed that the Acadian orogeny in the southern and central Appalachians was a transpressive event on the basis of diachronous, north-to-south deposition of the Catskill delta. Glover (1992) proposed that the Acadian and Alleghanian orogenies were in actuality one protracted transpressive event with periods of pure dextral transform motion preceded and followed by active dextral transpression.

Geologic evidence for the reactivation of older faults during the Mesozoic to form border and transfer faults for the formation of Triassic half-grabens also exists (Glover et al., 1980; Ratcliffe and Burton, 1985; Ratcliffe et al., 1986; Swanson, 1986; Manspeizer and Cousminer, 1988; Costain and Çoruh, 1989; Manspeizer et al., 1989; Olsen and Schlische, 1990; Withjack et al., 1995). Inherited structures from the Paleozoic were used to initiate rifting and basin formation, but trends of late Triassic and Jurassic mafic dikes in the southern and central Appalachians are not aligned with the preexisting structures or the basins, because they in general trend northwest in the southern, north-south in the central, and northeast in the northern Appalachians (deBoer et al., 1988). A younger set of north-south oriented dikes exists in the southern Appalachians along with an older northwest trending set (Ragland et al., 1983). Detailed studies of dike emplacement show that the dikes were injected episodically from the late Triassic through the middle Jurassic, with the largest volumes of mafic material emplaced in the rift zones during the early Jurassic, and in oblique-trending dikes near the end of extensional shearing in the mid-Jurassic (deBoer et al., 1988). deBoer and others (1988) discuss the tectonic implications of the episodic emplacement of the dikes and contend that the regional arching and the origin of the Appalachian (Piedmont) Gravity High are both a result of mafic magmatism during the Mesozoic. The injection of mafic material along preexisting zones of weakness and into planar and listric basin-bounding faults led to ponding and injection of the sills along the tilted bedding surfaces (de Boer et al., 1988; Bell et al., 1988). This could in part explain the enhanced reflectivity seen within some Mesozoic basins (Schorr, 1986; Costain and Çoruh, 1989; Domoracki, 1995).

Domoracki (1995) performed two-dimensional seismic and gravity modeling of the Dunbarton Triassic Basin in South Carolina and demonstrated that the surviving Triassic strata beneath the Atlantic Coastal Plain sediments are 5-6 km in thickness and are bounded by a steeply dipping border fault, the Pen Branch Fault. He also stated that the velocity increases rapidly with depth to velocities approaching that of the crystalline basement, making it difficult to image the base of this basin. Similar problems could exist for other Triassic basins (Costain and Çoruh, 1989). Domoracki (1995) could not conclusively demonstrate a relationship between this fault and other structures at depth. Peterson and others (1984) state that the Riddleville Basin to the southwest in Georgia and its border fault, the MacGruder Fault, were the result of reactivation of what was interpreted as the Augusta fault at depth. The Augusta fault has been variously interpreted as a thrust (Cook et al., 1979; 1981) or a normal fault reactivated as a dextral strike-slip fault during the late Paleozoic (Sacks and Secor, 1990; Maher et al., 1994).

Post-Jurassic faulting is fairly widespread in the sediments of the Atlantic Coastal Plain, and most faults that have been documented trend in the direction of preexisting basement structures (Mixon and Newell, 1977; Behrendt et al., 1981; Prowell, 1983, 1988; Reinhardt et al., 1984; Domoracki, 1995). Reverse faults are most common, but normal and strike-slip faults have also been documented. Faulting has been occurring at relatively steady rates since the late Cretaceous (Prowell, 1988). One of the best studied examples of the reactivation of a pre-Cretaceous fault is at the Savannah River Site near Aiken, South Carolina (see Figure 4.1). Domoracki (1995) reprocessed 270 km of seismic data from the site; his results clearly show the reactivation of the Pen Branch Fault, the Mesozoic border fault of the Dunbarton Triassic Basin, as a reverse fault at the top of basement deforming the Atlantic Coastal Plain strata above it (Figure 4.3).

From the above it would seem obvious that preexisting structures have strongly influenced the geologic history of the central and southern Appalachians. Thomas (1991, 1993) suggested that the pre-collisional Iapetan passive margin may have been the major controlling factor influencing the formation of structures along the entire Appalachian-Ouachita mountain belt. Gates (1997) has petrologic and structural evidence for reactivation of the Brookneal fault zone in the southern Virginia Piedmont during the Paleozoic and Mesozoic as both a fault zone and a conduit for the intrusion of felsic plutons during the Alleghanian. The Brookneal zone may be a part of the Eastern Piedmont Fault System first identified by Hatcher and others (1977) and postulated by Bobyarchick (1981) to be the locus of strike-slip faulting during the Alleghanian. In any event, preexisting faults must have maintained a preferred orientation to stress fields since at least the Taconic orogeny such that reactivation became the dominant way to produce new deformation within the Appalachian Piedmont and now within the onlapping Atlantic Coastal Plain sediments.

4.4 Seismic Reflectivity

Seismic reflectivity in the continental crust has multiple origins. In the brittle upper crust, reflectivity can usually be attributed to contrasts in physical properties (velocity and/or density) due to variations in lithology and porosity, unconformities, or juxtaposition of these by tectonic movements (faulting, folding, etc.). Considerable evidence exists for reflections originating in ductile shear zones of variable thickness with enhanced reflectivity due to seismic anisotropy or thin-bed effects (Jones and Nur, 1984; Fountain et al., 1984; Hurich et al., 1985; Christensen and Szymansky, 1988; Law and Snyder, 1997). These shear zones are interpreted to retain their reflectivity for long periods of time. Ductile shear zones are commonly interpreted on seismic reflection data from the central and southern Appalachians (e.g. Cook et al., 1979; Pratt et al., 1988). Several different ideas about the origin of deep crustal reflectivity have been discussed in the literature: 1) intrusive or magmatic layering (Meissner and Wever, 1986; McCarthy and Thompson, 1988; Holbrook et al., 1991); 2) metamorphic layering (Brown et al., 1986); 3) fluids (Fyfe, 1986; Meissner and Kusznir, 1987; Brown, 1987); and 4) tectonic layering

associated with subhorizontal shear zones (Meissner and Kusznir, 1987; DEKORP Research Group, 1990; Reston, 1990). These different explanations have all been associated with elevated heat flow in the lower crust and are often associated with extension (Klemperer, 1987; Wever et al., 1987; Meissner and Kusznir, 1987; Goodwin and Thompson, 1988). The age of the Moho in the southern and central Appalachians is also a subject of debate, with some preferring a post-collisional origin (Brown, 1987; Glover et al., 1997), and others place its origin during or after extension (Pratt et al., 1987; McBride and Nelson, 1991).

Previous studies of the overall nature of seismic reflectivity in the Appalachians have concentrated on the geometric aspects of seismic reflectivity (e.g. Allmendinger et al., 1987; Quinlan et al., 1993). Most interpretations of seismic data from the central and southern Appalachians have emphasized the compressive or transpressive nature of the Paleozoic orogenies (e.g. Cook et al., 1979, 1981; Pratt et al., 1988; Gates et al., 1988; McBride and Nelson, 1991). Offshore data from most of the North Atlantic region have been interpreted as an expression of extensional basin formation and post-extensional sedimentation due to thermal subsidence during and after Mesozoic rifting, although some preexisting structures have been implicated (e.g. Hutchinson et al., 1988; Keen et al., 1991; Sheridan et al., 1993). Heck (1989) suggested that events recorded in the COCORP southern Appalachian transect were more related to Mesozoic rifting than to the prior compressional episodes.

The reflectivity seen on seismic data is difficult to correlate and quantify between seismic lines. It depends on a large number of factors, including the source, recording parameters, processing, line orientation, surface and subsurface geologic factors, etc. (Hatcher, 1986). The reflection signatures from two lines in the same area are often different using identical recording and processing parameters (Figure 4.4). However, when similar features are seen on similarly oriented transects hundreds of kilometers apart, comparisons can be made if differences in recording and processing parameters and local geology are taken into account.

One way of looking at reflection seismic data is to produce sketches ("line drawings") of features that are judged to be significant by the interpreter. The problem with this approach is that it is *subjective*, i.e. the prejudices of the interpreter can strongly influence the final product. We prefer to apply a poststack process to the seismic data called Automatic Line Drawing (ALD). The ALD technique is a more objective process that produces unconventional line drawings in which *the seismic waveform and relative amplitude information are preserved*. The processing is based upon the Fresnel zone concept that acknowledges that the reflections from a subsurface reflecting "point" must be on several traces on a seismic section in the space-time domain. The ALD process converts the seismic amplitudes into two-dimensional coherency estimates using a moving window in which a scanning procedure searches for the angular direction with the highest correlation. The results are then subjected to an exponential amplitude adjustment that forces the background noise outside of the dynamic range of the plotter. The result can be considered as a section *of relative seismic reflectivity*. The ALD process is especially useful for crustal seismic data because of the larger size of the Fresnel zone at depth. Excellent results have been obtained from reprocessed seismic reflection data using the ALD technique (e.g.

Çoruh et al., 1987; Çoruh et al., 1988; Hubbard et al., 1991; Lampshire et al., 1994). Similar methods are also used to enhance noisy seismic record sections (e.g. Kong et al., 1985). Because the ALD technique gives sections of relative seismic reflectivity, comparisons between sections can more easily be made and the *reader* can judge for him- or herself which reflections are more important. In addition, it should be stressed that *anything that appears on the ALD is also in the data*. An ALD is just a different approach to displaying seismic data for ease of interpretation and reproduction. All of the following seismic data panels shown in this paper were generated using the ALD process.

Two transects have been generated for this paper, one across the southern Appalachians, and a second across the central Appalachians. The southern Appalachian transect (Figure 4.5) is a combination of COCORP Georgia seismic lines 1, 5 and 8 and extends from the middle of the Blue Ridge geologic province out onto the Atlantic Coastal Plain. The central Appalachian transect (Figures 4.6 and 4.7) consists of two separate lines reprocessed at Virginia Tech: line WV2, an industry line in western Virginia and eastern West Virginia (Lampshire, 1992), and the USGS I-64 seismic line in central Virginia (Pratt, 1986). Line WV2 crosses from the Appalachian Plateau on the west into the westernmost Piedmont on the east and USGS I-64 begins in the Valley and Ridge Province and continues eastward onto the Atlantic Coastal Plain. All of the data have been split into smaller panels and the interpretation placed below for the convenience of the reader.

An analysis of the two transects leads to the following general observations:

1. A dominant reflection package at 3-4 seconds on the western end of both transects (labeled ‘A’ in Figures 4.5 – 4.7);

2. A general lack of reflectivity below ‘A’;

3. Higher reflectivity throughout the crust in the central and eastern portions of both transects (Figures 4.5 – 4.7);

4. East-dipping reflections in the mid- and upper crust (labeled ‘B’ in Figures 4.5 – 4.7);

5. Antiformal reflectivity patterns in the upper crust in the eastern portions of both transects (labeled ‘C’ in figures 4.5 and 4.7);

6. Gently east-dipping mid-crustal reflections starting at ~7 seconds separating the east-dipping fabric from the more planar fabric in the lower crust (labeled ‘D’ in Figures 4.5 and 4.7);

7. A west-dipping reflection package the base of which is interpreted as the Moho (labeled 'M' in Figures 4.5 and 4.7); and

8. An apparent merging of the east dipping reflectors ('B') with the mid-crustal reflections ('D') on both transects, with the mid-crustal reflections merging with the Moho ('M') to the east (Figures 4.5 and 4.7).

These observations are discussed below.

4.5 Interpretation of Reflectivity Patterns

During the Alleghanian orogeny, dextral transpression in the Piedmont was coincident with thin-skinned compressional folding and faulting in the Valley and Ridge province. The coincidence of these events have led some authors to propose a multi-stage deformational event including both dominant strike-slip and compressive phases (Sacks and Secor, 1990). Deformation in the Valley and Ridge has been shown to be diachronous, with major folding occurring in the southern Appalachians first, then later in the central Appalachians (Dean et al., 1988). This analysis fits well with paleomagnetic evidence presented by Miller and Kent (1988) showing a similar remagnetization pattern. Stamatakos and others (1996), however, find that remagnetization was relatively rapid and between ca. 255-285 Ma in the central Appalachians, and postdates folding toward the hinterland and predates the folding toward the structural front. Geologic analysis of jointing and cleavage development in the northern Appalachian Valley and Ridge (Faure et al., 1996) and the central Appalachian Plateau (Evans, 1994) display a counter-clockwise rotation of the stress field during the late Paleozoic. The counterclockwise rotation could be interpreted to support dextral transpression with an irregular continental edge (Faure et al., 1996), or a gradual change of relative plate motion with time.

The stratigraphy of the Valley and Ridge province is shown in Figure 4.8. These strata were either flat-lying or gently dipping towards the east or southeast before major deformation occurred during the Alleghanian. There are alternate mechanically weak and strong zones within the stratigraphic column, with shales and evaporites making up the bulk of the weak zones, and sandstones and carbonates the mechanically stronger zones. The mechanically stronger zones form large thrust sheets bounded by thrust faults through the weak zones (Boyer and Elliot, 1982). As deformation progresses, the thrust sheets may deform by folding and by the formation of ramps within these stronger units and flats within the weaker units, sometimes producing either an array of hinterland-dipping or an antiformal stack of thrust blocks (Boyer and Elliot, 1982). In addition, the mechanically weak zones may deform by layer parallel shortening (Ferrill and Dunne, 1989). The leading or western edge of major deformation in the Appalachians is the Allegheny Structural Front, which is at the Valley and Ridge/Plateau transition (Figure 4.1). The deformation has the effect of compressing or shortening the stratigraphic section laterally. Total shortening in the Valley and Ridge is estimated from cross section balancing to be up to 250

km in the southern Appalachians (Hatcher, 1989), and ranges up to 100 km in the central Appalachians (Evans, 1989). This does not include layer parallel shortening, which could be significant (Ferrill and Dunne, 1989; Evans, 1994). As pointed out above, the structural style of Valley and Ridge in the southern and central Appalachians is different, with the central Appalachians being dominated by folding and the southern Appalachians being dominantly a thrust province. The overall structural style − that of thin-skinned deformation above a master decollement − is the same in both cases.

The partitioning of deformation between dominant strike-slip in the Piedmont and dominant compression in the Valley and Ridge and Plateau during the Alleghanian orogeny is related to the orientation of preexisting zones of weakness relative to the stress field during orogenesis. Sub-horizontal, planar weak zones dictated by stratigraphy in the Valley and Ridge sedimentary section allowed most of the deformation to occur above sub-horizontal detachment surfaces with shortening being accommodated by thrust faulting, folding, imbrication of thrust sheets and layer parallel shortening within and between the mechanically weak zones. This deformation can be seen in seismic sections as the complex deformation above reflector 'A' on line WV2 (Figure 4.6). In the Piedmont, the weak zones were moderate to steeply dipping thrust, reverse, or possible strike-slip faults from the Taconic and/or Acadian orogenies which could more easily be reactivated as transpressive shear zones. This modified the Piedmont crust significantly, producing transpressive structures and through-going zones of crustal weakness.

The boundary zone between the differing stress fields was located near the current eastern edge of the Blue Ridge in the central Appalachians, and the current eastern edge of the Inner Piedmont in the southern Appalachians (see Figures 4.5 and 4.7). Both the Blue Ridge and Inner Piedmont are allochthonous and were thrust over the lower Paleozoic sedimentary succession. In Figures 4.5 and 4.6, possible duplexing is interpreted to have occurred beneath the Blue Ridge. This duplexing is believed to have involved the lower Paleozoic sedimentary succession (Hubbard et al., 1991; Lampshire et al., 1994). To the west of this boundary zone, mid- to lower crustal reflectivity is much reduced in comparison to the Piedmont immediately to the east. Also, mid-crustal reflection 'D' does not extend very far to the west of this boundary zone between the highly reflective Piedmont crust and the less reflective crust to the west. This can be interpreted as an expression of the fact that 1) there were no favorably oriented structures in the basement beneath reflection 'A' to be reactivated during orogenisis or the succeeding Mesozoic extension, or 2) the strain was somehow partitioned at this boundary zone and it was mechanically more attractive for the deformation to take place on the sub-horizontal weak zones in the sediments than by forming new faults or reactivating preexisting ones in the underlying Precambrian basement. This boundary zone could be related to the location of the hinge zone of the Laurentian continent (Cook and Oliver, 1981), or perhaps the edge of significant rifting during the opening of the Iapetus. Thomas (1991, 1993) postulated that the shape and location of the continental edge were a major controlling factor on the entire deformational history of the Appalachian-Ouachita mountain belt.

The east dipping reflectivity seen in the reflection seismic data ('B' in Figures 4.5 and 4.7) is interpreted to not penetrate the entire crust and is interpreted to merge with the zone of mid-crustal reflectivity at ~7 seconds ('D') in both the southern and central Appalachian transects. If the upper to mid-crustal zone of east-dipping reflectivity merges into the mid-crustal reflections, then the corresponding reflections must be related. Since many of the east-dipping reflections have been interpreted as ductile shear zones and many of these shear zones have been shown to have experienced strike-slip motion during the Alleghanian, the merging of the dipping reflections with a sub-horizontal reflection boundary means that either reflection 'D' was a deep crustal strike-slip transfer detachment allowing for horizontal motions above the mantle during transpression (i.e. 'orogenic float'; see Oldow et al., 1990), or that reflection 'D' postdates the transpressional deformation episode(s).

A recent series of finite-element models by Harry and others (1995) show that under compression, horizontal mechanically weak zones within the mid- and lower crust could give rise to sub-horizontal ductile shear zones. These shear zones could have formed during the Taconic and then were used during subsequent transpression and extension. Glover and others (1997) developed new tectonic models for the central Appalachians on the basis of new seismic data from offshore (EDGE seismic lines 801 – 803; see Sheridan et al., 1993), and a reinterpretation of the USGS I-64 seismic line. These models show an interpretation of the mid-crustal reflection along I-64 as a preexisting structure reactivated under an extensional stress field during the Mesozoic and merging with the Moho to the east.

If reflection 'D' postdates the transpression, then perhaps reflection 'D' represents an extensional detachment and the brittle reactivation of many of those zones during the Mesozoic was a ductile reactivation at depth. Bell and others (1988) suggested that the presence of mafic material in the mid-crust could produce the long wavelength part of the gravity anomaly pattern across Mesozoic basins in the eastern United States. In their model, the conduit for mafic material would be a crustal-scale detachment that would allow mafic magma from a remote source to migrate into the mid- and upper crust, forming thick sills in the mid-crust and dike swarms and sills within and surrounding the Mesozoic basins. An interesting observation about reflection 'D' in the central Appalachians is that earthquakes of the Central Virginia Seismic Zone are rare or absent beneath the mid-crustal reflection (Çoruh et al., 1988). This being the case, perhaps the intrusion of mafic material during extension strengthened the crust at and below the mid-crustal reflection as suggested by others (Serpa and deVoogd, 1987; Goodwin and Thompson, 1988).

The orientation of the Moho reflector ('M' in Figures 4.5 and 4.7) and its merging with the mid-crustal reflector ('D') to the east is intriguing. If the current Moho were formed during or after extension (McBride and Nelson, 1991), then the mid-crustal reflector was probably significantly modified during extension. However, if the Moho formed soon after collision (Brown, 1987), then reflector 'D' is mostly of a result of compression or transpression during the Paleozoic and was little effected by Mesozoic extension. Given the relatively high reflectivity of the crust in the Piedmont and the merging of both the east-dipping reflections into

the mid-crustal reflection and that reflection into the interpreted Moho reflection, it is likely that these reflections were at least in part reactivated during the Mesozoic.

The antiformal reflectivity patterns ('C' in Figures 4.5 and 4.7) have been interpreted as either a result of dextral transpression (Gates, 1987; Gates et al., 1988) or as a result of block rotation above a detachment horizon during the Mesozoic (Costain and Çoruh, 1989). Whatever their origin, they are in the seismic data and have to be accounted for. We favor the latter interpretation as being more likely given the amount of extension in the central Appalachians implied by the number and size of exposed and buried Mesozoic basins (Figure 4.2) and the amount of mafic material of Mesozoic age found throughout the orogen. This in conjunction with the thinning of the crust towards the east and the merging reflections discussed above suggests that the orientation of reflectors within the crust of the Piedmont and eastward was strongly affected by Mesozoic extension and this must be taken into account during interpretations of seismic data from the southeastern United States.

Finally, the reactivation of faults during multiple tectonic episodes would most likely increase the reflectivity within the fault zones, particularly in the ductile portions of the zones. As mentioned earlier, studies have shown that ductile shear zones can have enhance reflectivity due to seismic anisotropy and thin bed effects (e.g. Jones and Nur, 1984).

4.6 Conclusions

The reflectivity seen in seismic profiles in the southern and central Appalachians is due in part to the reactivation of preexisting zones of weakness in the crust of the Piedmont to the east, and to sub-horizontal zones of mechanical weakness in the Paleozoic sedimentary succession to the west. There is ample geologic evidence for episodic reactivation of major faults in the southern and central Appalachian Piedmont. As discussed above, these faults were reactivated several times and each episode affected the orientation and reflectivity of the fault zones. To the west, either basement faults were oriented poorly for reactivation, or it was simply mechanically easier for new faulting to take place on subhorizontal detachments within weak zones in the sedimentary succession. This boundary between the highly reflective and less reflective mid-and lower crust may be related to the original location of the Laurentian continental edge. The final major deformational episode − extension during the Mesozoic − has probably had a profound effect on the picture revealed by reflection seismic data. Therefore, seismic reflectivity beneath the Piedmont of the southeastern U.S. is most likely the result of its participation in multiple episodes of deformation from the early Paleozoic through the Mesozoic.

Given the complex deformation history of the eastern United States, it might not be possible to extract the correct picture of the history of an orogen from analyses of seismic reflectivity and surface geology alone. Even the inclusion of potential fields and magnetotelluric data (see Ogawa et al., 1996), given their non-uniqueness, might not provide the complete picture considering the history of fault reactivation in the central and southern Appalachians. We believe the best course is to consider all the tectonic events and try to estimate their possible

effects on geophysical and geologic interpretations, for it is only through understanding the complete geologic history that the origins of crustal reflectivity can be resolved.

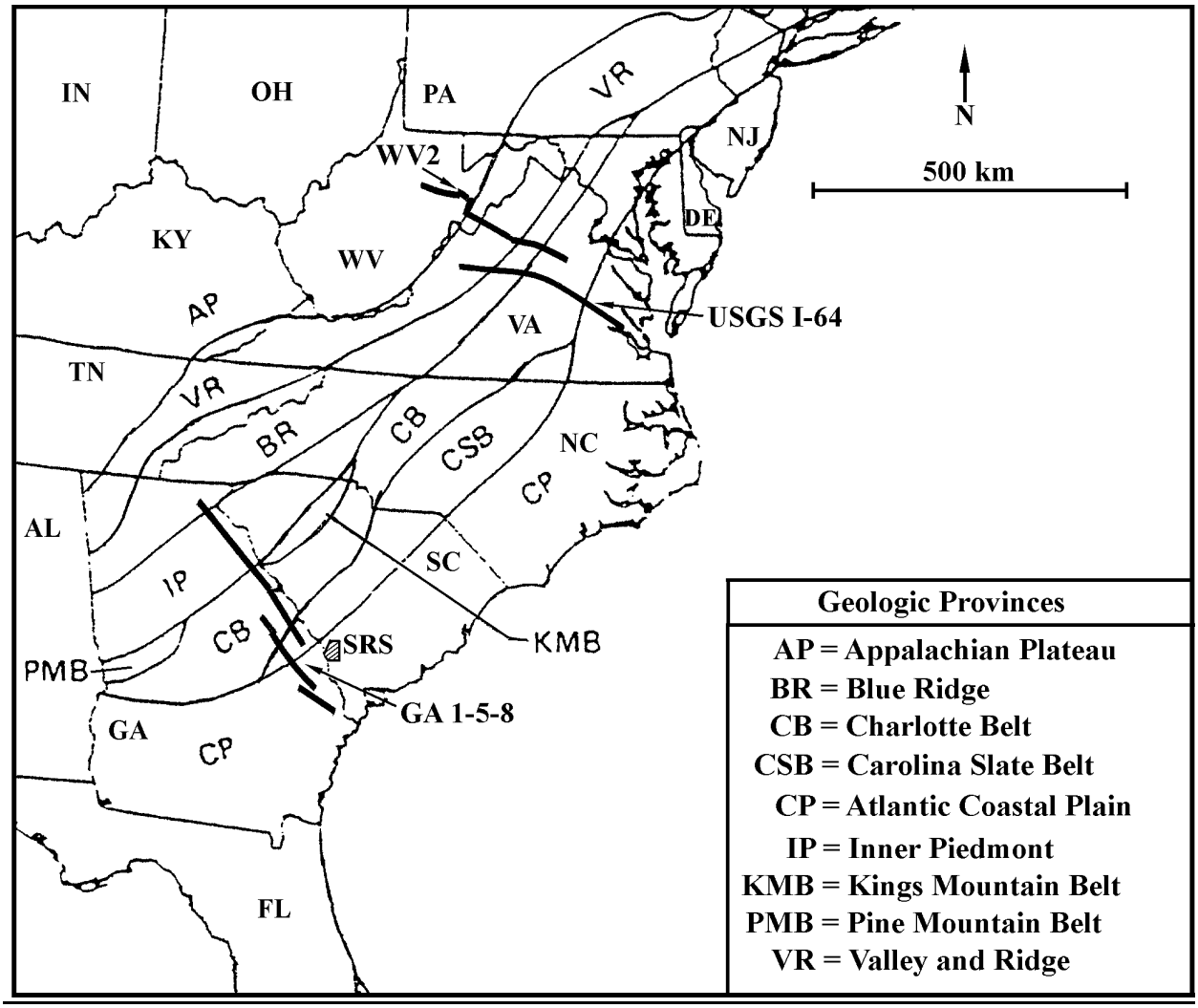

Figure 4.1: Locations of seismic lines (thick lines) and geologic provinces in the southeastern United States. Hachured area in South Carolina shows the location of the Savannah River Site (SRS). (Modified from Taylor, 1989).

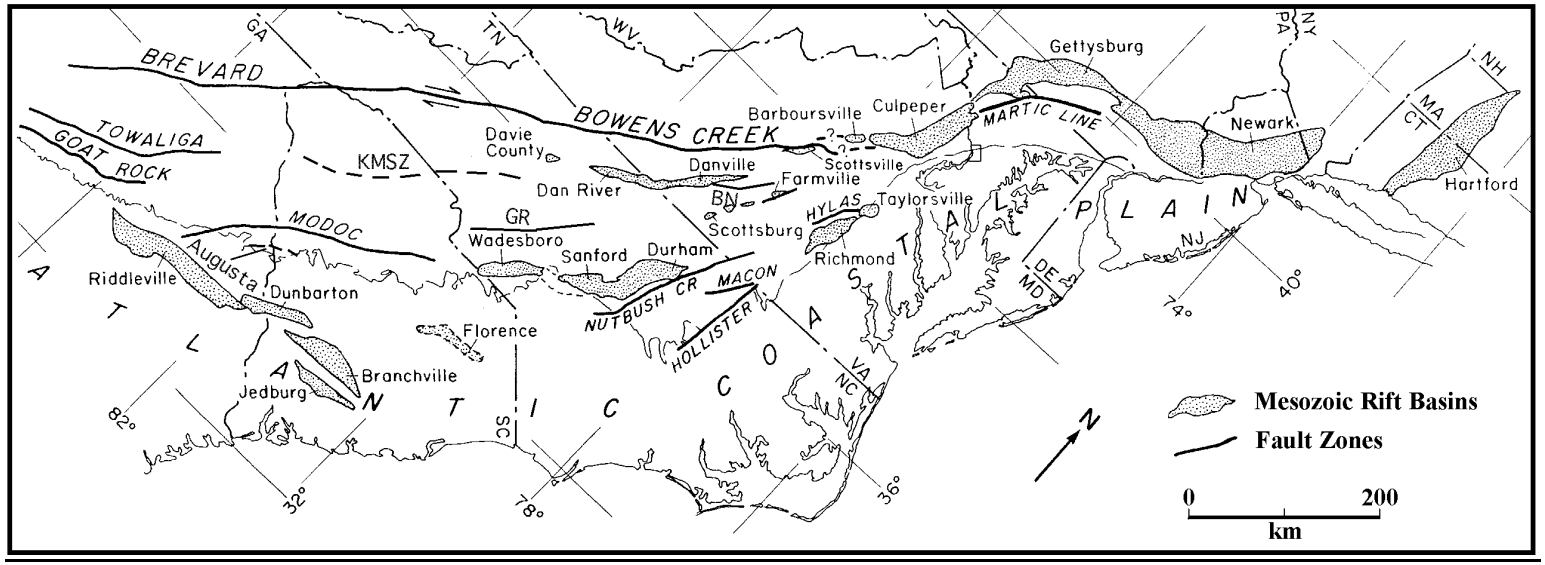

Figure 4.2: Map showing locations of some of the exposed and buried Mesozoic basins along the East Coast of North America. Major mylonite zones that were reactivated during the Alleghanian in a dextral sense are also shown: BN, Brookneal shear zone; GR, Goat Rock shear zone; KMSZ, Kings Mountain shear zone (modified from Costain and Çoruh, 1989 and Gates, 1988).

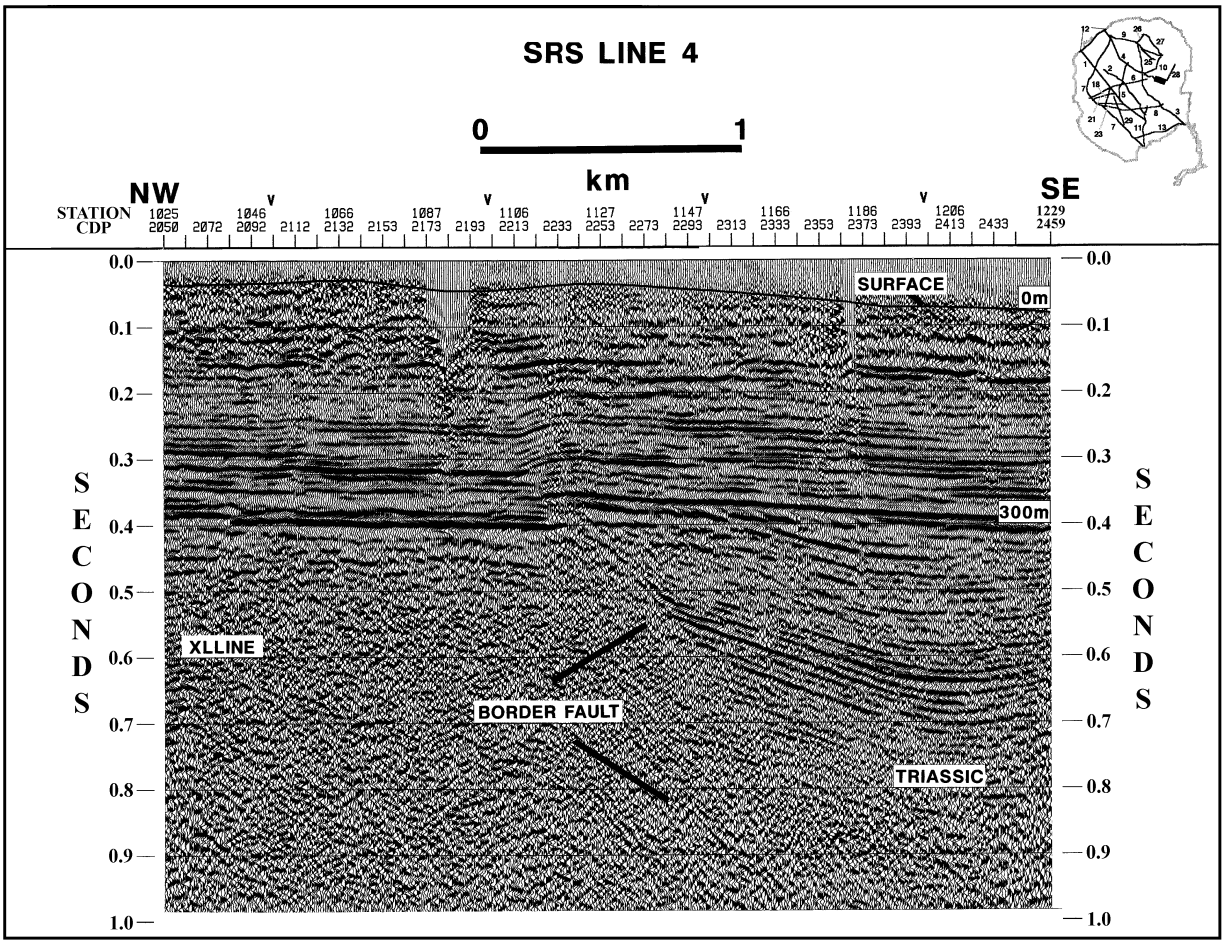

Figure 4.3: Seismic data from the Savannah River Site in South Carolina (Domoracki, 1995). Atlantic Coastal Plain sediments are deformed and offset by the reactivation of the Pen Branch Fault, the border fault of the Dunbarton Triassic Basin (near station 1106). Abbreviation 'XLLINE' = crystalline basement rocks.

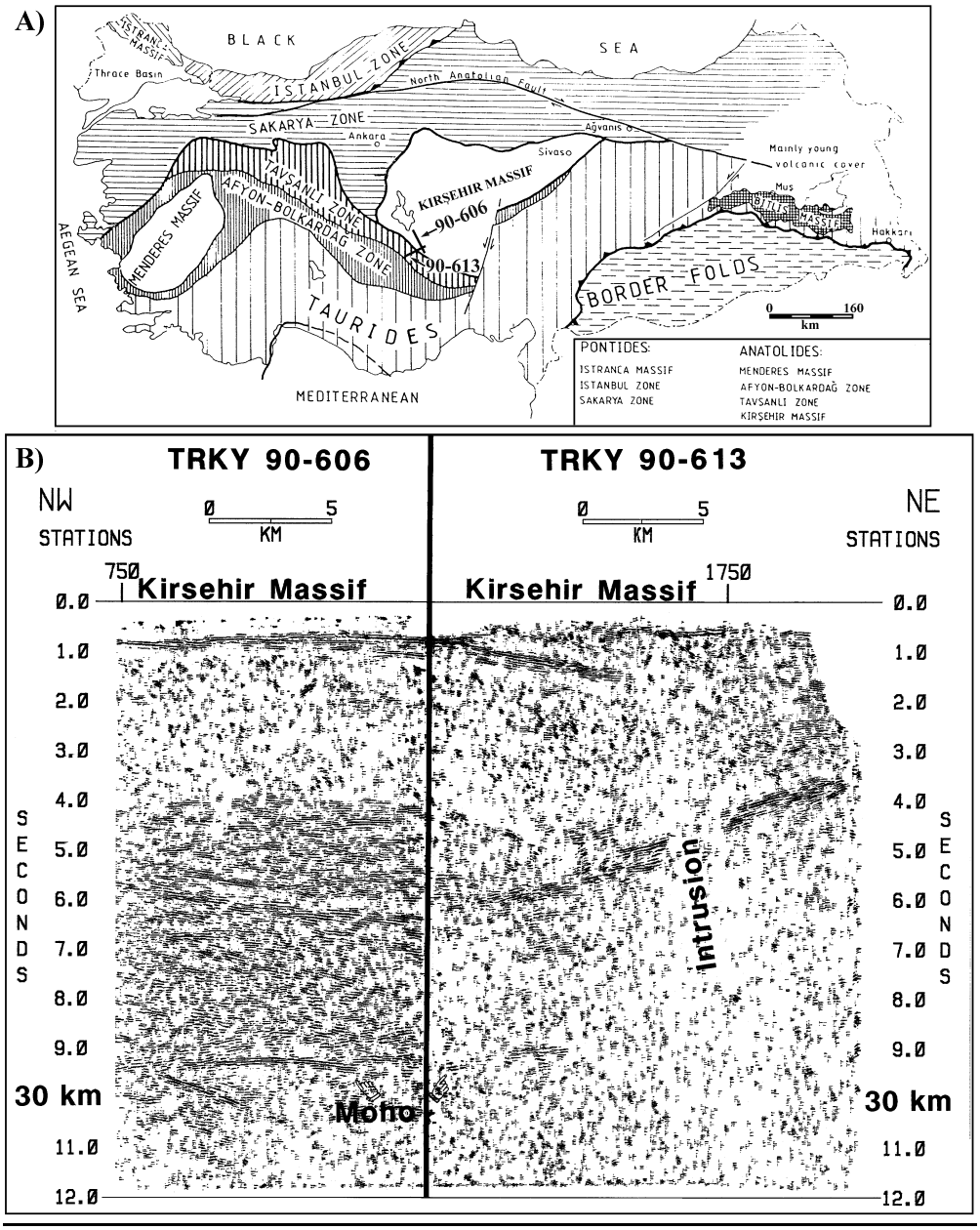

Figure 4.4: Illustration of the problem of relying solely on reflectivity in the interpretation of seismic data. Lines 90-606 and 90-613 were shot perpendicular to each other on the Kirsehir Massif in central Turkey. Recording, source, and processing parameters were identical for the two lines (Çoruh, personal comm. 1996). A) Tectonic map of Turkey, showing the location of the seismic lines (after Okay, 1986). B) ALD of line tie showing contrast in reflectivity at the point of intersection. Is the lower crust reflective or not? Line orientation can make a difference in the overall reflectivity of the data.

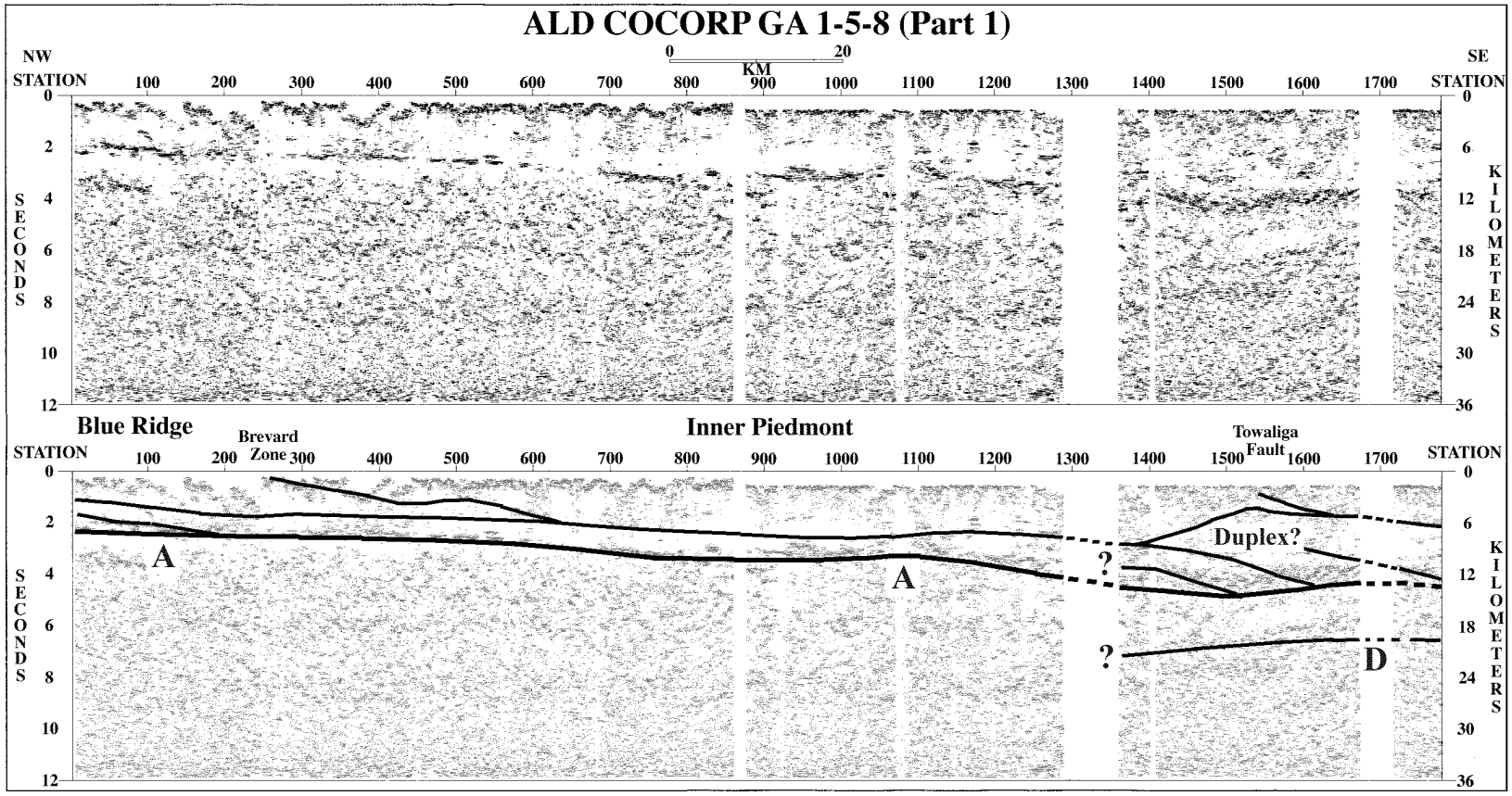

Figure 4.5: ALD of combined COCORP Georgia lines 1, 5, and 8. Abbreviations: A, reflection above which thin-skinned deformation takes place; B, east-dipping reflections; C, antiformal reflections; D, mid-crustal reflections; M, lower crustal reflection package whose base is interpreted at the Moho. Geologic information from papers of Cook and others, 1979 and 1981. Seismic data is plotted at 1:1 for 6 km/s. (Large PDF can be viewed by clicking on the figure.)

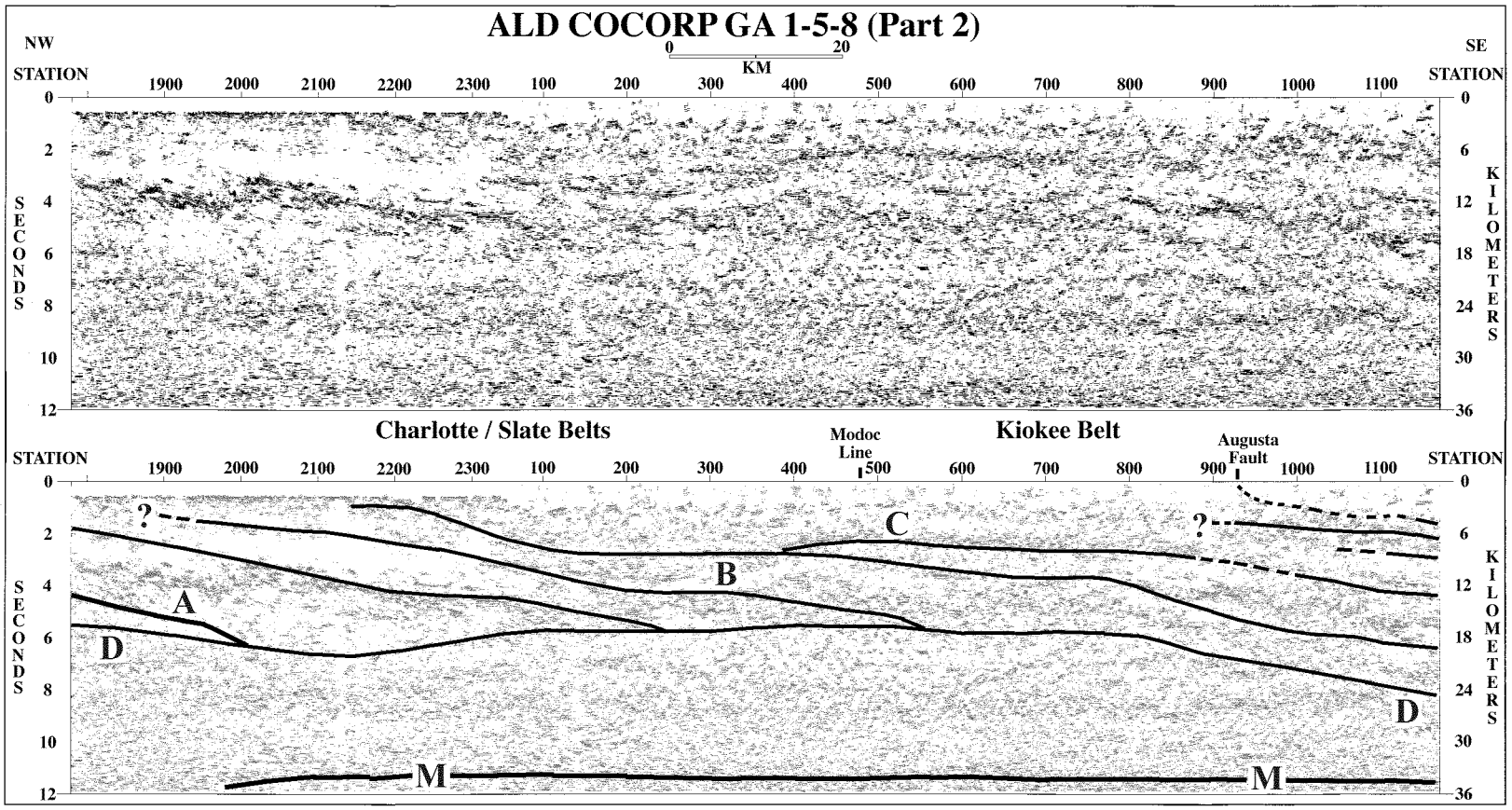

Figure 4.5: (continued; Large PDF can be viewed by clicking on the figure.)

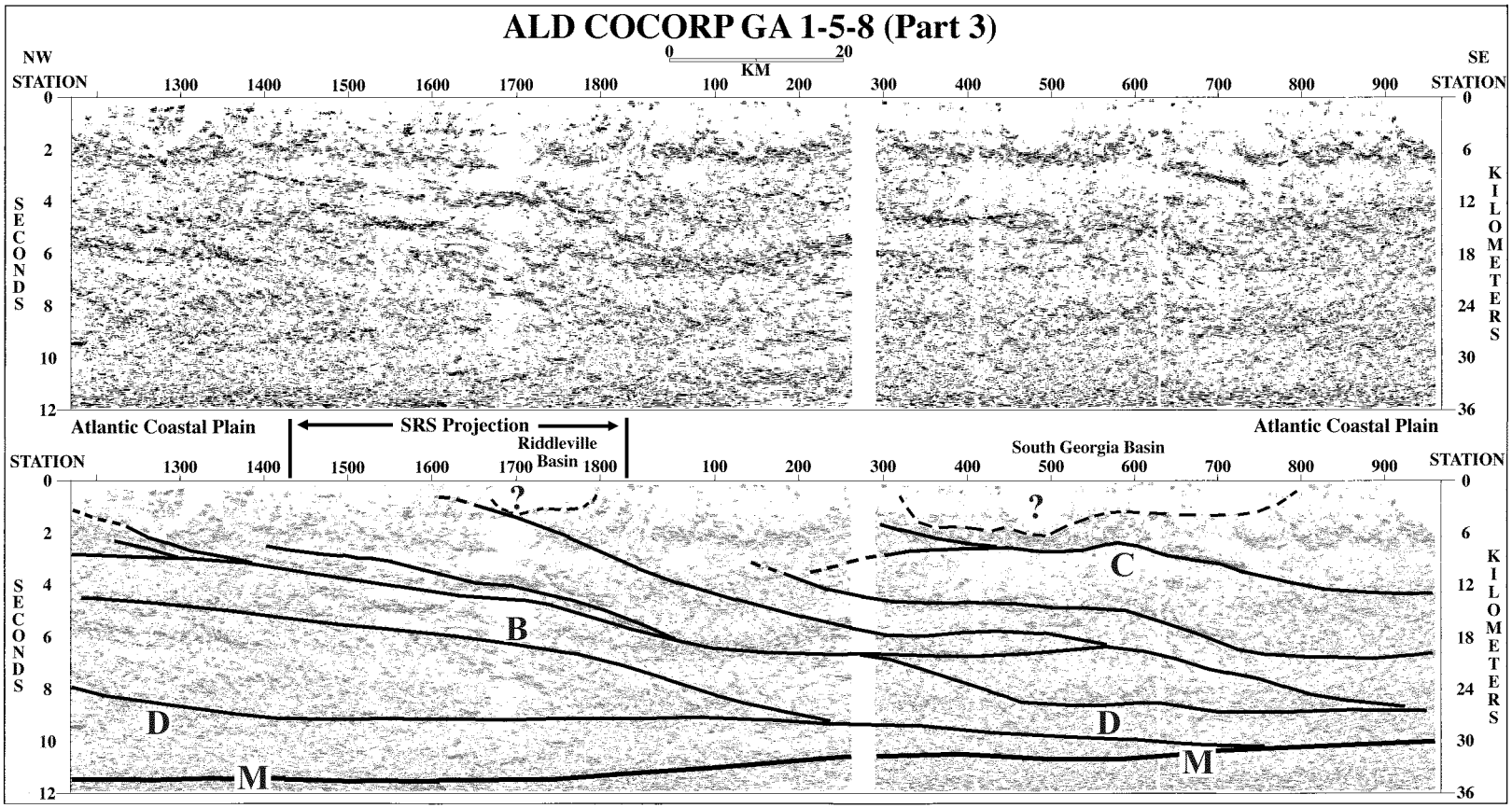

Figure 4.5: (continued; Large PDF can be viewed by clicking on the figure.)

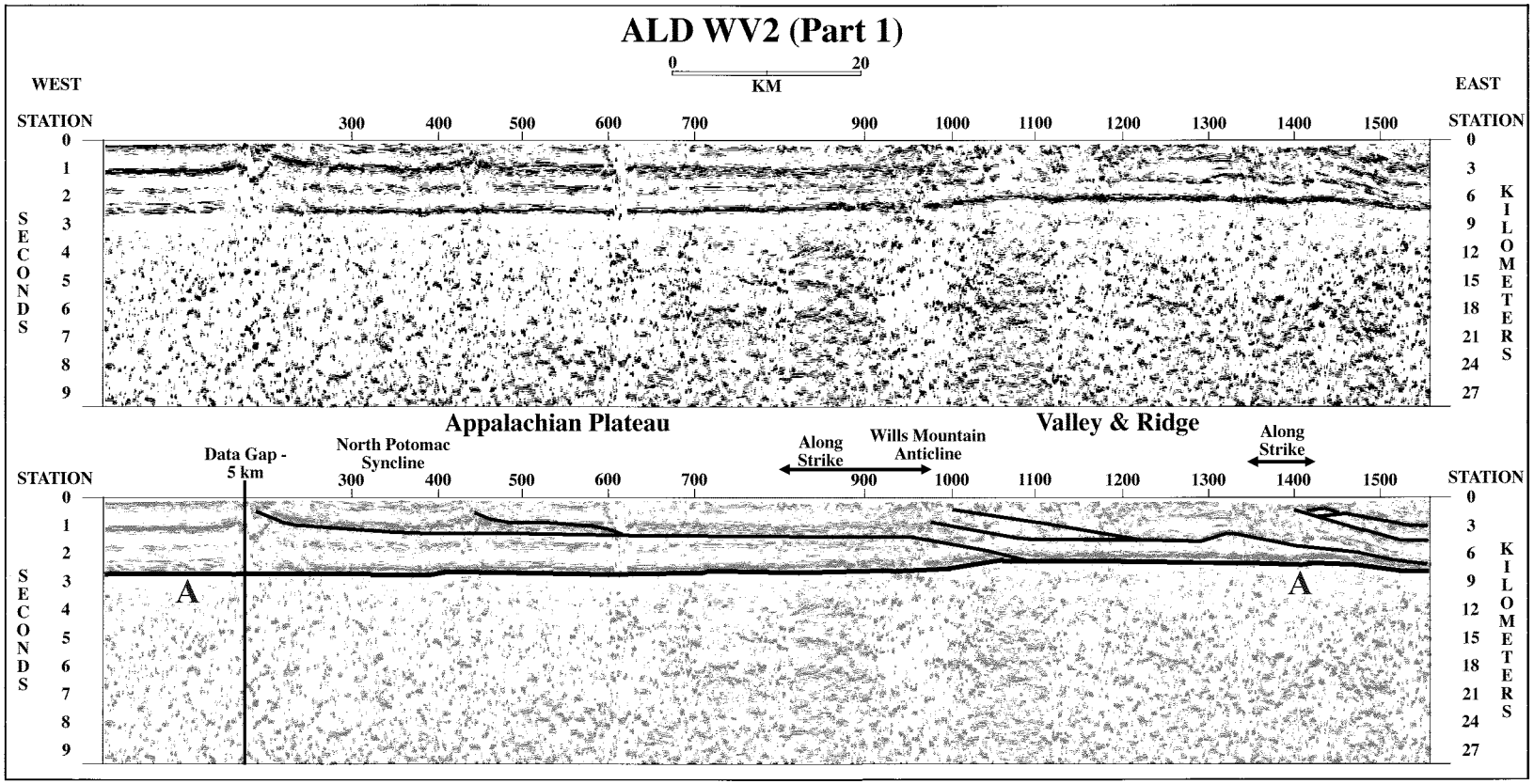

Figure 4.6: ALD of reprocessed industry line WV2. Abbreviations: A, reflection above which thin-skinned deformation takes place; B, east-dipping reflections; C, antiformal reflections; D, mid-crustal reflections; M, lower crustal reflection package whose base is interpreted at the Moho. Geologic information from paper of Lampshire and others (1994). Seismic data is plotted at 1:1 for 6 km/s. (Large PDF can be viewed by clicking on the figure.)

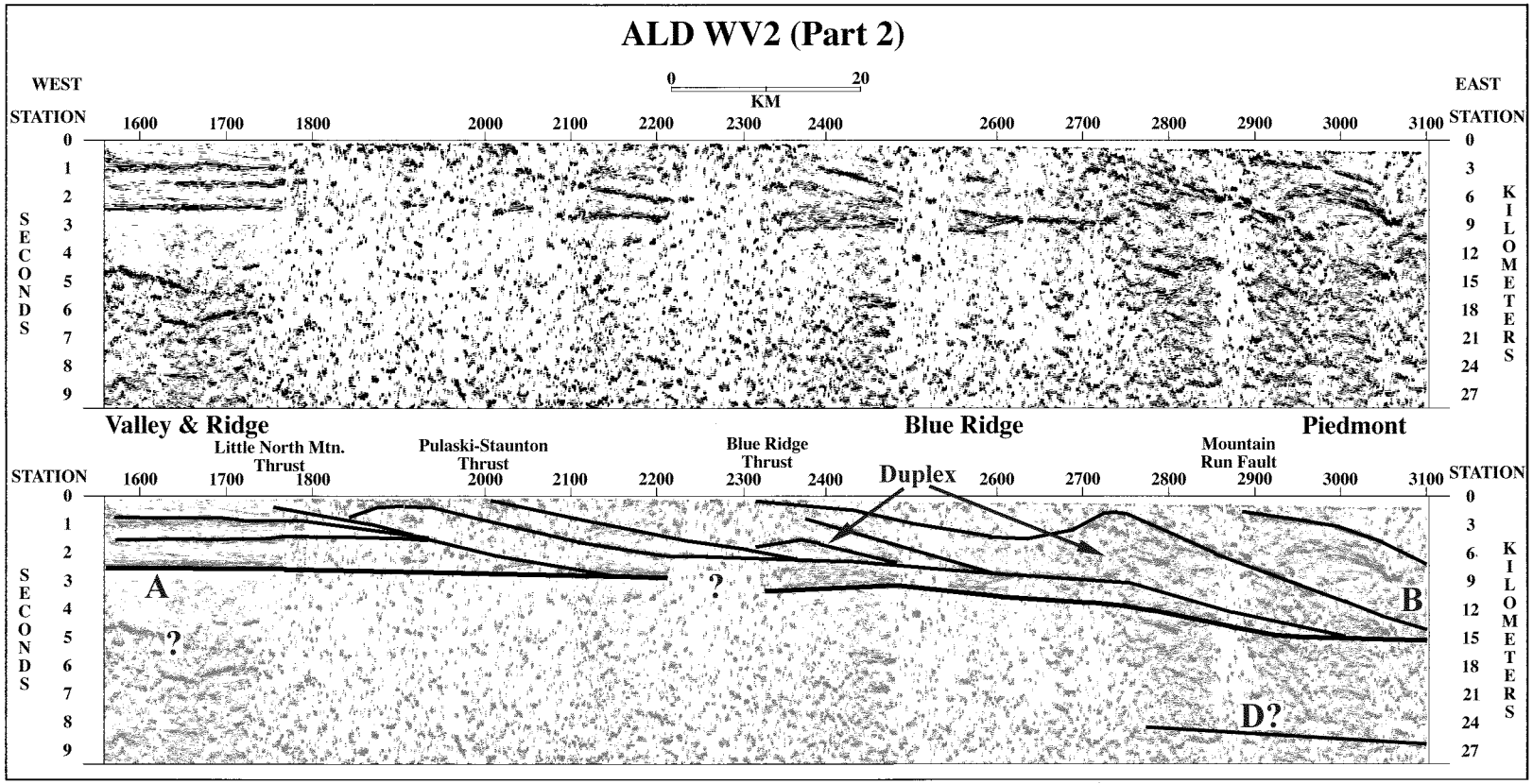

Figure 4.6: (continued; Large PDF can be viewed by clicking on the figure.)

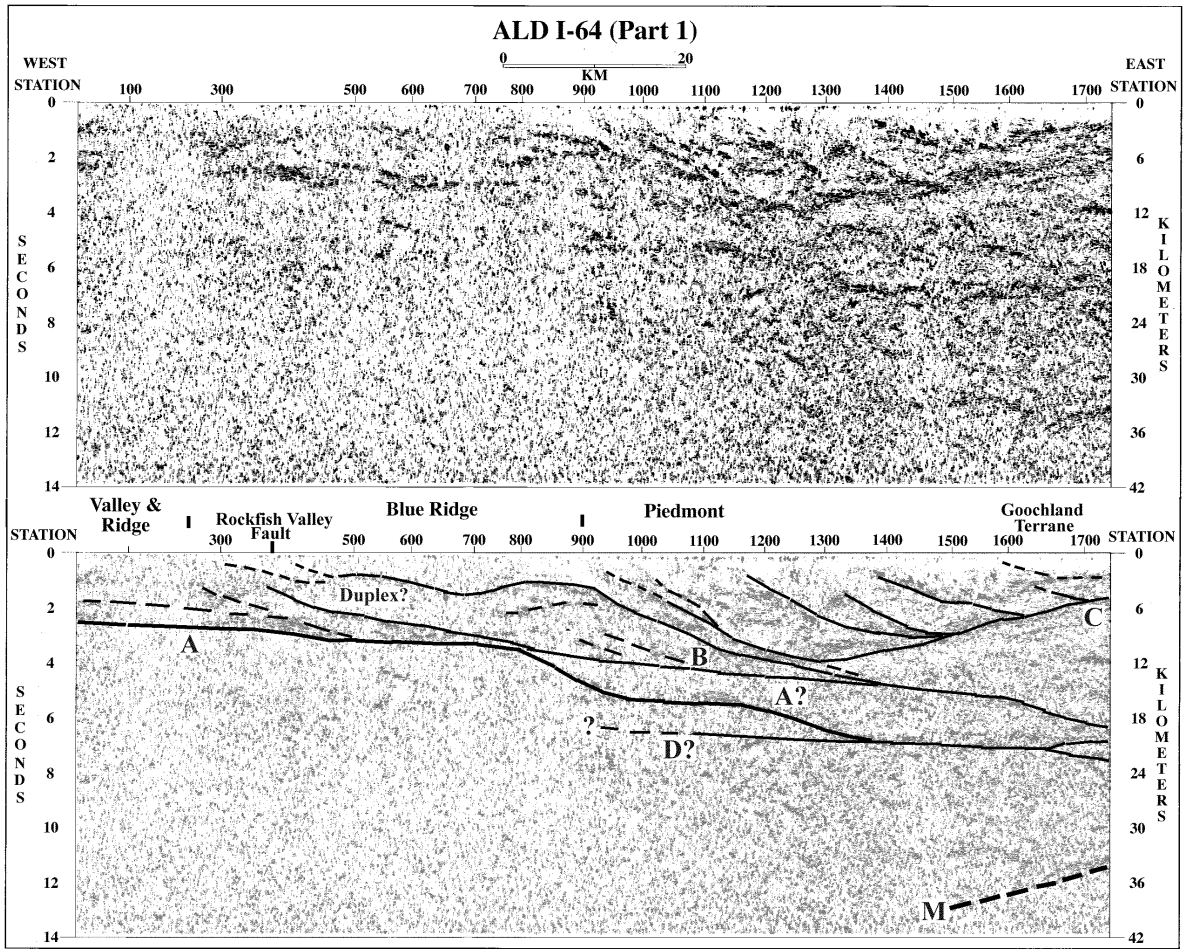

Figure 4.7: ALD of USGS line I-64. Abbreviations: A, reflection above which thin-skinned deformation takes place; B, east-dipping reflections; C, antiformal reflections; D, mid-crustal reflections; M, lower crustal reflection package whose base is interpreted at the Moho. Geologic information from dissertation of Pratt (1986). Seismic data is plotted at 1:1 for 6 km/s. (Large PDF can be viewed by clicking on the figure.)

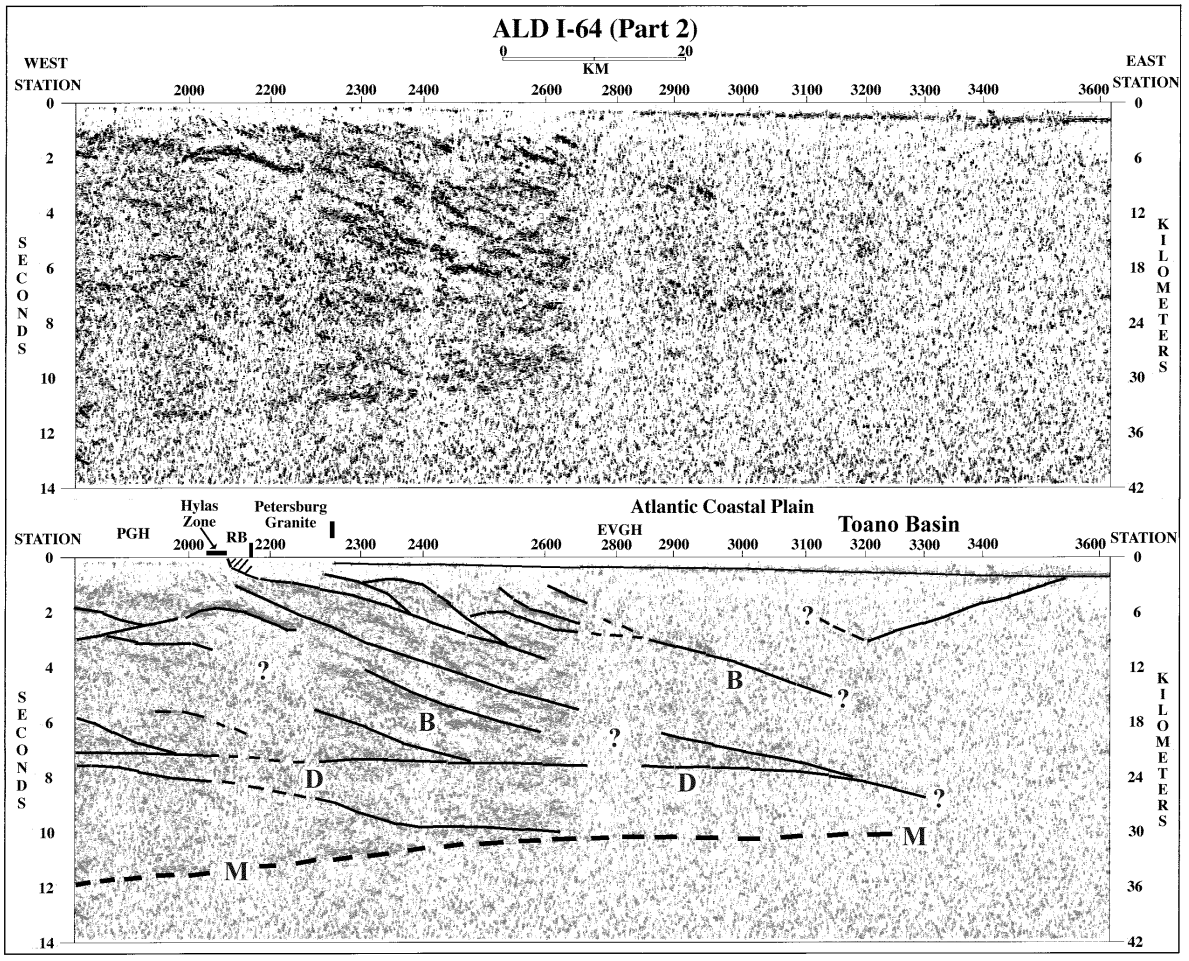

Figure 4.7: (continued; Large PDF can be viewed by clicking on the figure.)

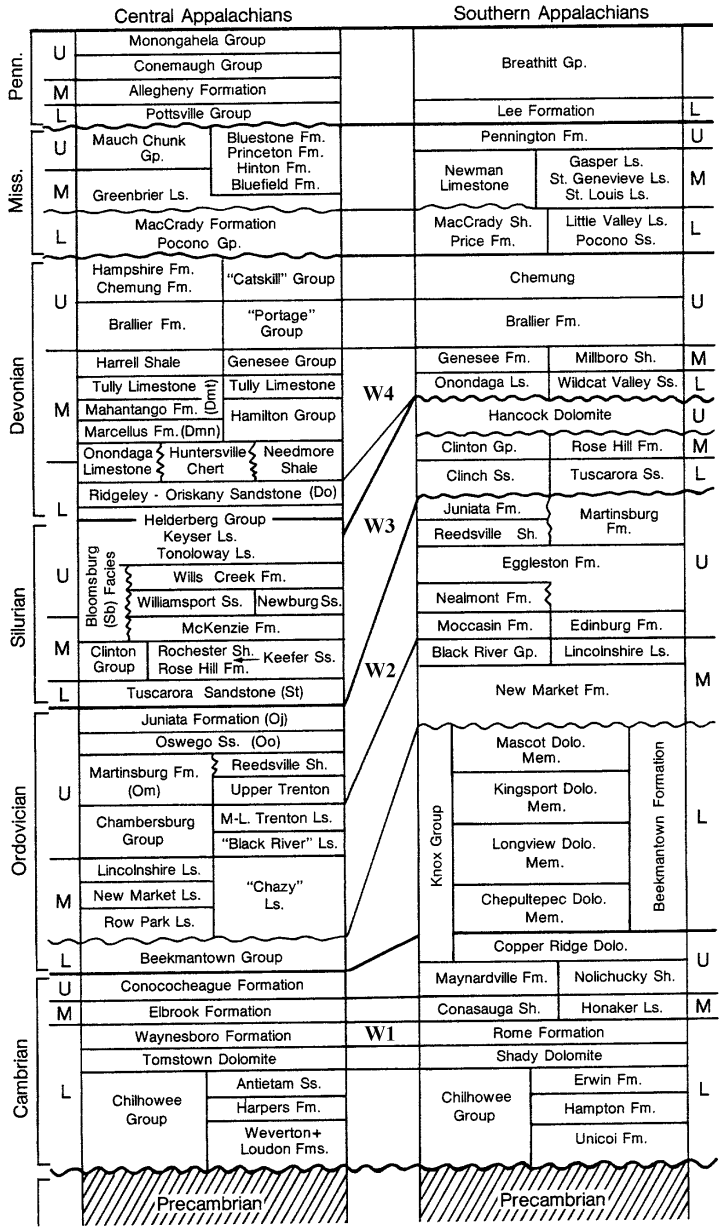

Figure 4.8: Generalized stratigraphic correlation chart for the central and southern Appalachians. Undulating and vertical sawtooth boundaries indicate unconformities and lateral facies variations. Letters W1 – W4 indicate relatively weak zones in the stratigraphy where decollements can form. W1, Rome/Waynesboro shale; W2, Martinsburg and other upper Ordovician shales; W3, locally weak horizon in central Appalachians; W4, Devonian shales (modified from Kulander and Dean, 1986, and Wilson and Shumaker, 1988).

Chapter 5: Lateral Continuity of Major Structures in the Central Appalachians: An Integrated Geophysical Interpretation

Abstract

Over 700 km of industry vibroseis reflection were combined with regional Bouguer gravity data, deep well and geologic information in a study of the continuity of major structures in the central Appalachians of Virginia and West Virginia. The seismic data were reprocessed using a new method – *dip projection* – which projects the original crooked-line data onto a straight line oriented in the general dip direction. These new stack data were then migrated and the results combined with *potential field attribute* (PFA) analysis to ascertain the lateral extent of major structures imaged on the reflection data. The following interpretations resulted:

1) The Blue Ridge basement complex of the central Appalachians of Virginia is underlain by an imbricate stack of high density Cambrian-Ordovician carbonates near its leading edge; and
2) The large-scale blind thrust sheet of Cambrian-Ordovician carbonates underlying the Nittany Anticlinorium in West Virginia is replaced by imbrication of the carbonate layer to the southwest in Virginia.

The utility of dip-projected reflection seismic sections and PFA analysis in the interpretation of these features is emphasized.

5.1 Introduction

Much progress has been made in recent years on understanding the structural and geologic history of the central Appalachians. A major contributor to this progression has been the utilization of geophysical data sets, in particular reflection seismic data, in combination with more traditional structural and stratigraphic analyses. The availability of regional-scale reflection data sets from industry has greatly enhanced this effort.

Petty Ray Geophysical conducted a series of seismic surveys in the central and southern Appalachians of West Virginia, Virginia, and Tennessee from the late 1970's into the early 1980's. These data were made available through Halliburton Geophysical Services (now a subsidiary of Western Geophysical) to us both in stacked and field data formats. Several recent papers made use of these as well as other reflection data to analyze structures within the folded Valley and Ridge province in the central Appalachians (e.g. Evans, 1989; Wilson and Shumaker, 1992; Lampshire et al., 1994).

As a part of this study, over 700 km of Petty Ray reflection data were reprocessed at the Regional Geophysics Laboratory at Virginia Tech (Figure 5.1). The initial results of the reprocessing effort were published by Lampshire and others (1994). They looked at the structures along one particular line (labeled WV2 in Figure 5.1) and showed duplexing of Cambrian-Ordovician carbonates beneath the Blue Ridge province, and the possibility of a basement structure near the Allegheny Structural Front in West Virginia (Figure 5.2). This study extends the previous effort both to the north and south, thus allowing the lateral continuity of major structures to be investigated. In addition to standard reflection data processing, a new processing sequence was developed to project the crooked-line seismic data onto a straight line perpendicular to regional strike; i.e. parallel to regional dip. This process, called *dip projection*, allows for better seismic migration and interpretation of the seismic section. All three seismic lines discussed include the dip projection processing step.

In addition to the seismic reflection data, gravity, well and geologic information have also been merged to obtain integrated interpretations. Specialized derivative processing was applied to the gravity data and potential field attribute maps were produced to aid in the delineation of major subsurface structures. The generation of synthetic seismograms to tie the well information to the seismic data was a critical step in the evaluation of structures associated with the Allegheny structural front. The combination of these data sets allowed verification of the lateral continuity of two major structures in the subsurface: 1) an imbricate stack of carbonates beneath the Blue Ridge crystalline thrust sheet, and 2) the structure of the Nittany Anticlinorium.

5.2 General Geology

The central Appalachians can be divided into five geologic provinces. From west to east these are the Appalachian Plateau, Valley and Ridge, Blue Ridge, Piedmont and the Atlantic

Coastal Plain. For this study, we investigated only the geologic structures associated with the Appalachian Plateau, Valley and Ridge, and Blue Ridge provinces.

The Appalachian Plateau and Valley and Ridge Provinces consist of carbonate shelf strata and foreland basin clastics deposited on Precambrian basement (Colton, 1970; Figure 5.2). A stratigraphic correlation chart for the central Appalachians is shown in Figure 5.3. The chart shows the presence of several zones of structural weakness in the sedimentary succession. These zones are horizons wherein decollement surfaces can form between the more competent stiff layers (Evans, 1989; Wilson and Shumaker, 1992). The stiff layers will deform by imbrication and duplexing. The imbricate blocks are bound by thrust faults within the weaker layers (Boyer and Elliot, 1982). There are three primary weak zones in the central Appalachians: the Cambrian Waynesboro Formation, the Ordovician Martinsburg and Juniata formations, and the Devonian shales (Figure 5.3). Silurian shales and evaporite horizons may also provide a locally weak zone for the propagation of thrust faults (Shumaker, 1974; Evans, 1989; Wilson and Shumaker, 1992). Figure 5.4 shows a generalized geologic map of the region.

Structurally, the Plateau is characterized by horizontal to relatively gently folded strata. Within the Appalachian Plateau, there is an intraplateau structural front separating the folded or high plateau on the east from the Allegheny Plateau on the west (Kulander and Dean, 1986). The folded Plateau and Valley and Ridge provinces widen to the northeast over a postulated deepening basement (Kulander and Dean, 1986; Figure 5.2). Estimates of depth to basement in this portion of the Valley and Ridge are primarily based on magnetic data (Kulander and Dean, 1978). To the north and west of the intraplateau structural front, the Salina Salt and associated evaporites provide a weak zone within the Silurian strata, thus providing an additional decollement surface in the sedimentary strata and allowing deformation to develop at higher levels. Frey (1973) and Shumaker (1974) postulated that the folded Plateau was a result of the extent of the evaporite basin during the Silurian.

The Valley and Ridge consists of a series of anticlinal and synclinal structures interspersed with thrust faults. The central Appalachian Valley and Ridge mainly exhibits folding above blind thrusts, with the few breakthrough thrusts occurring towards the Blue Ridge in the eastern part of the province. On the basis of surface geologic mapping, reflection seismic data and well information, the Valley and Ridge province is interpreted to be the result of thin-skinned deformation above a master decollement in the lower Cambrian Rome/Waynesboro formations (Gwinn, 1964; Rodgers, 1970; Jacobeen and Kanes, 1974, 1975; Harris and Milici, 1977; Perry, 1978; Clark et al., 1978; Harris and Bayer 1979; Kulander and Dean 1986; Evans, 1989; Wilson and Shumaker 1992; Lampshire, et al., 1994).

The Blue Ridge Province consists of crystalline metamorphic and igneous rocks varying in age from Grenvillian (~1.1 billion years) in the Blue Ridge through the earliest Paleozoic (Glover, 1992). A regional summary of metamorphic ages in the Blue Ridge and Piedmont is given by Glover and others (1983). The Blue Ridge is allochthonous and thrust over the lower Paleozoic carbonate platform (Harris and Bayer, 1979; Pratt et al., 1987; Lampshire et al., 1994).

In addition to the sources cited above, geologic information used in the interpretation of the seismic and gravity data was also taken from the following sources: Butts (1933; 1940), Bick (1960), Brent (1960), Allen (1963;1967), Young and Rader (1974), Gathright (1976), Rader and Biggs (1976), West Virginia Geologic and Economic Survey (1986), Lampshire (1992), and Virginia Division of Mineral Resources (1993).

5.3 Geophysical Data Sets

Three different geophysical data sets were used in this study. They include: 1) seismic reflection data, 2) Bouguer gravity data, and 3) geophysical well logs from deep wells in the area. Details about the data sets follow.

5.3.1 Vibroseis Reflection Data

Over 700 km of vibroseis reflection seismic data provided by Halliburton Geophysical Services (now a part of Western Geophysical) were reprocessed using both conventional and specialized processing sequences. The conventionally processed stack data follow the usual seismic reflection data processing sequence (demultiplexing, vibroseis correlation, crooked-line geometry definition, datum and elevation statics, spatially varying deconvolution, sort, velocity analysis, residual statics, stack, filtering, and migration) with the addition of extended vibroseis correlation (Pratt, 1982; Okaya and Jarchow, 1989) and vibroseis whitening (Çoruh and Costain, 1983). All three seismic lines, WV1, WV2, and WV3, were correlated beyond the original 5 s full correlation time to a total of 10 s. Lines WV2 and WV3 had vibroseis whitening applied to balance the effects of spherical divergence and frequency attenuation. The application of vibroseis whitening to line WV1 made no appreciable difference in the data, and so it was not included in the final processing sequence for that line.

After conventional processing was completed, a newly developed processing sequence called *dip projection* was implemented. The dip-projection processing sequence takes common mid-point gathers (CMPs) from conventional crooked-line processing and projects them onto a straight line that is perpendicular to regional strike. For these data, the average strike of structures in the Valley and Ridge in the study area − N35°E − was used to define the direction along which the data were projected. The dip-projected stacks along straight lines have the advantage of being more interpretable because they more closely approximate conventional, dip-oriented geologic cross sections. They are also attractive from a geophysical point of view, as both velocity analysis and migration work better because they represent straight line stacks (for more information on the process, see Chapter 2 in this dissertation).

The resulting stacks were migrated using a Kirchhoff algorithm at 90% stacking velocities. The migrated stacks are shown after *automatic line drawing* (ALD) processing in Figures 5.5 − 5.7. The ALD technique is an objective process that produces unconventional line drawings in which *the seismic waveform and relative amplitude information are preserved*. The processing is

based upon the Fresnel zone concept that requires the reflections from a subsurface reflecting "point" be on several traces on seismic sections in the space-time domain. The ALD process converts the seismic amplitudes into two-dimensional coherency estimates using a moving window in which a scanning procedure searches for the angular direction with the highest correlation. The results are then subjected to an exponential amplitude adjustment that forces the background noise outside of the dynamic range of the plotter. The result is a section *of relative seismic reflectivity*. The ALD process is especially useful for crustal seismic data because of the larger Fresnel zone size at depth. Excellent results have been obtained from reprocessed seismic reflection data using the ALD technique (e.g. Çoruh et al., 1987; Çoruh et al., 1988a; Hubbard et al., 1991; Lampshire et al., 1994). Similar methods are also used to enhance noisy seismic record sections (e.g. Kong et al., 1985).

The strong reflections located at 2-3 seconds on all the seismic lines is interpreted to be the contact between lower Cambrian Waynesboro Formation and the underlying Tomstown Dolomite (see Figure 5.3). These formations have a significant velocity and density contrast and should, therefore, provide a strong reflection (Çoruh et al., 1988b). General features that can be seen on the seismic stack sections are: 1) the thin-skinned nature of the deformation above a decollement in the Waynesboro Formation just above the strong reflection at 2-3 seconds across most of the line, and 2) an increase in the time-depth to the strong Waynesboro/Tomstown reflection from south (~2.2 seconds) to north (~3 seconds). The increase in time-depth could be attributed to a deepening basement to the north as stated by Kulander and Dean (1978; 1986).

5.3.2 Bouguer Gravity Data

Over 17,000 gravity stations provided by the Defense Mapping Agency (DMA) for the region of interest were taken from a CD-ROM published by the National Geophysical Data Center (Hittleman et al., 1994). Terrain corrected data from the National Geodetic Survey (NGS) was not used due to insufficient data coverage in the region. the error associated with using the DMA data was estimatied by computing differences between the data sets at the same stations. The differences were less than 0.2 mgal which is smaller than the maximum station error of ~0.5 mgal in either data set, therefore the DMA data set was used for its superior coverage. The original data distribution is shown in Figure 5.8. The DMA point data were gridded at an initial spacing of 4 km. Missing grid values were added by linear interpolation. The resulting gravity field is shown in Figure 5.9. The gravity field is dominated by a large regional low attributed to the thickness of the crust in the region (Kulander and Dean, 1978), and a sharp positive gradient trending northeast. This gradient is well known as the Appalachian Gravity Gradient and has been shown to be a result of crustal thinning to the east (Cook, 1984; Pratt et al., 1987).

Removal of the regional field was accomplished by the removal of a 3rd-order trend surface from the original data grid. The resulting residual field is shown in Figure 5.10. The final residual gravity grid of 56x61 points was interpolated onto a 1x1 km grid for ***potential field attributes*** (PFA) analysis. Potential field attributes are based on combinations of horizontal and

vertical derivatives of the gravity field and are mathematically analogous to seismic attribute analysis routinely performed on stacked seismic sections. The three attributes are the *analytic signal* (Nabighian, 1972, 1984; Roest et al., 1992), *tilt angle* (Miller and Singh, 1994), and the gradient of the tilt angle, herein called the *wavenumber*. In general, the analytic signal peaks over the edges of subsurface lateral density contrasts and is more sensitive to near surface changes. The tilt angle peaks over the center of mass of the body and is relatively insensitive to depth. The zero degree contour approximates the location of the edges of a subsurface body. Positive values of the tilt angle indicate a positive relative density contrast; negative values indicate a negative relative density contrast. The wavenumber, being the horizontal derivative of the tilt angle, highlights the steeper slopes on the tilt angle map that could be indicative of the edges of bodies in the subsurface and their proximity to the surface. (For more details on the analysis procedure, see Chapter 3, this dissertation.) The results of this analysis on the data from the study area is discussed in a later section.

5.3.3 Well Logs

Data from two wells, the Rockingham-Whetzel well in Virginia and the Pocahontas-21 well in West Virginia, were used to tie subsurface geology to the reflection seismic data (Figure 5.11). Geophysical well logs provided by the West Virginia Geologic and Economic Survey included sonic, gamma ray, and neutron logs that were used to correlate the log responses to geologic information provided in various reports. Sonic logs were used to generate synthetic seismograms that were tied to the seismic lines along strike.

The Rockingham-Whetzel well (Virginia Division of Mineral Resources No. W-1432) was drilled in 1965 by Shell Oil Company to a total depth of 14,176' (4,320 m) in northern Rockingham County, Virginia (Cardwell, 1977). The well is located between lines WV1 and WV2 on the relatively undeformed Broad Top Synclinorium (Figures 5.2, 5.5, 5.6, and 5.11. The proximity of the well to the seismic lines (~ 25 km), its location on a structure with only minor deformation, and the completeness of the lithologic section from the Upper Cambrian Conococheague Formation to the Upper Devonian Chemung Formation make it nearly ideal for this purpose. Formation tops were picked by combining information from reports (Brent, 1960; Johnson, 1965; Cardwell, 1977; Bartlett & Associates, 1981) with the well logs provided (Table 5.1).

The Tidewater-U.S. Forest Service No. 1 well (West Virginia Geologic and Economic Survey No. Pocahontas-21) was drilled in 1963 by Tidewater to a total depth of 11,932' (3468 m) in Pocahontas County, West Virginia. The well is located within 2 km of seismic line WV3 and is drilled into the culmination of the Browns Mountain Anticline, a major structure at the intraplateau deformation front. The well contains evidence for imbricate faulting within the structure because of duplication of the geology encountered in the well. The deepest formation encountered in the well was the lower Ordovician New Market or equivalent. Formation tops

were picked by combining information from reports (Cardwell, 1977; Diecchio, 1985; Kulander et al., 1986) with the well logs provided (Table 5.2).

5.4 Interpretation

The results of potential field attribute (PFA) analysis are shown in Figures 5.12 – 5.14. Major features are labeled on the maps and discussed below. The integration of the PFA maps and well data sets with the seismic data was accomplished by projecting the gridded PFA output onto the seismic lines and then plotting both the seismic data and their associated attributes. The projection program chooses the grid point closest to the location of each seismic station and outputs the station number and the associated attributes. These attributes can then be plotted above the seismic data for analysis.

The analytic signal map (Figure 5.12) has few large-scale anomalies with the exception of the two northeast-trending linear features labeled 'C'. These anomalies appear to correspond to the surface location of outcrops of Catoctin metavolcanics (see Figure 5.4). The Catoctin rocks have an average density of ~ 3.00 g/cm^3, a sharp contrast with the surrounding Precambrian basement rocks whose density is ~ 2.70 g/cm^3 (Edsall, 1974; Kolich, 1974). A large lateral density contrast in the near surface should produce a well-defined analytic signal anomaly. The near-surface density contrasts in the Valley and Ridge are either too small to produce a significant peak, or not of sufficient width to be detected using the chosen grid interval. The anomalies labeled 'C' also appear on the wavenumber map (Figure 5.14), but only the eastern outcrop belt of Catoctin rocks appears as a high on the tilt angle map (Figure 5.13). The reason for this could be that the western outcrop belt is located under a local low residual anomaly (see Figure 5.10).

The results of PFA analyses over the Blue Ridge are combined with seismic data in Figures 5.15 – 5-17. The seismic data are interpreted to show an imbricate stack of Cambrian-Ordovician carbonates beneath the leading edge of the Blue Ridge allochthon. The structure formed in response to the westward movement of the Blue Ridge and Piedmont over the lower Paleozoic shelf strata during the Alleghanian orogeny (Hatcher et al., 1989; Boyer, 1992). This duplex was interpreted to be present under line WV2 on the basis of seismic data (Lampshire et al., 1994); the data presented here indicates that the imbricate stack is laterally continuous beneath the Blue Ridge from northern to central Virginia over a distance of more than 150 km.

The local peak labeled 'A' on the tilt angle map (Figure 5.13) is just to the east of the surface location of the North Mountain Thrust (Figure 5.2). The seismic data in this area show a possible small-scale duplex of carbonates beneath the local gravity high (Figure 5.18).

The major anomaly on the tilt angle map (labeled 'B' in Figure 5.13) is a relatively wide (~20 km) high region extending off the map to the northeast. The edges of this feature approximate the mapped location of the Nittany Anticlinorium in West Virginia and Maryland. This feature does not continue southward as a positive feature indicating that the positive density contrast responsible for the tilt angle high is less prominent to the southwest. The wavenumber map shows a series of local highs along the western edge of this same anomaly

Table 5.1: Depths to formation tops and compressional wave velocities in the Rockingham-Whetzel well, Rockingham County, Virginia. The well has a nearly complete stratigraphic section from the Upper Cambrian to the Upper Devonian. Formation tops were evaluated using gamma ray, neutron, and sonic logs, then correlated to geology using various reports (Brent, 1960; Johnson, 1965; Cardwell, 1977; Bartlett & Associates, 1981). For generalized stratigraphy, see Figure 5.3.

Depth Interval (m)	Formation	Avg. Interval Velocity of Formation (m/s)
0 - ~620	Chemung	4550
~620 - ~950	Brallier	4170
~950 - ~1020	Millboro / Needmore	4350
~1020 - ~1070	Ridgely / Oriskany	5880
~1070 - ~1360	Helderburg	5710
~1360 - ~1480	Cayuga Group	5260
~1480 - ~1670	Bloomsburg	4760
~1670 - ~1730	Tuscarora	6060
~1730 - ~1890	Juniata	5400
~1890 - ~2010	Oswego	5000
~2010 - ~2380	Martinsburg	4350
~2380 - ~ 2650	Edinburg	5080
~2650 - ~2930	New Market	5880
~2930 - ~3520	Beekmantown	6450
~3520 - ~3720	Stonehenge	6670
~3760 - 4320	Conococheague	6350

Table 5.2: Depths to formation tops and compressional wave velocities in the Tidewater-U.S. Forest Service No. 1 well (Pocahontas 21), Pocahontas County, West Virginia. Only a limited portion of the well was logged using the sonic tool. The well was drilled into the Browns Mountain Anticline. The lithologic sequence in the anticline is highly faulted and has several repeated sections. Formation tops were evaluated using gamma ray and neutron logs, then correlated to geology using various reports (Cardwell, 1977; Diecchio, 1985; Kulander et al., 1986). For generalized stratigraphy, see Figure 5.3.

Depth Interval (m)	Formation	Avg. Interval Velocity of Formation (m/s)
0 - ~90	Rose Hill	not available
~90 - ~170	Tuscarora	" "
~170 - ~200	Fault / Wills Creek	" "
~200 - ~215	Williamsport	" "
~215 - ~265	McKenzie	" "
~265 - ~415	Rose Hill	" "
~415 - ~460	Tuscarora	" "
~460 - ~654	Juniata	" "
~654 - ~671	Oswego	" "
~671 - ~780	Martinsburg	" "
~780 - ~786	Fault	" "
~786 - ~811	Rose Hill	" "
~811 - ~825	Fault / McKenzie	" "
~825 - ~890	Wills Creek	" "
~890 - ~985	Williamsport	" "
~985 - ~1030	Fault / Wills Creek	" "
~1030 - ~1100	Williamsport	" "
~1100 - ~1350	McKenzie	" "
~1350 - ~1500	Rochester Shale?	" "
~1500 - ~1600	Rose Hill	" "
~1600 - ~1690	Tuscarora	" "
~1690 - ~1880	Juniata	" "
~1880 - ~1915	Oswego	" "
~1915 - ~2240	Martinsburg	5260
~2240 - ~2690	Trenton	5880
~2690 - ~2810	Black River	6450
~2810 - ~3050	New Market	6450
~3050 - ~3225	Beekmantown	6060
~3225 - ~3300	Fault / Black River	not available
~3300 - 3468	New Market	not available

(Figure 5.14). The change in trend on the tilt angle map could be indicative of a change in structural style from north to south beneath the Nittany Anticlinorium.

An interpretation combining reflection seismic, gravity, and well data over the Nittany Anticlinorium in Virginia and West Virginia is shown in Figures 5.19 – 5-21. Synthetic seismograms generated from the well log sonic and density information were used to tie the subsurface lithology to seismic reflectivity. The seismic data in Figures 5.19 and 5.20 were tied to the Rockingham-Whetzel well. Some of the stronger reflections in the data are not at formation boundaries, a result predicted by Christensen and Szymansky (1991) from synthetic seismograms constructed for a similar sequence of rocks in the southern Appalachians in Tennessee. They postulated that the high-amplitude reflections were from constructive interference of reflections from alternating shales, siltstones or carbonates, producing a thin-bed 'tuning' effect (Sengbush et al., 1961).

The seismic data for the northern two lines, WV1 and WV2 (Figures 5.19 and 5.20), are interpreted as a large-scale blind thrust of Cambrian-Ordovician carbonates overriding a deeper section across the entire width of the Nittany Anticlinorium. This produces a large lateral density contrast over a significant area and is reflected in the tilt angle map (Figure 5.13). This is the same general conclusion reached by Wilson (1989) and Wilson and Shumaker (1992) for the same area using gravity and reflection seismic data. To the south, line WV3 also shows a ramp with an overlying thrust imbricate above it (Figure 5.21); this particular thrust imbricate is interpreted to extend only a short distance, thereby generating a smaller response on the tilt angle map ('D' in Figure 5.13). The rest of the seismic data to the west in Figure 5.21 is interpreted to contain a series of smaller imbricate blocks that are of a size below the limit of resolution for the tilt angle method. The wavenumber map (Figure 5.14) does indicate a small contrast at the western edge of the Nittany Anticlinorium, though the seismic data are inconclusive as to its cause. One possibility is a change in the level of deformation at the Allegheny Structural Front to detachments at higher levels in the sedimentary section (e.g. Hatcher, 1989). The smaller density contrasts in the overlying upper Ordovician through Devonian strata could produce a small anomaly on the wavenumber map as the higher density carbonates stayed at their original level. This interpretation is supported by the lack of lower Ordovician carbonates and the extensive faulting at the Browns Mountain Anticline to the west (Kulander et al, 1986).

The tilt angle and seismic data would therefore indicate that the structure beneath the Nittany Anticlinorium changes to the south in Virginia from large-scale blind thrusting to imbricate thrusting. This could be a reflection of the change in structural style from blind thrusting in the central Appalachians to break-through thrusting in the southern Appalachians that occurs just to the south of this area (e.g. Hatcher et al., 1989). The change in structural style is indicated also by the imbrication at the nearby intraplateau deformation front in the Pocahontas 21 well (Table 5.2).

5.5 Conclusions

Integration of seismic, gravity, well, and geologic information has allowed for an investigation of the lateral continuity of two major structures in the Valley and Ridge and Blue Ridge provinces of the central Appalachians. The application of new processing and analysis methods to seismic (dip projection processing) and gravity (potential field attributes) data have greatly improved the interpretation of these data.

In dip projection, conventionally processed, crooked-line common midpoint gathers are projected onto a straight line in the general dip direction. The resultant stack better approximates a dip-oriented geologic cross section and is therefore more interpretable. Potential field attribute (PFA) analysis uses three maps generated from a combination of vertical and horizontal derivatives of the gravity field. The three maps – analytic signal, tilt angle, and wavenumber – highlight different aspects of the gravity field and enhance its overall interpretation. Deep well information established a tie between the seismic data and lithologies on seismic lines WV1 and WV2, also aiding interpretation.

A imbricate stack of Cambrian-Ordovician carbonates is interpreted to extend under the western edge of the crystalline Blue Ridge thrust sheet for at least 150 km along strike. The Nittany Anticlinorium is underlain in West Virginia by a broad (~20 km wide) blind thrust sheet of Cambrian-Ordovician carbonates. To the south in Virginia, the structural style changes to that of smaller imbricate blocks in the lower part of the section. This contrast in styles along the Nittany Anticlinorium could be related to the transition between the southern and central Appalachian deformation styles.

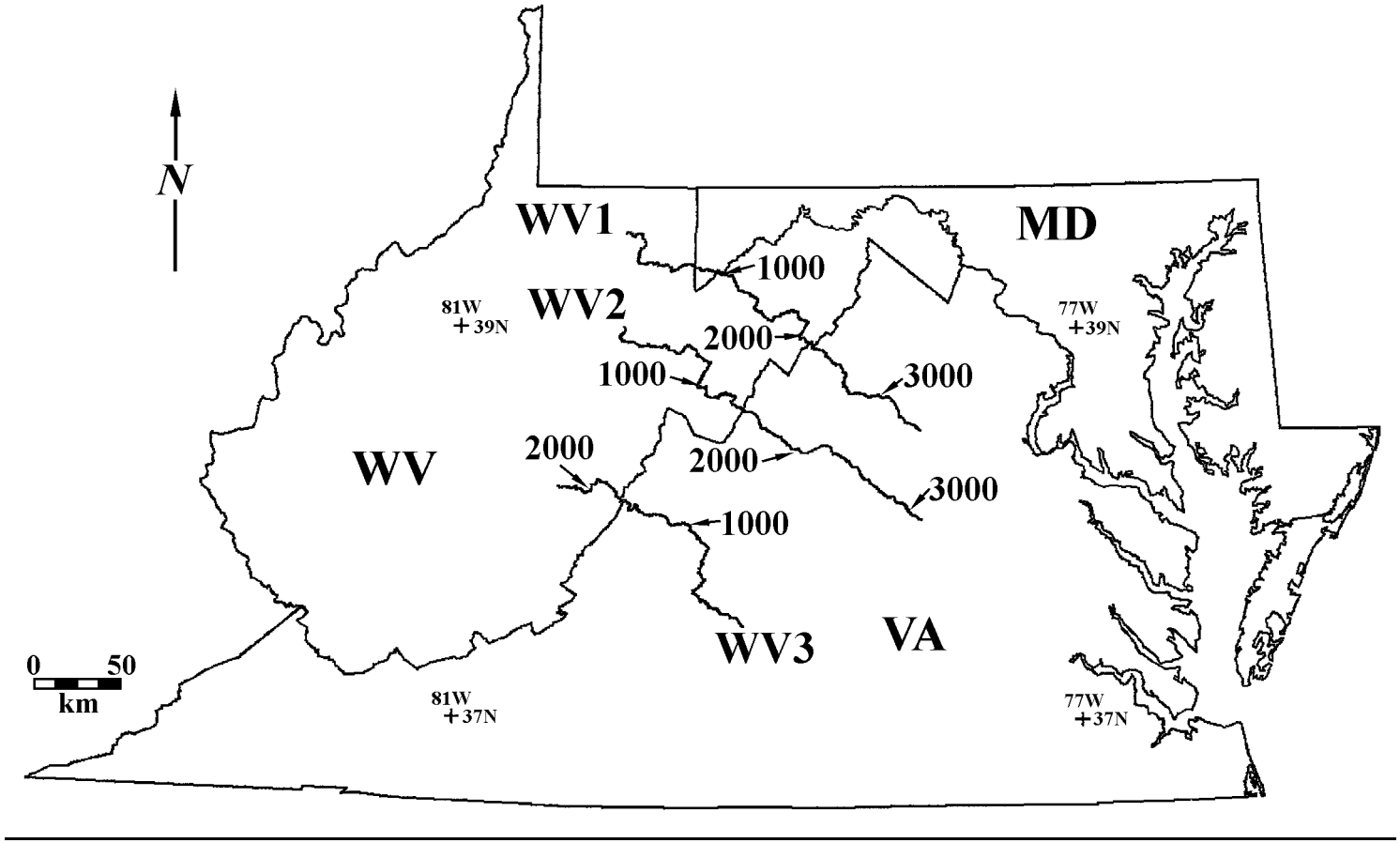

Figure 5.1: Location of seismic profiles used in this study. Map projection is Virginia North state plane. Scale is 1:4000000.

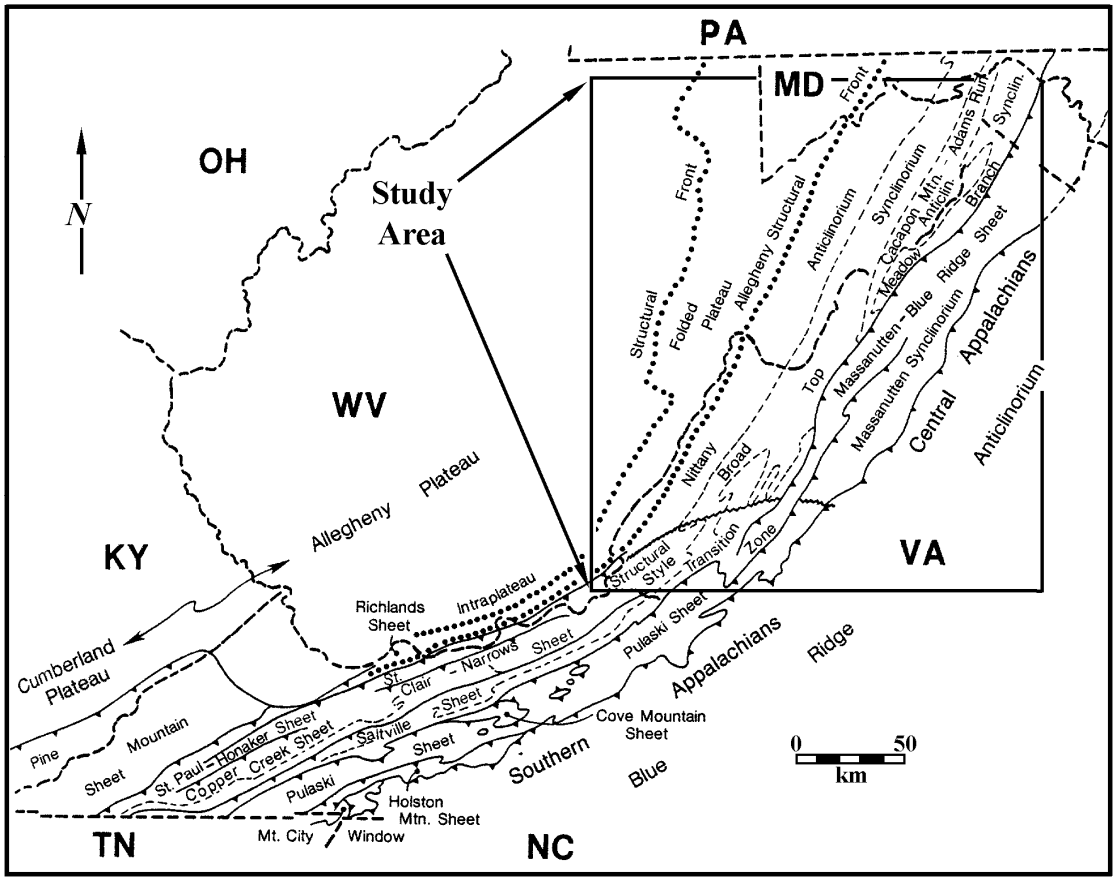

Figure 5.2: Major structural features in the central Appalachian Valley and Ridge. Box indicates approximate location of study area. (Modified from Kulander and Dean, 1986).

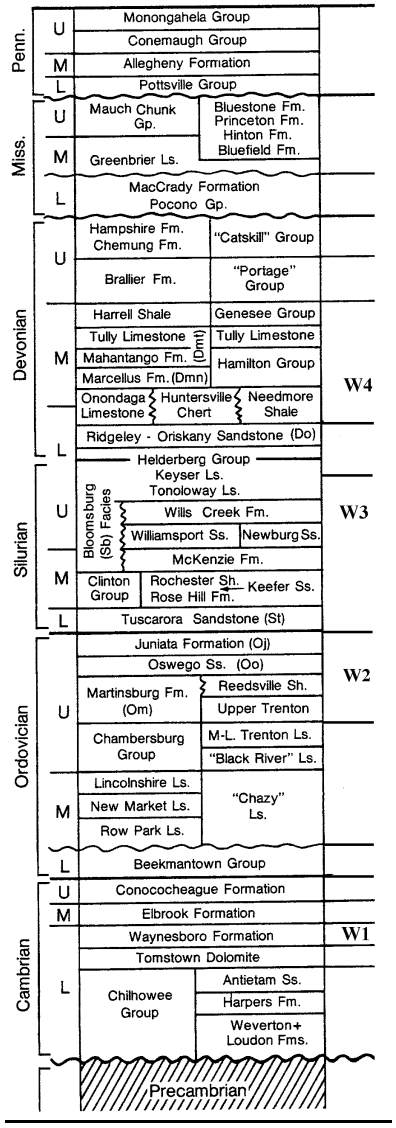

Figure 5.3: Stratigraphic correlation chart for the central Appalachians. Undulating and vertical sawtooth boundaries indicate unconformities and lateral facies variations. Letters W1 – W4 indicate relatively weak zones in the stratigraphy where decollements can form. W1, Rome/Waynesboro shale; W2, Martinsburg and other upper Ordovician shales; W3, locally weak horizon in central Appalachians; W4, Devonian shales (modified from Kulander and Dean, 1986, and Wilson and Shumaker, 1988).

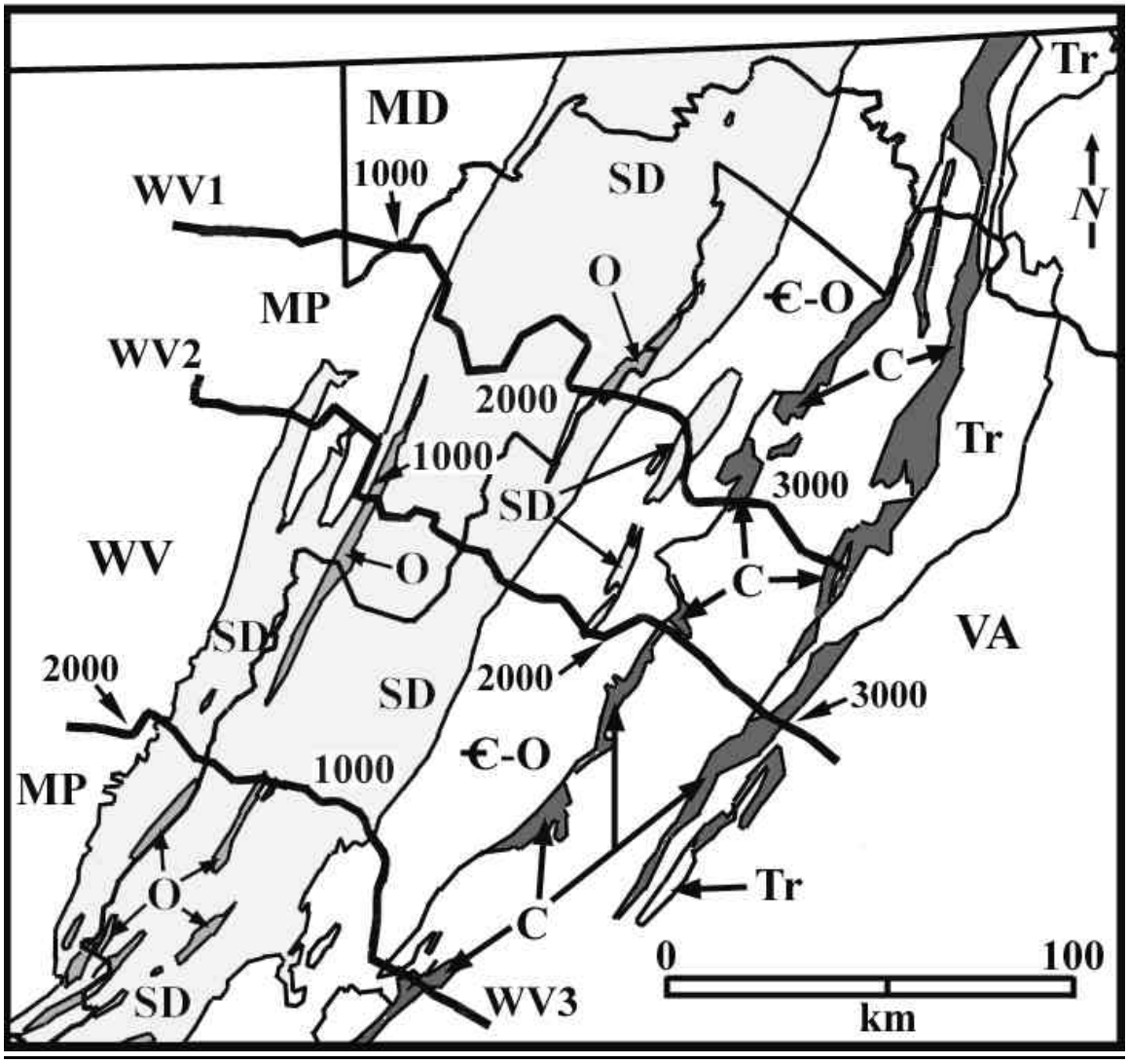

Figure 5.4: Geologic map of the study area. Heavy lines represent the locations of reflection seismic data used in this study. **C** (dark shading) = Catoctin metavolcanics; **C-O** = Cambrian and Ordovician sedimentary rocks; **O** (medium shading) = Ordivician rocks; **SD** (light shading) = Silurian and Devonian sedimentary rocks; **MP** = Mississippian and Pennsylvanian sedimentary rocks; and **Tr** = Triassic basin sedimentary and igneous rocks.

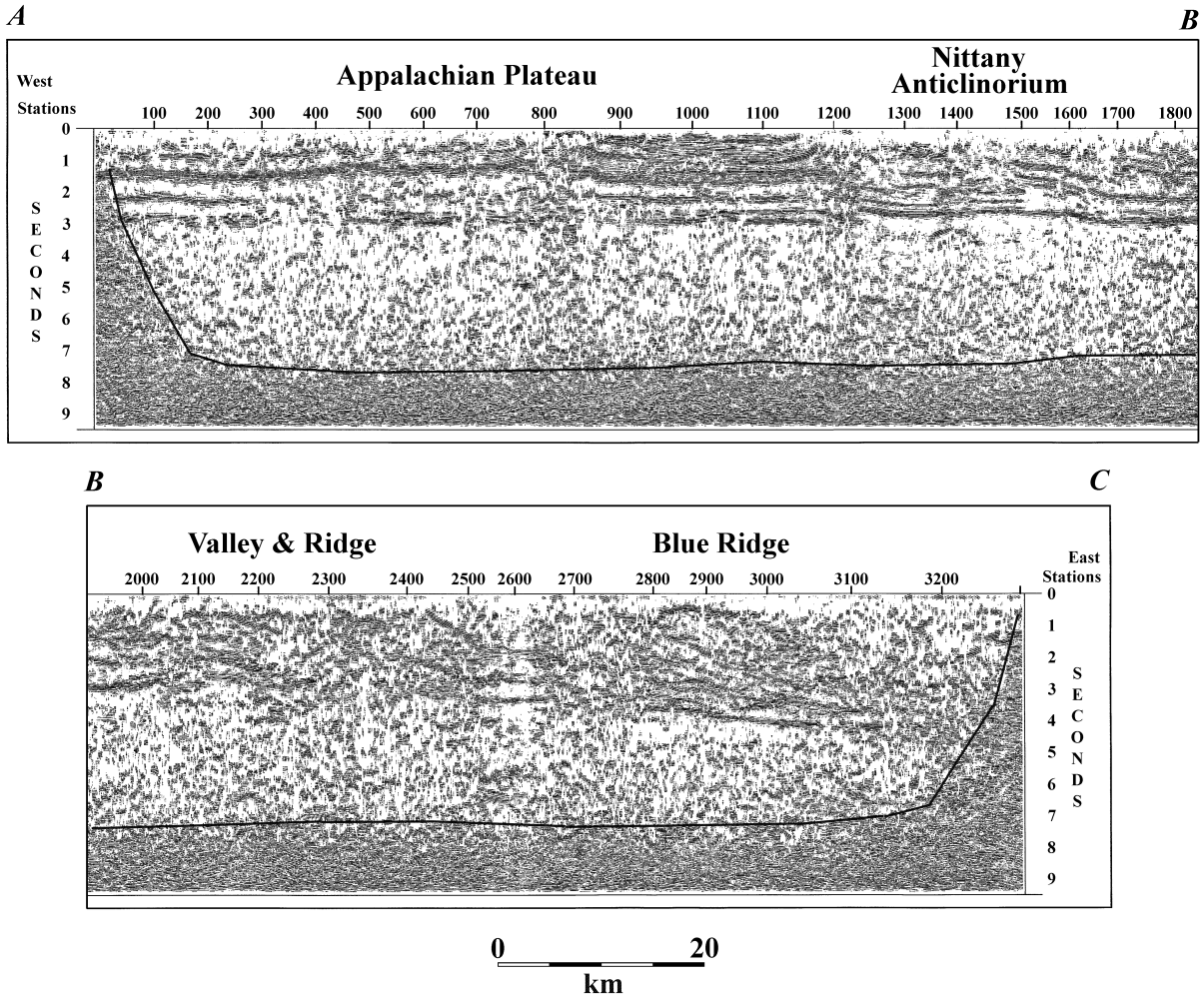

Figure 5.5: Dip-projectied and migrated version of seismic line WV1. Kirchhoff post stack migration using 90% stacking velocities. Data show thin-skinned deformation above a master decollement at ~ 3.0 seconds. Black line highlights the zone of migration smearing in the data; only data above this line is interpretted. Data plotted at 1:1 for 6 km/s. (Large PDF can be viewed by clicking on the figure.)

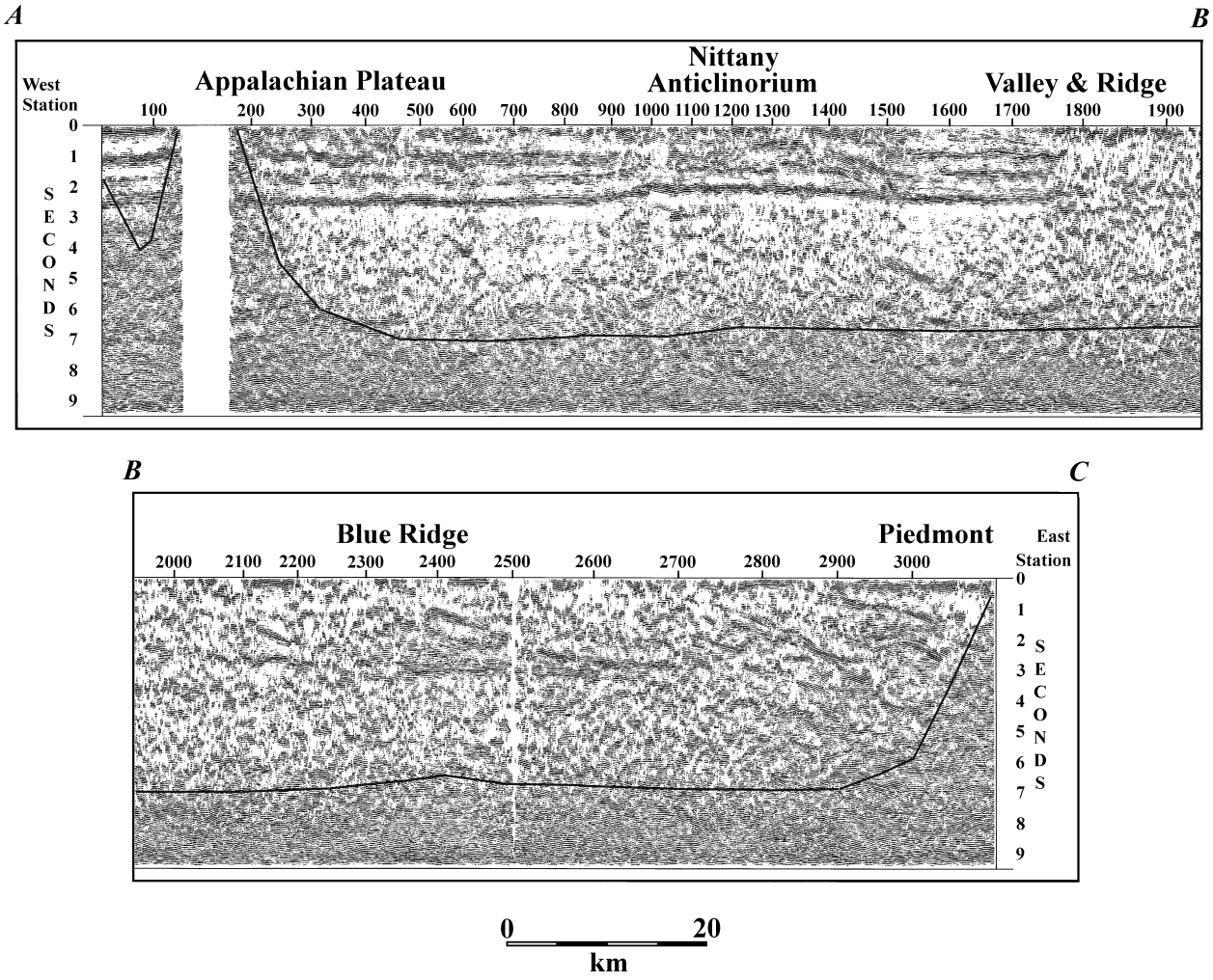

Figure 5.6: Dip-projectied and migrated version of seismic line WV2. Kirchhoff post stack migration using 90% stacking velocities. Data show thin-skinned deformation above a master decollement at ~ 2.5 seconds. Black line highlights the zone of migration smearing in the data; only data above this line is interpretted. Data plotted at 1:1 for 6 km/s. (Large PDF can be viewed by clicking on the figure.)

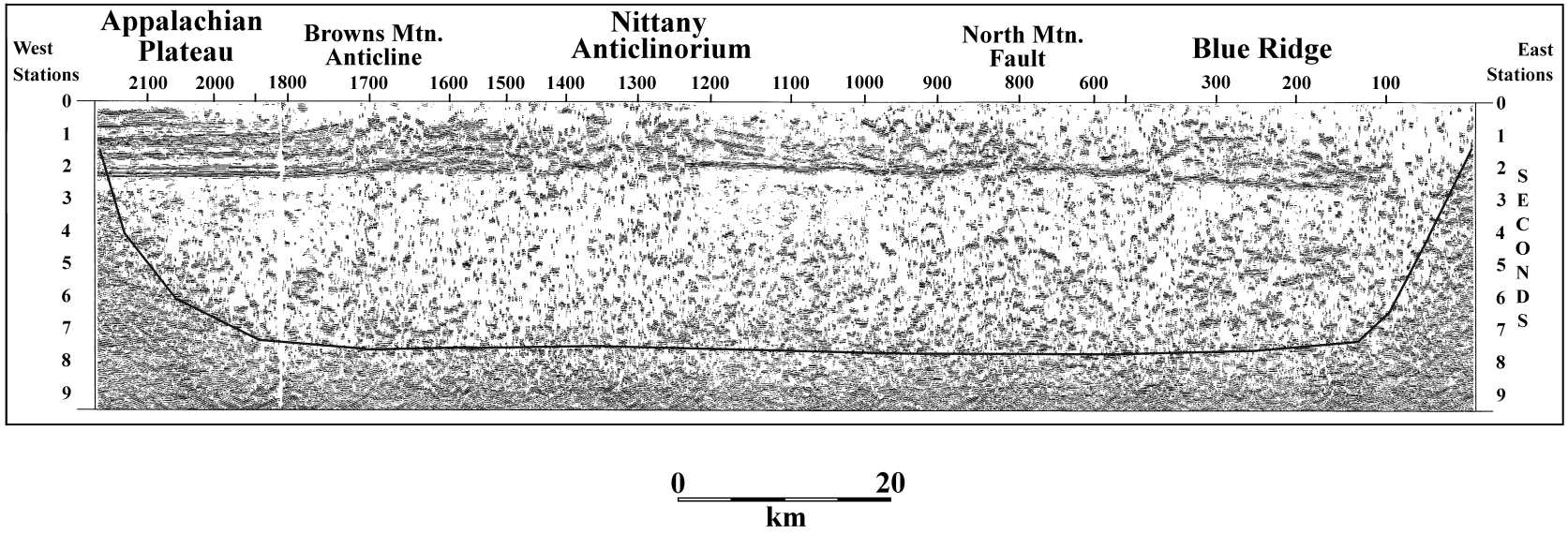

Figure 5.7: Dip-projectied and migrated version of seismic line WV3. Kirchhoff post stack migration using 90% stacking velocities. Data show thin-skinned deformation above a master decollement at ~ 2.0 seconds. Black line highlights the zone of migration smearing in the data; only data above this line is interpretted. Data plotted at 1:1 for 6 km/s. (Large PDF file can be viewed by clicking on the figure.)

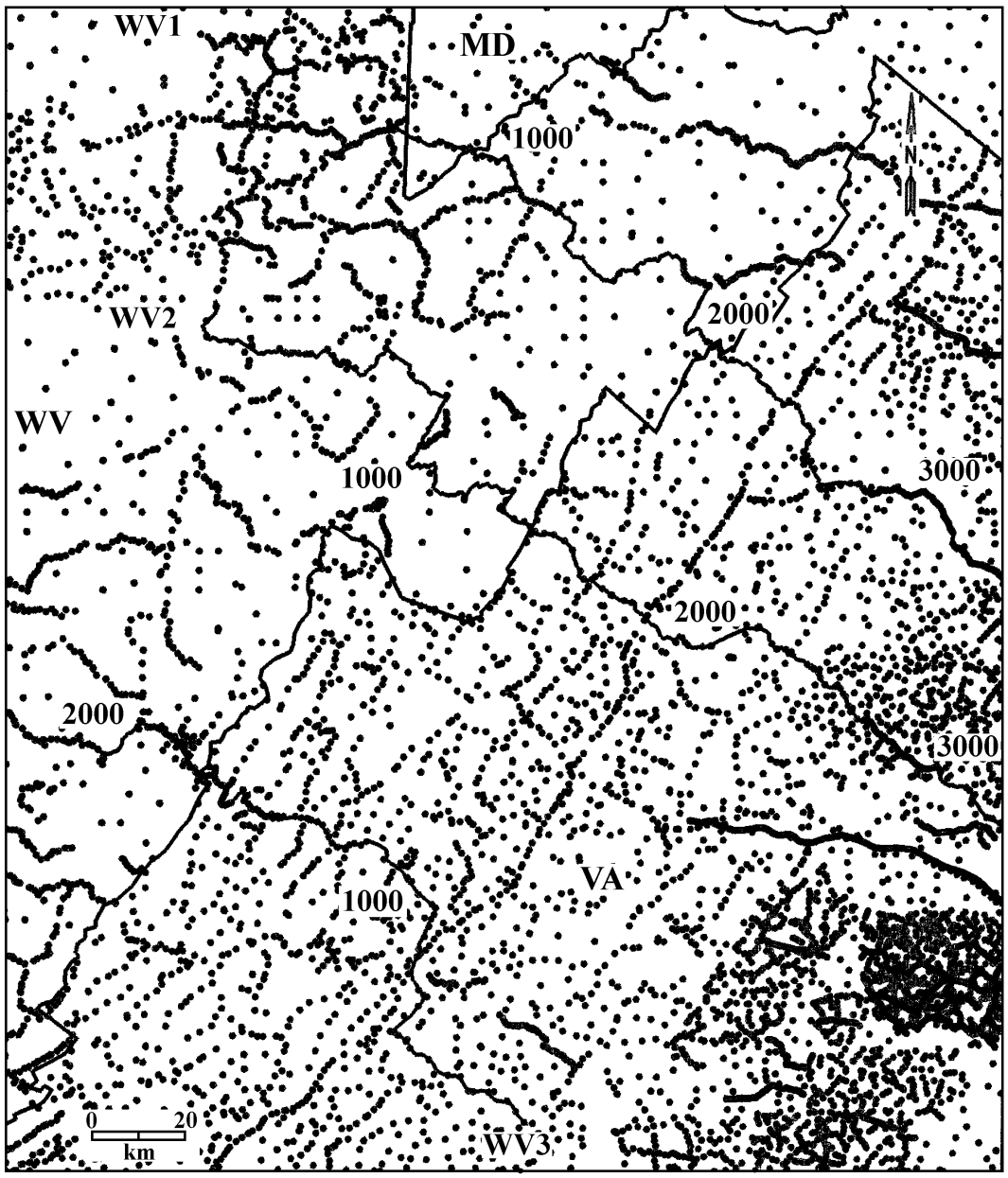

Figure 5.8: Original distribution of gravity stations within the study area before gridding. The gravity station data are from the Defense Mapping Agency (Hittleman et al., 1994). Contour interval 5 mgal. Scale is 1:100000. Projection: Virginia North State Plane.

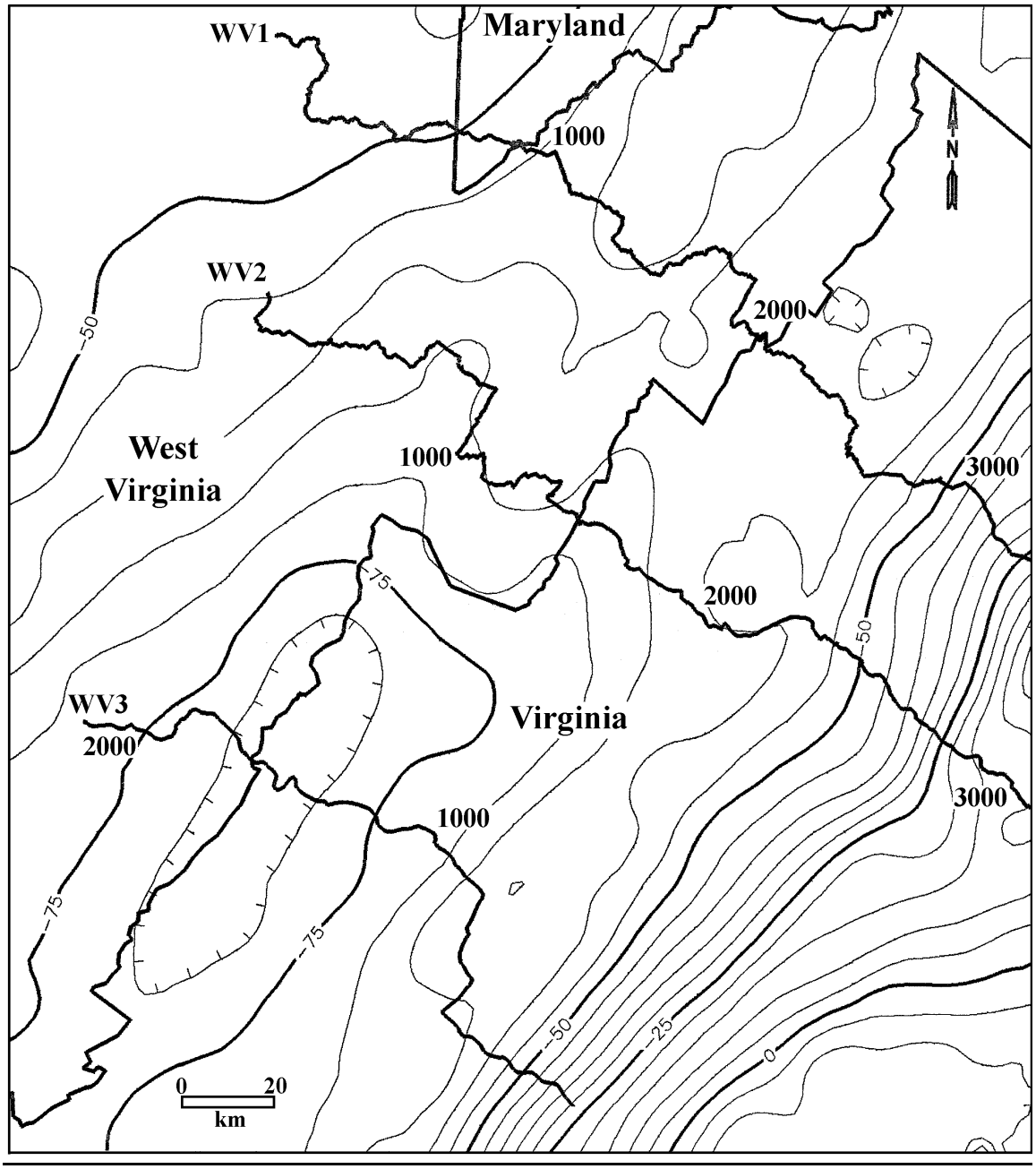

Figure 5.9: Bouguer gravity anomaly map prepared using Defense Mapping Agency data from the Gravity CD-ROM of the National Geophysical Data Center (Hittleman, et al., 1994). The Appalachian Gravity Low and the Piedmont Gravity Gradient can easily be seen. Map projection Virginia North state plane; scale 1:1000000. Contour interval 5 mgal.

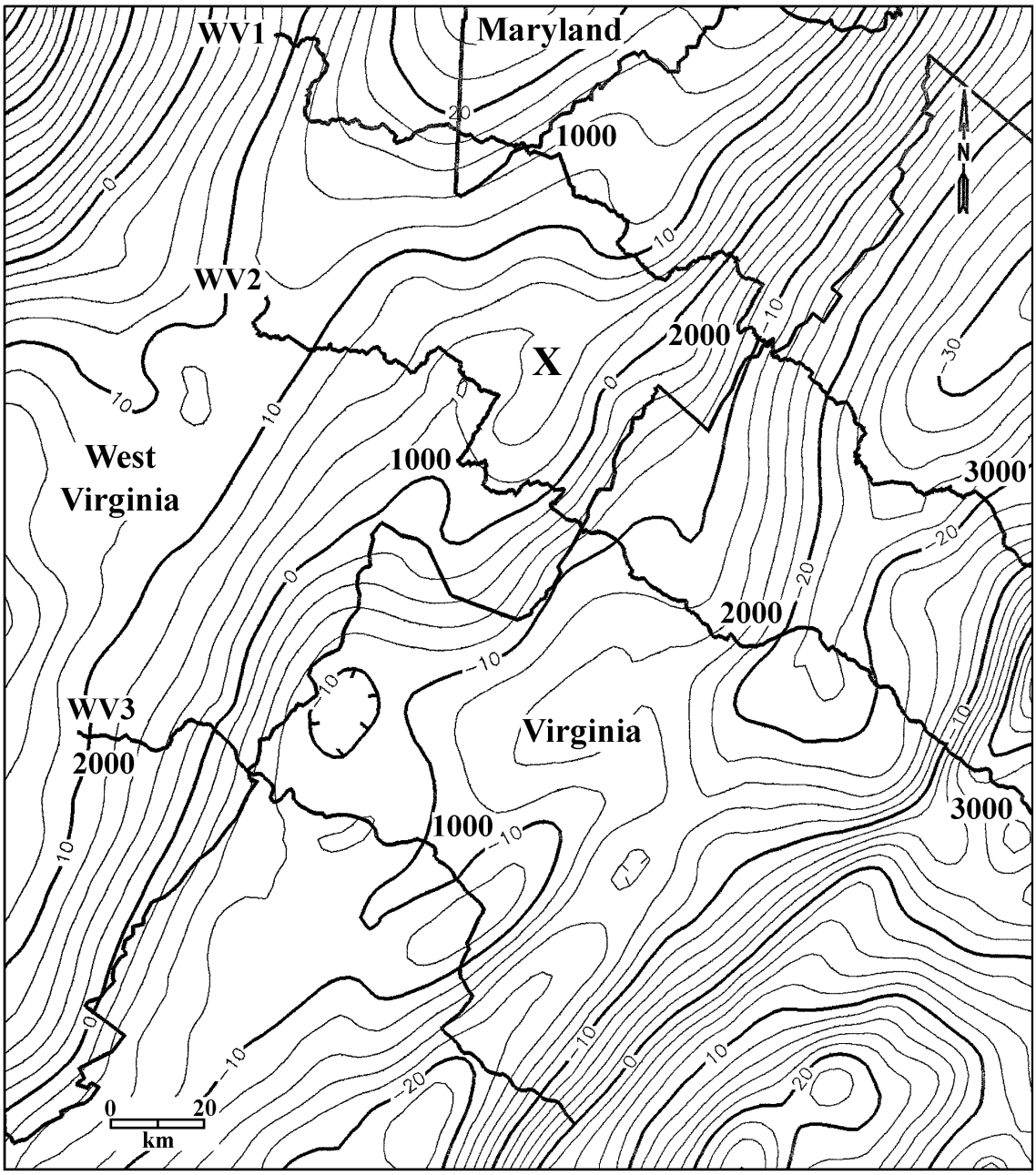

Figure 5.10: Residual gravity anomaly map obtained from the data shown in Figure 5.7 by the removal of a third-order trend surface. The Appalachian Gravity Low has been removed by the trend surface. Note the divergence ('X') of the contours between seismic lines WV1 and WV2. Map projection Virginia North state plane; scale 1:1000000. Contour interval 2 mgal.

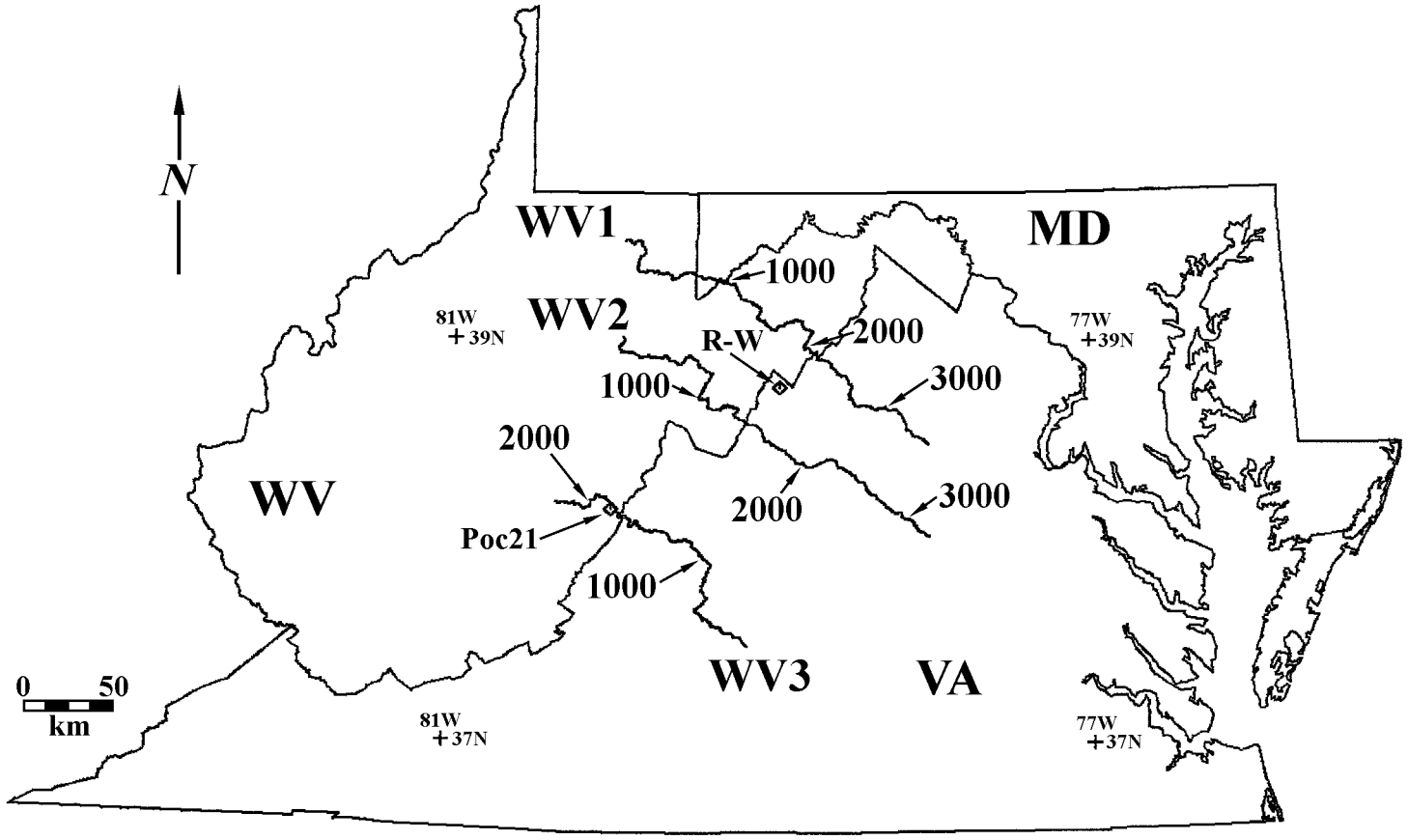

Figure 5.11: Well location map. Both the Rockingham-Whetzel ('R-W') and the Pocahontas Co. #21 ('Poc21') are shown. Map projection Virginia North state plain; scale is 1:4000000.

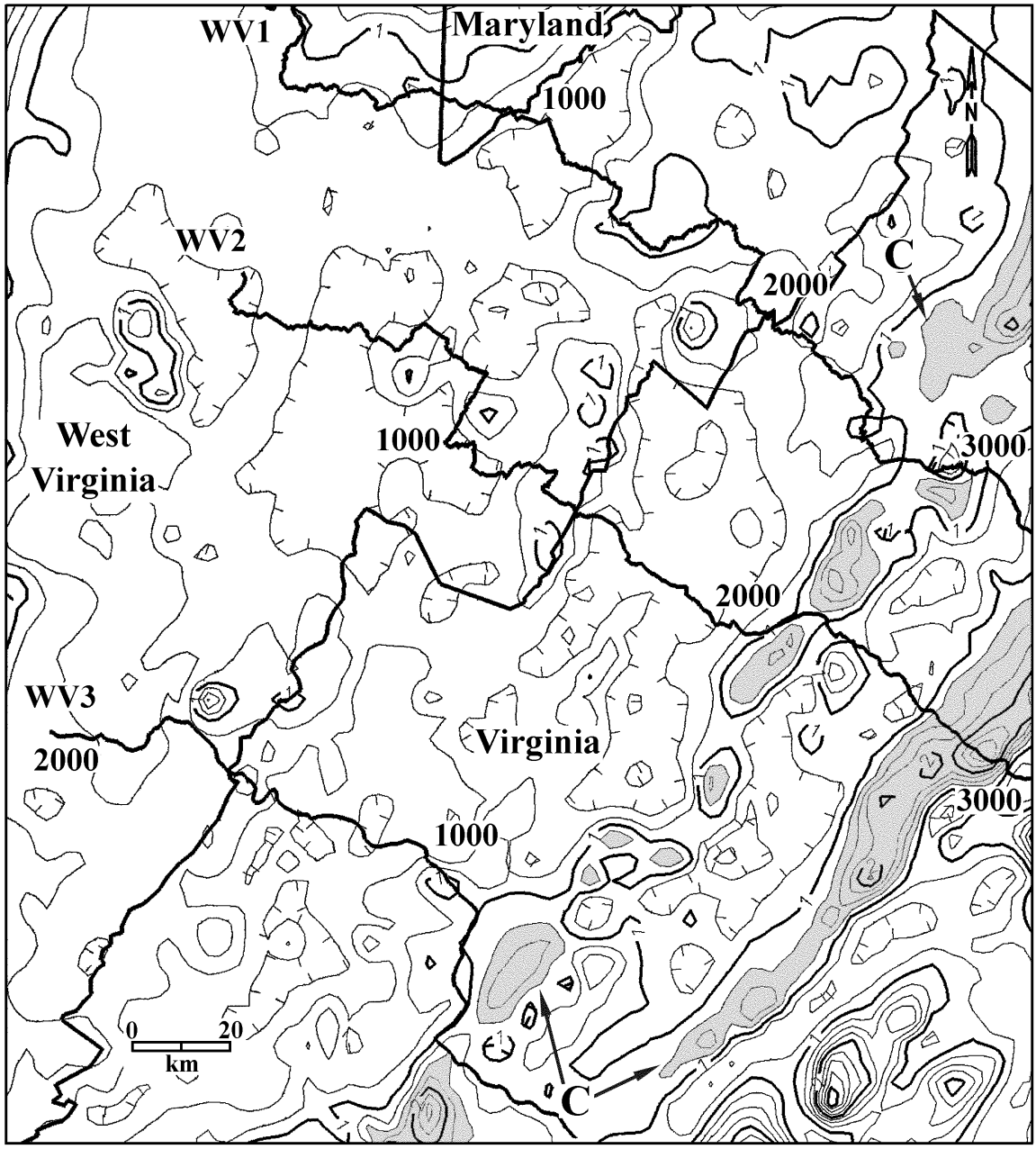

Figure 5.12: Map showing the calculated analytic signal over the study area. Gray color highlights a series of highs possibly associated with the Catoctin metavolcanics flanking the Blue Ridge (labeled 'C'). Map projection Virginia North state plane; scale is 1:1000000. Contour interval = 0.25 mgal/km.

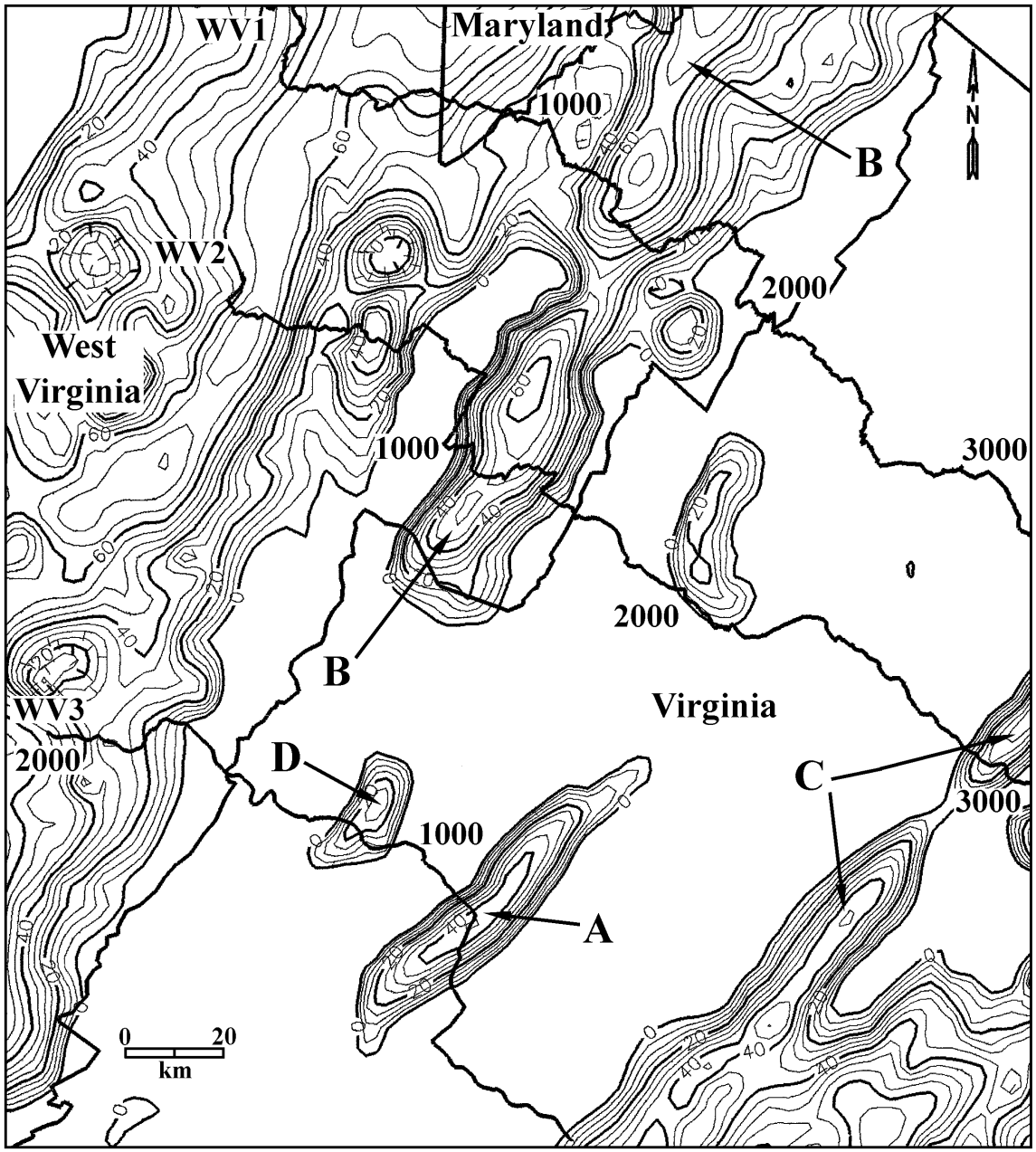

Figure 5.13: Map showing the calculated tilt angle over the study area. Only positive values are shown. The map shows highs over areas of smaller ('A' and 'D') and a large thrust sheet ('B') of higher-density Cambrian-Ordovician carbonates, and the eastern flank of the Blue Ridge and the associated high density Catoctin metavolcanics ('C'). Area 'B' approximates the location of the Nittany Anticlinorium in West Virginia; 'D' is associated with the same structure in Virginia (see text for details). Map projection Virginia North state plane; scale is 1:1000000. Contour interval = 5 degrees.

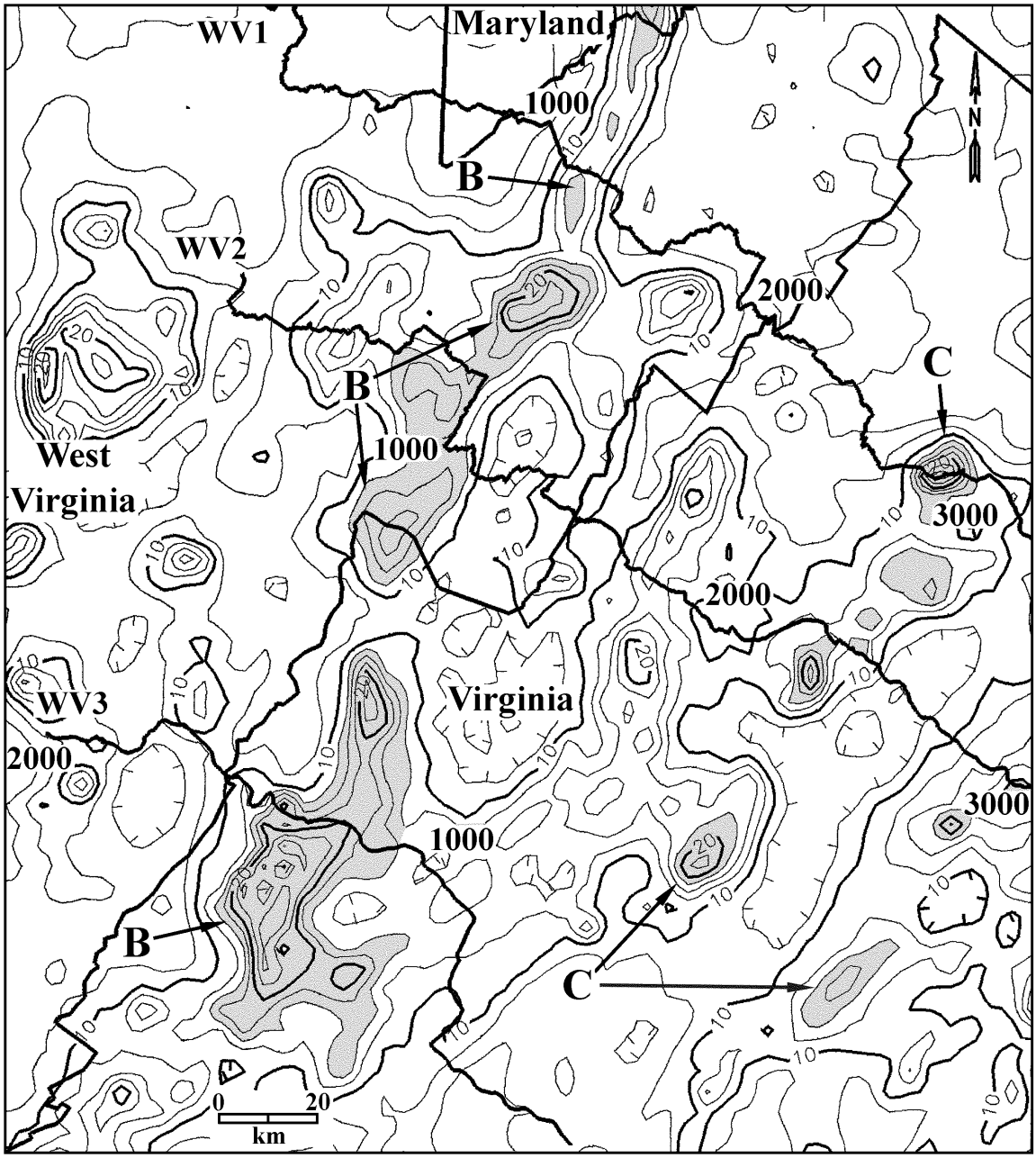

Figure 5.14: Map showing the calculated wavenumber over the study area. The map shows pronounced highs trending north-northeast ('B' and 'C'; shaded gray on map) The westernmost belt of highs ('B') are associated with the leading edge of the Nittany Anticlinorium and the Alleghany structural front in Virginia and West Virginia. The eastern set of highs ('C') are associated with high density Catoctin metavolcanics . (See text for details). Map projection Virginia North state plane; scale is 1:1000000. Contour interval = 2 degrees/km.

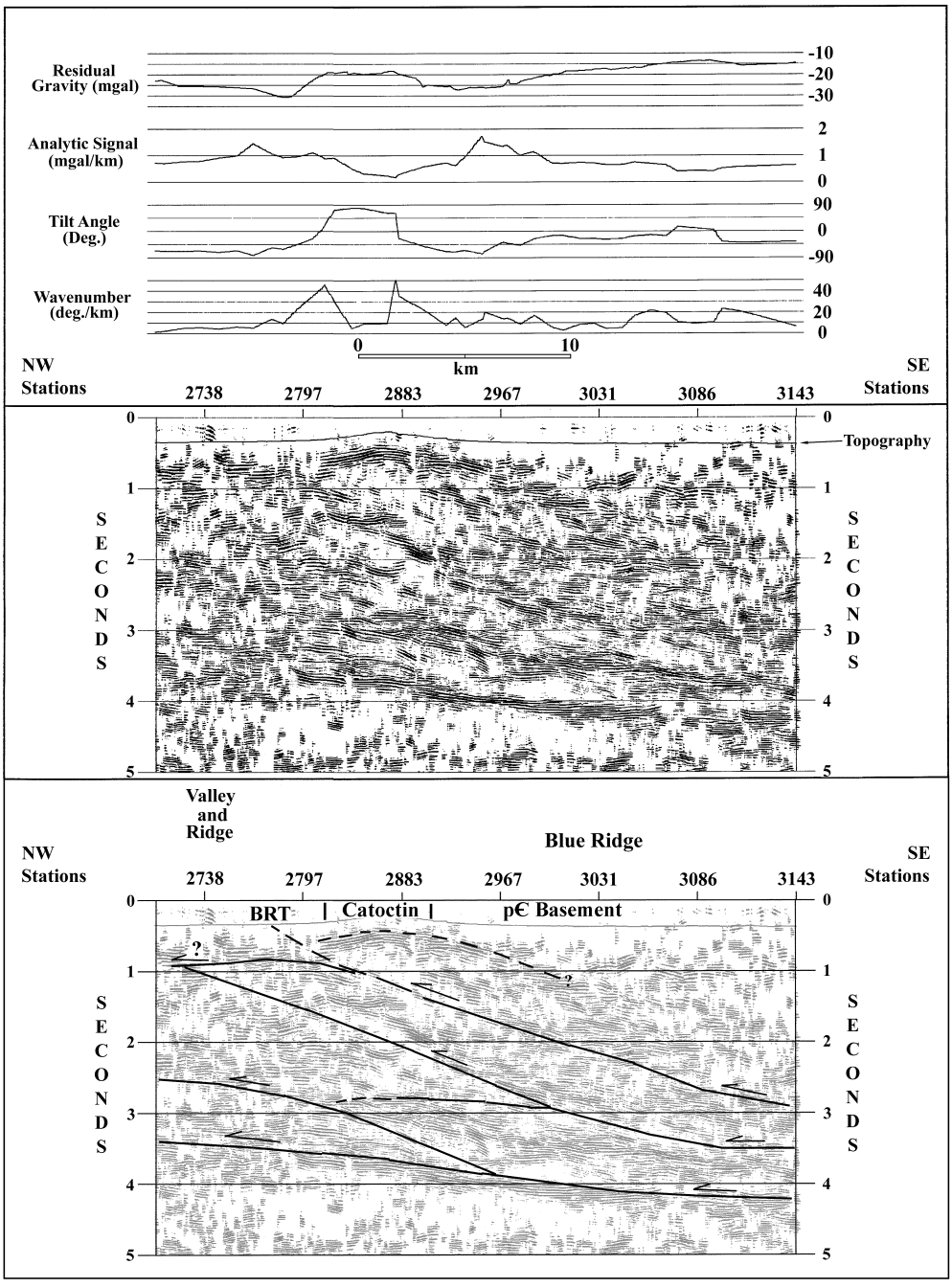

Figure 5.15: Dip-projected and migrated line WV1 over the western Blue Ridge province in Virginia with residual gravity and potential field attributes (PFAs) plotted above. Seismic data image a large duplex of lower Paleozoic strata; PFA analysis highlights the surface location of the Catoctin metavolcanics. 'BRT' is the Blue Ridge thrust. Seismic data plotted at 1:1 for 6 km/sec.

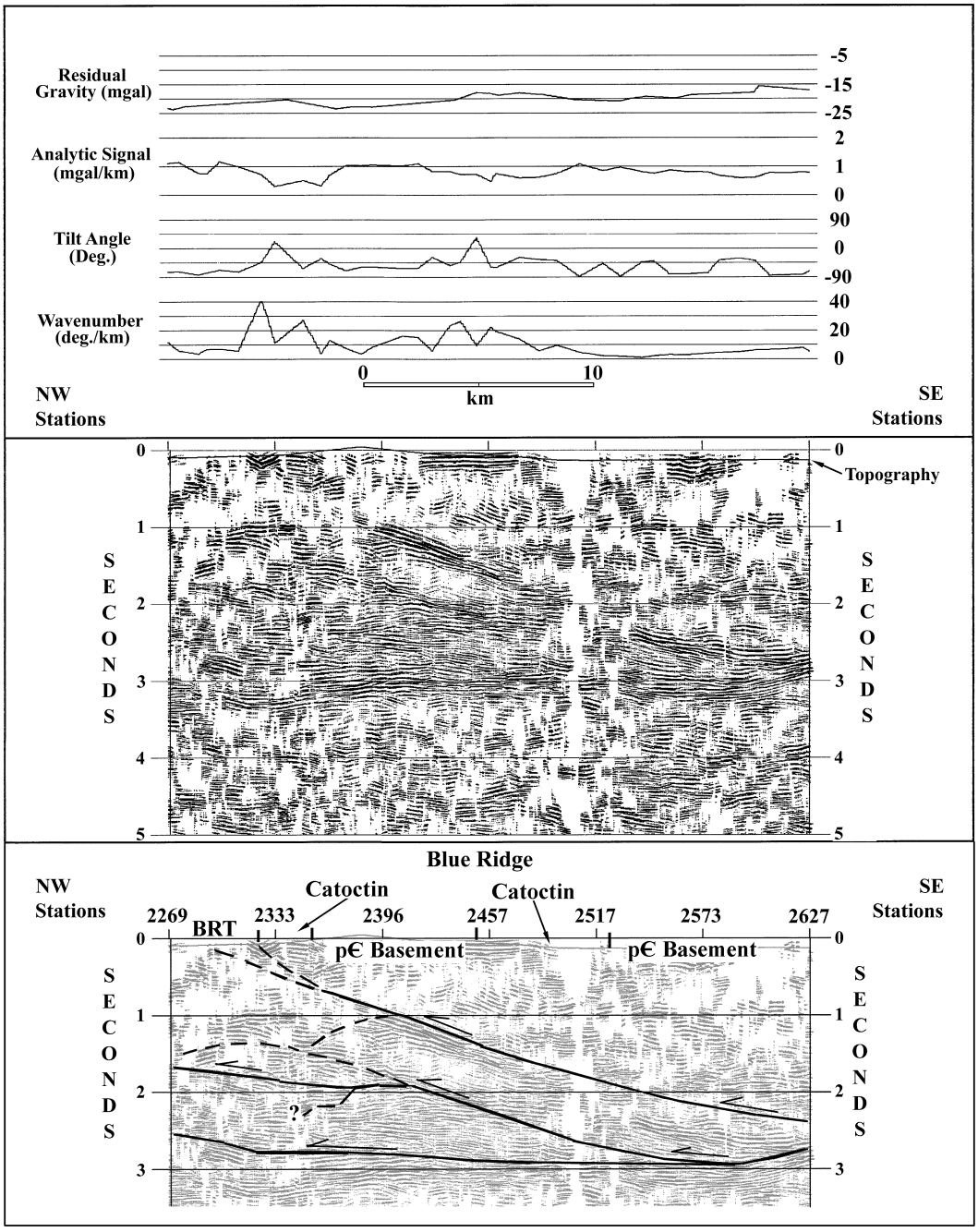

Figure 5.16: Dip-projected and migrated line WV2 over the western Blue Ridge province in Virginia with residual gravity and potential field attributes (PFAs) plotted above. Seismic data image an imbricate fan duplex of lower Paleozoic strata and possible Precambrian basement. PFA analysis again highlight the surface locations of the Catoctin metavolcanics. 'BRT' is the Blue Ridge thrust. Seismic data plotted at 1:1 for 6 km/sec.

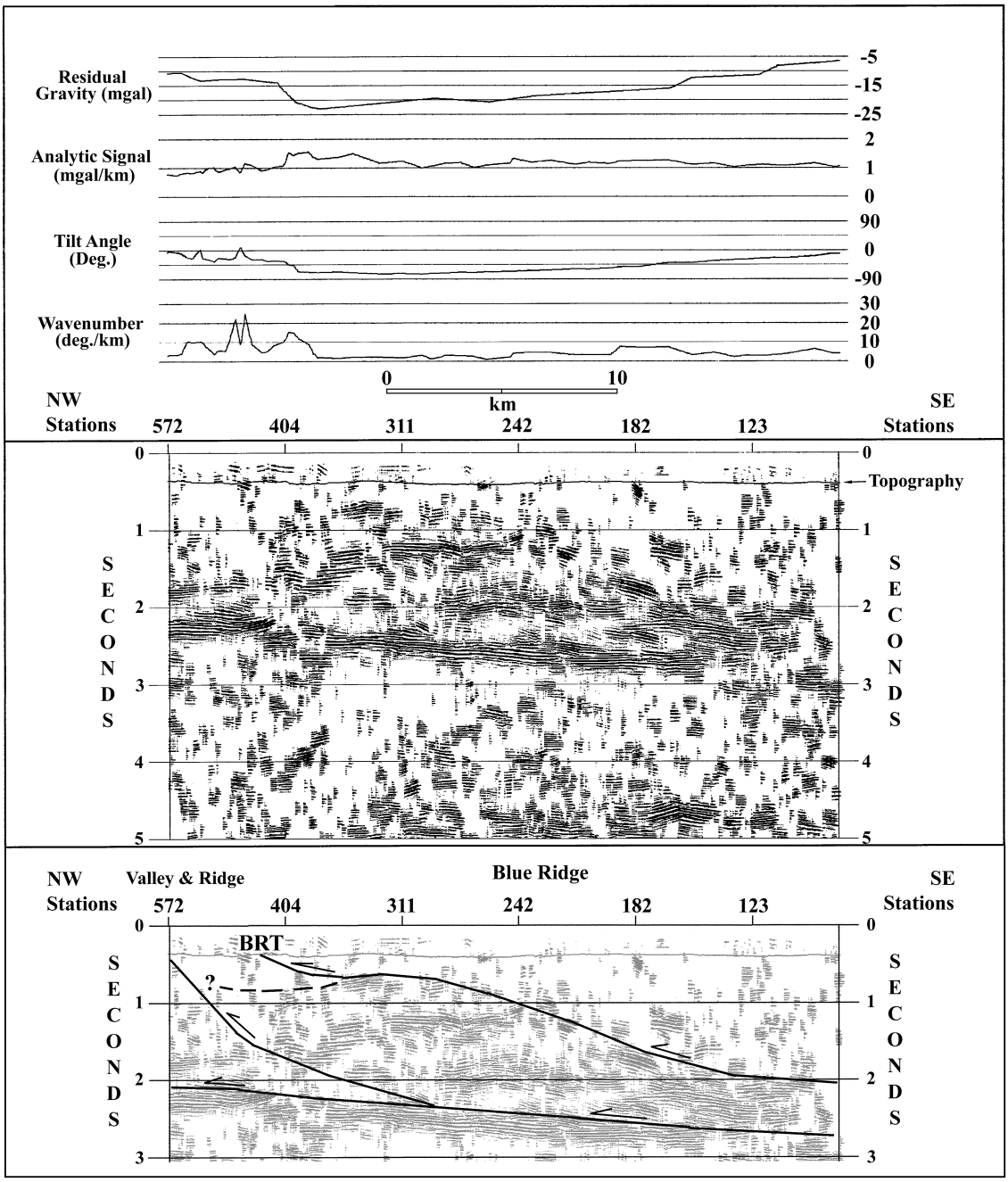

Figure 5.17: Dip-projected and migrated line WV3 over the western Blue Ridge province in Virginia with residual gravity and potential field attributes (PFAs) plotted above. Seismic data image a large duplex of lower Paleozoic strata; PFA analysis shows little in this instance. 'BRT' is the Blue Ridge thrust. Seismic data plotted at 1:1 for 6 km/sec.

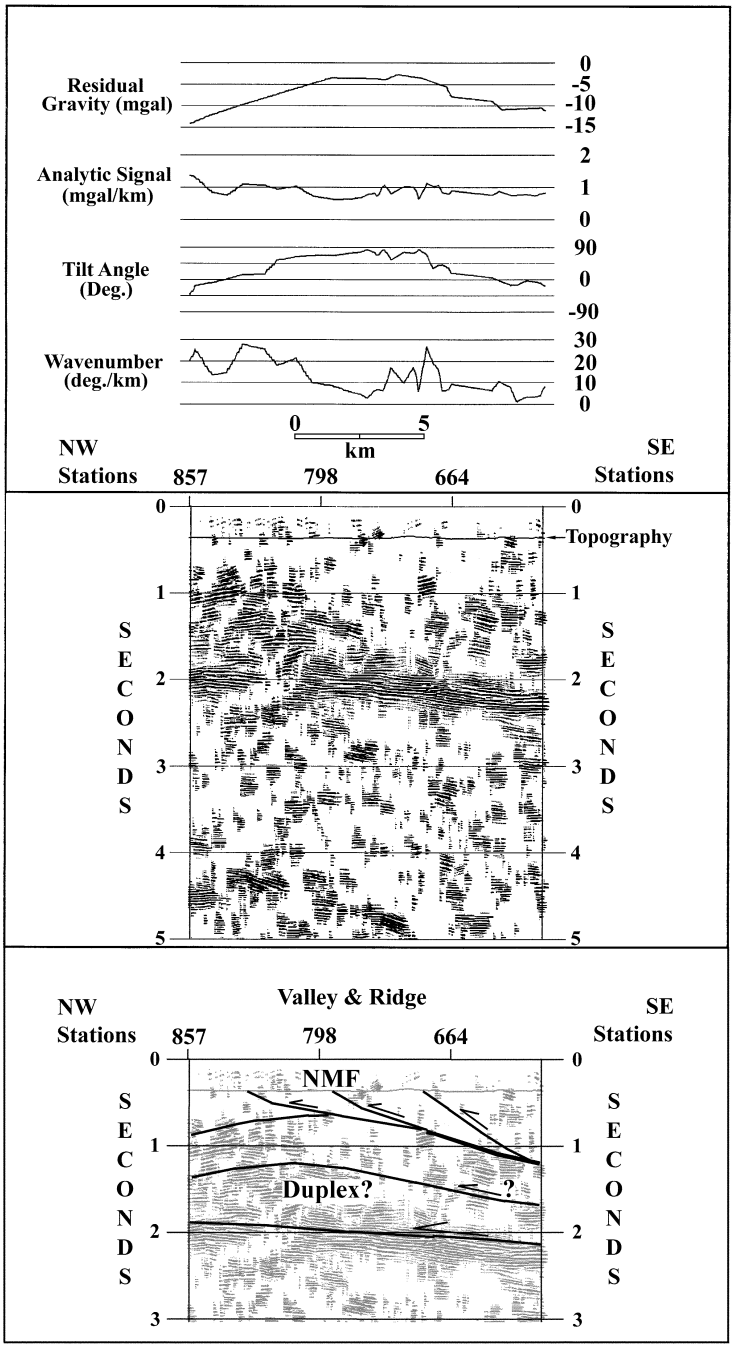

Figure 5.18: Dip-projected and migrated line WV3 crossing the location on the tilt angle map (Figure 5.13) marked 'A' with residual gravity and potential field attributes (PFAs) plotted above. Seismic data image a small duplex (?) of lower Paleozoic carbonates; PFA analysis shows the lateral density change associated with the duplex. 'NMF' is the North Mountain fault. Seismic data plotted at 1:1 for 6 km/sec.

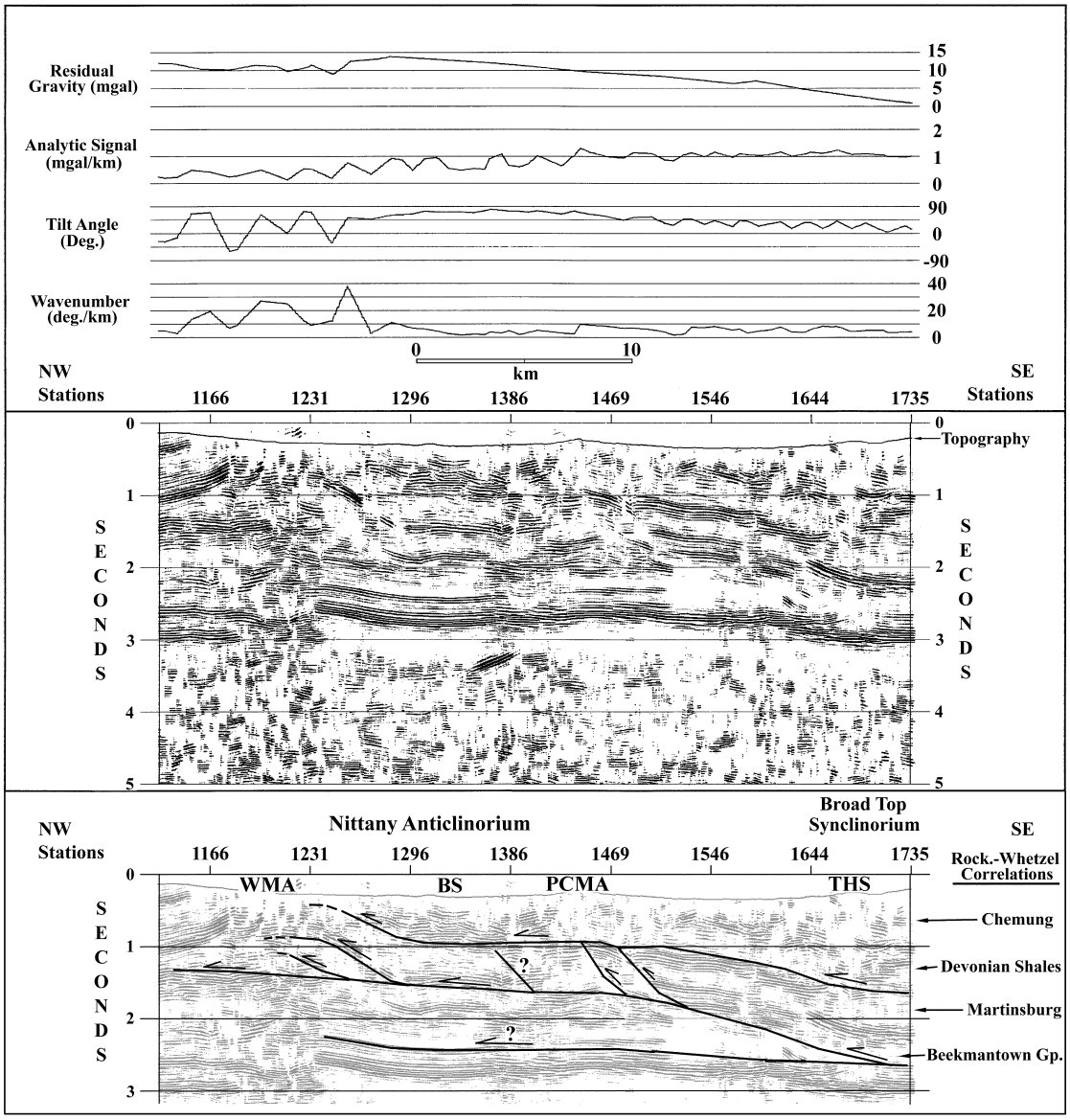

Figure 5.19: Dip-projected and migrated line WV1 over the Nittany Anticlinorium in eastern West Virginia with residual gravity and potential field attributes (PFAs) plotted above. The broad high on the tilt angle and high on the wavenumber show the location of the large thrust sheet and its leading edge as revealed by the seismic data below. Lower section also shows lithologic correlation to the Rockingham-Whetzel log made from a synthetic seismogram. 'WMA' is the Wills Mountain Anticline, 'BS' the Bedford Syncline, 'PCMA' the Paterson Creek Mountain Anticline and 'THS' the Town Hill Syncline. Seismic data plotted at 1:1 for 6 km/sec.

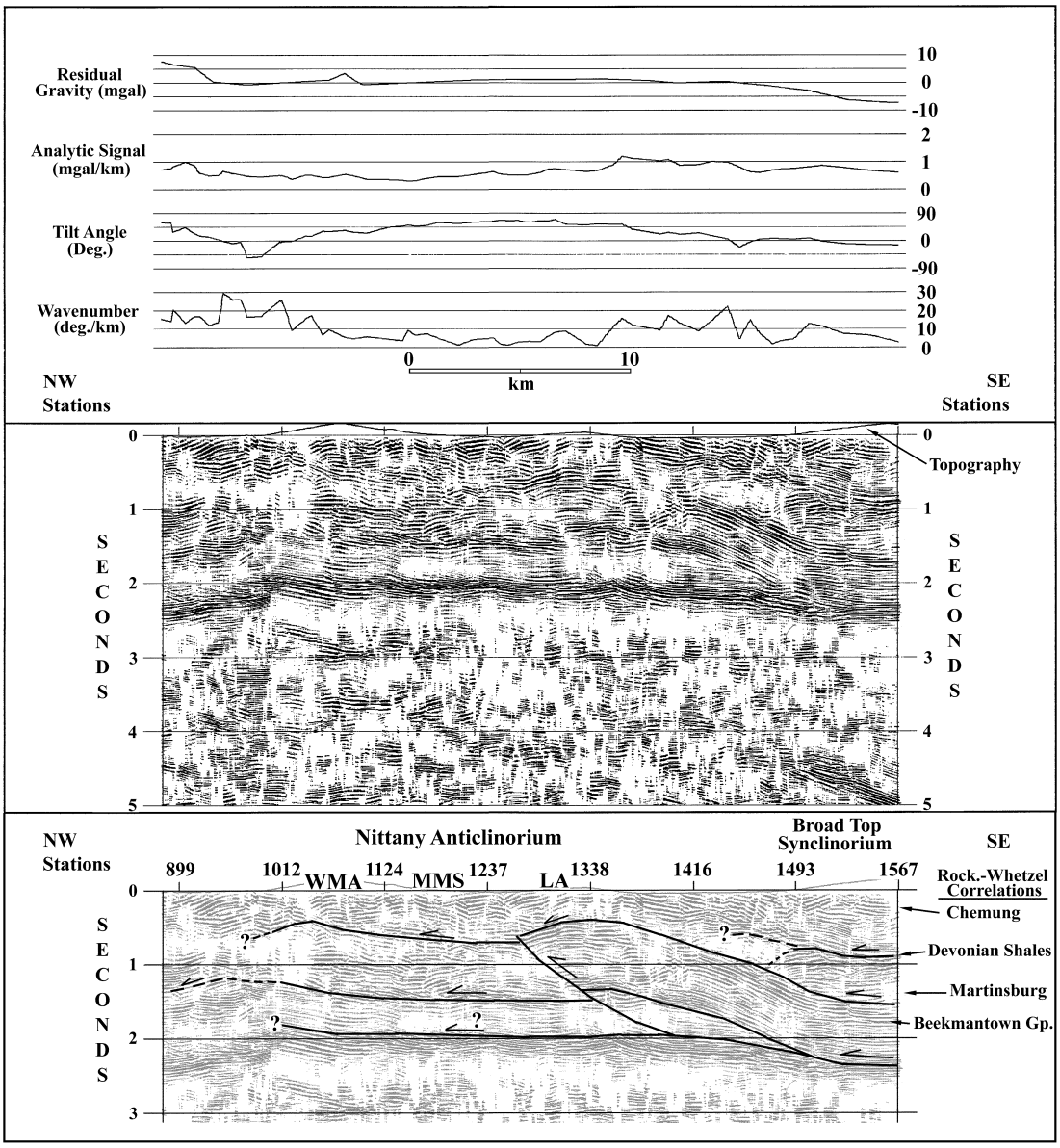

Figure 5.20: Dip-projected and migrated line WV2 over the Nittany Anticlinorium in eastern West Virginia with residual gravity and potential field attributes (PFAs) plotted above. The broad high on the tilt angle and highs on the wavenumber show the location of the large thrust sheet as revealed by the seismic data below. Lower section also shows lithologic correlation to the Rockingham-Whetzel log made from a synthetic seismogram. 'WMA' is the Wills Mountain Anticline, 'MMS' the Middle Mountain Syncline, and 'LA' the Long Anticline. Seismic data plotted at 1:1 for 6 km/sec.

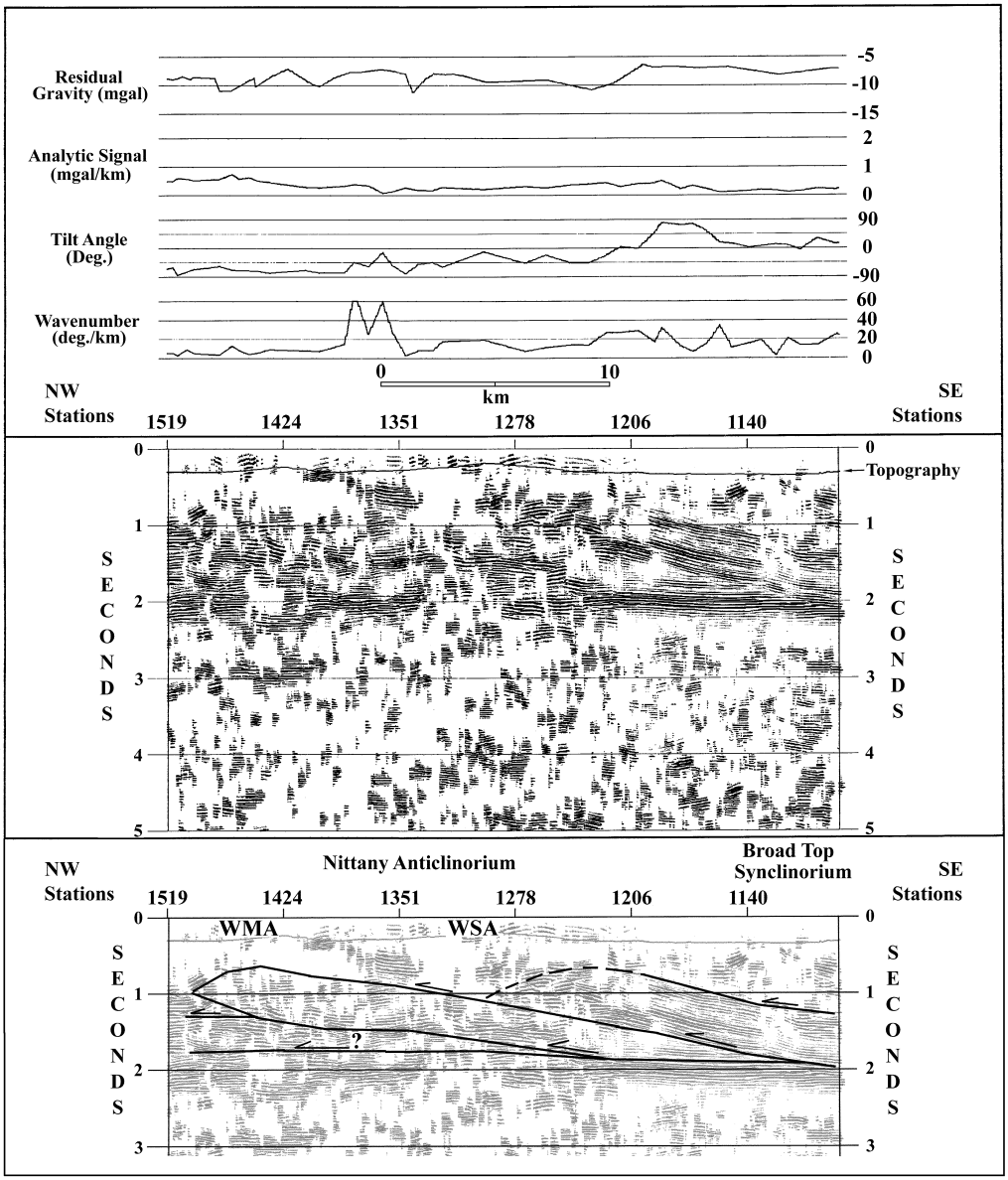

Figure 5.21: Dip-projected and migrated line WV3 over the Nittany Anticlinorium in western Virginia with residual gravity and potential field attributes (PFAs) plotted above. The tilt angle high between stations 1140 and 1206 corresponds to location 'D' in Figure 5.13, and is associated with a ramp anticline of higher density lower Paleozoic carbonates as seen in the seismic data. The wavenumber shows the location of the leading edge of a smaller imbricate block beneath the Wills Mountain Anticline (WMA) and 'WSA' the Warm Springs Anticline. Seismic data plotted at 1:1 for 6 km/sec.

Chapter 6: Conclusions and Suggestions for Future Research

This study is an attempt to integrate a large data set including reprocessed seismic reflection data, gravity data, deep well data, and geologic information in order to understand the lateral extent of major structures in the central Appalachians of Virginia and West Virginia. More than 700 km of seismic reflection data were reprocessed using a new processing sequence called *dip projection*. Dip projection relocates the crooked-line reflection data onto a straight line aligned in the user-defined dip direction, and yields final stacked sections that were demonstrated to be both more interpretable and more migration friendly. This method might have some utility in separating differing dip domains at different structural levels as shown with the model example in chapter 2.

The study also utilized over 17,000 Bouguer gravity values from a 52,800 sq. km area in the central Appalachians of Virginia and West Virginia. These data were gridded and then subjected to potential field attribute (PFA) analysis. The results shown in chapters 3 and 5 illustrate the utility of this method for locating hidden density contrasts in the subsurface. Large-scale duplexes of high density Cambrian-Ordovician carbonates were located on the basis of the gravity data analysis. Confirmation of these structures was achieved through the use of seismic reflection data.

An analysis of overall reflectivity along two major reflection transects across the central and southern Appalachians was made in chapter 4. Several similarities between the reflection character of data in both regions were noted, most importantly the change in reflectivity from the Piedmont westward. Along both transects highly reflective crust is imaged from the near-surface to the interpreted Moho beneath the Piedmont. To the west, most of the reflectivity is confined to the upper 3-4 seconds of the data sets above an apparent detachment at that level. This change in reflectivity is interpreted as a manifestation of a change in the orientation of mechanically weak zones in the crust. There is substantial geologic evidence to suggest that the crust of the Piedmont has undergone modification during each major tectonic event since the early Paleozoic. The preexistence of preferentially oriented weak zones in the crust allowed many of these zones to be reactivated during all of the different tectonic events, leading to a high reflectivity throughout the crust. To the west of the Piedmont, the sub-horizontal weak zones in the sedimentary succession were used as detachment surfaces during the late Paleozoic Alleghanian orogeny generating Valley and Ridge folding and thrust faulting. The lack of apparent deformation below that zone might be a consequence of either having no basement structures oriented properly for reactivation, or of it being mechanically more efficient to generate the near surface detachments within the sedimentary section.

Chapter 5 takes the results of dip-projection processing of industry seismic reflection data from the central Appalachians and combines it with PFA analysis, well data, and surface geologic information to investigate the along strike continuity of major structures within the Valley and Ridge and Blue Ridge. On the basis of this analysis, an imbricate stack of higher

density Cambrian-Ordovician carbonates is shown to exist beneath the western edge of the Blue Ridge for a lateral extent of over 150 km in Virginia. In addition, the Nittany Anticlinorium is shown to change its structural style from West Virginia into Virginia. A transition from the overthrusting of a large sheet of higher density Cambrian-Ordovician carbonates in West Virginia to more of an imbricate thrust style to the south in Virginia was inferred from PFA analysis and confirmed by interpretation of dip-projected seismic reflection data. This change in the Nittany Anticlinorium could be attributed to the transition from the deformation style of the Central to that of the Southern Appalachians.

The results summarized above are based on a 3.5 year effort of data reprocessing and analysis. There is more that can and should be done in order to fully confirm or refute the results presented here. Some of the possibilities for future work include:

1. Completion of the reprocessing effort of industry seismic reflection data in the central Appalachians of Virginia and West Virginia. There are three major lines left to reprocess: 1) a dip line to the south of WV3 close to the transition zone from the southern to central Appalachians; 2) a second dip line between WV2 and WV3 near the area identified by PFA analysis where the change in the structural style beneath the Nittany Anticlinorium takes place; and 3) a strike line tying all of the data set together. If the reprocessing effort includes the dip-projection step, perhaps many of the controversies regarding interpretations of the reflection data in the central Appalachians of Virginia and West Virginia could be resolved by utilizing the entire data set

2. Extension of PFA analysis to other regions. The success of the method in detecting the existence of large-scale thrust sheets and duplex structures in the subsurface might be of use in other areas of the Appalachians where a lack of good seismic reflection makes interpretation difficult. Also, the method could be used to define more clearly structures beneath the Atlantic Coastal Plain.

3. The use of the dip projection method to scan for dips at different crustal levels offers additional advantages. The possibility that the lack of reflectivity in the middle and lower crust to the west of the Piedmont in the southeastern United States might be the result of the line direction with respect to the actual dip of the structures. This issue is an intriguing one and needs to be investigated.

These are only a few of the possibilities for derivative work from this effort. I hope to work on some of this myself, but I also hope that others may find this as interesting and challenging as I did, and will perhaps develop even better tools to help us all better understand the world around us.

References

Allen, R. M., Jr., 1963, Geology and mineral resources of Greene and Madison Counties, Bulletin 78, Virginia Division of Mineral Resources, Charlottesville, Virginia, 102p., 1 plate.

Allen, R. M., Jr., 1967, Geology and mineral resources of Page County, Bulletin 81, Virginia Division of Mineral Resources, Charlottesville, Virginia, 78p., 1 plate.

Allmendinger, R. W., Nelson, K. D., Potter, C. J., Barazangi, M., Brown, L. D., and Oliver, J. E., 1987, Deep seismic reflection characteristics of the continental crust, *Geology*, v.15, n.4, p.304-310.

Bartlett & Associates, 1981, Geologic Log of W-141 (W-1432), Rockingham Co., Virginia, Virginia Division of Mineral Resources, 4p.

Behrendt, J. C., 1986, Structural interpretation of multichannel seismic reflection profiles crossing the southeastern United States and the adjacent continental margin – decollements, faults, Triassic (?) basins and Moho reflections, *in* Barazangi, M., and Brown, L.D., eds., **Reflection Seismology, The Continental Crust**, AGU Geodynamics Series Volume 14, Washington, D.C., p.201-214.

Behrendt, J. C., Hamilton, R. M., Ackermann, H. D., and Henry, V. J., 1981, Cenozoic faulting in the vicinity of the Charleston, South Carolina 1886 Earthquake, *Geology*, v.9, p.117-122.

Bell, R. E., Karner, G. D., and Steckler, M. S., 1988, Early Mesozoic rift basins of eastern North America and their gravity anomalies: The role of detachments during extension, *Tectonics*, v. 7, no. 3, p. 447-462.

Bick, K. F., 1960, Geology of the Lexington quadrangle, Virginia, Report of Investigations 1, Virginia Division of Mineral Resources, Charlottesville, Virginia, 40p., 1 plate.

Blakley, R. J., and Simpson, R. W., 1986, Approximating edges of source bodies from magnetic or gravity anomalies, *Geophysics*, v.51, p.1494-1498.

Bobyarchick, A. R., 1981, The Eastern Piedmont fault system and its relationship to Alleghanian tectonics in the southern Appalachians, *J. Geology*, v.89, p.335-347.

Bobyarchick, A. R., and Glover, L. G., III, 1979, Deformation and metamorphism in the Hylas zone and adjacent parts of the eastern Piedmont in Virginia, *GSA Bulletin*, v.90, p.739-752.

Boyer, S. E., 1992, Sequential development of the southern Blue Ridge province in northwest North Carolina ascertained from the relationships between penetrative deformation and

thrusting, *in* Mitra, S., and Fisher, G.W., eds., **Structural Geology of Fold and Thrust Belts**, Johns Hopkins University Press, Baltimore, Maryland, p.161-188.

Boyer, S. E., and Elliot, D., 1982, Thrust systems, *AAPG Bulletin*, V.66, p.1196-1230.

Bracewell, R. N., 1965, **The Fourier Transform and Its Applications**, McGraw-Hill Book Company, New York, 381p.

Brent, W. B., 1960, Geology and Mineral Resources of Rockingham County, Virginia Division of Mineral Resources Bulletin 76, 174p., 2 plates.

Brown, L. D., 1987, Lower continental crust: Variations mapped by COCORP deep seismic profiling, *Ann. Geophys.*, v.5B, p.325-330.

Brown, L., Barazangi, M., Kaufman, S., Oliver, J., 1986, The first decade of COCORP: 1974-1984, *in* Barazangi, M., and Brown, L.D., **Reflection Seismology: A Global Perspective**, AGU Geodynamics Series Volume 13, Washington, D.C., p.107-120.

Butts, C., 1933, Geologic map of the Appalachian Valley in Virginia with explanatory text, Bulletin 42, Virginia Geological Survey, University, Virginia, 56p., 1 plate.

Butts, C., 1940, Geology of the Appalachian Valley in Virginia, Part 1: Geologic text and illustrations, Bulletin 52, Virginia Geologic Survey, University, Virginia, 568p.

Cardwell, D. H., 1977, West Virginia Gas Development in Tuscarora and Deeper Formations, Mineral Resources Series MRS-8, West Virginia Geologic and Economic Survey, 34 p., 1 plate.

Chowns, T. M., and Williams, C. T., 1983, Pre-Cretaceous Rocks Beneath the Georgia coastal plain -- regional implications, .us in Gohn, G.S., ed., Studies Related to the Charleston, South Carolina, Earthquake of 1886 -- Tectonics and Seismicity, USGS Professional Paper 1313, p. L1-L42.

Christensen, N. I., and Szymansky, D. L., 1988, Origin of reflections from the Brevard fault zone, *J. Geoph. Res.*, v.93, p.1087-1102.

Christensen, N. I., and Szymansky, D. L.,1991, Seismic properties and the origin of reflectivity from a classic Paleozoic sedimentary sequence, Valley and Ridge province, southern Appalachians, *GSA Bulletin*, v.103, p.277-289.

Clark, H. B., Costain, J. K., and Glover, L. G., III, 1978, Structural and seismic reflection studies of the Brevard ductile deformation zone near Rosman, North Carolina, *American Journal of Science*, v.278, p.419-441.

Colton, G. W., 1970, The Valley and Ridge and Appalachian Plateau; stratigraphy and sedimentation; the Appalachian basin; its depositional sequences and their geologic relationships, *in* **Studies in Appalachian Geology, Central and Southern**, Interscience Publications, New York, p.5-47.

Cook, F. A., 1984, Geophysical anomalies along strike of the southern Appalachian Piedmont, *Tectonics*, v.3, p.45-61.

Cook, F. A., Albaugh, D. S., Brown, L. D., Kaufman, S., Oliver, J. E., and Hatcher, R. D., Jr., 1979, Thin-skinned tectonics in the crystalline southern Appalachians: COCORP seismic reflection profiling of the Blue Ridge and Piedmont: Geology, v. 7, p. 563-567.

Cook, F. A., Brown, L. D., Kaufman, S., Oliver, J. E., and Peterson, T. A., 1981, COCORP seismic reflection profiling of the Appalachian orogen beneath the Coastal Plain of Georgia, *GSA Bulletin*, v.92, p.738-748.

Cook, F. A., and Oliver, J. E., 1981, The late Precambrian-early Paleozoic continental edge in the Appalachian Orogen, *Am. J. Science*, v.281, p.993-1008.

Cordell, L., and Grauch, V. J. S., 1985, Mapping basement magnetization zones from aeromagnetic data in the San Juan Basin, New Mexico, *in* Hinze, W.J., Ed., **The Utility of Regional Gravity and Magnetic Anomaly Maps**, Society of Exploration Geophysicists, p.181-197.

Çoruh, C., Bolliger, G. A., and Costain, J. K, 1988a, Seismogenic structures in the central Virginia seismic zone, *Geology*, v.16, p.748-751.

Çoruh, C., and Costain, J. K., 1983, Noise attenuation by Vibroseis whitening (VSW) processing, *Geophysics*, v.48, p.543-554.

Çoruh, C., Costain, J. K., Glover, L., III, Pratt, T. L., and Brennan, J., 1988b, Seismicity, seismic reflection, gravity, and geology of the Central Virginia Seismic Zone: Part 1, reflection seismology, *in* Glover, L, III, Costain, J. K., and Çoruh, C., Studies of the pattern and ages of post-metamorphic faults in the Piedmont of Virginia and North Carolina, NUREG/CR-5123, p.1-32.

Çoruh, C., Costain, J. K., Hatcher, R. D., Jr., Pratt, T. L., Williams, R. T., and Phinney, R. A., 1987, Results from regional vibroseis profiling: Applachian Ultra-deep Core Hole study, *Geoph. J. Royal Astr. Soc*., v.89, p.147-156.

Costain, J. K., and Çoruh, C., 1989, Tectonic settings of Triassic half-grabens in the Appalachians: Seismic data acquisitin, processing, and results, *in* Tankard, A.J., and Balkwill, H.R., eds., **Extensional Tectonics and Stratigraphy of the North Atlantic Margins**, AAPG Memoir 46, American Association of Petroleum Geologists − Canadian Geological Foundation, p.155-174.

Costain, J. K., and Çoruh, C., 1991, "True dip" seismic images from crooked-line recording in mountainous terrain: an example from the Appalachian Blue Ridge, Southeastern U.S., *GSA Abstracts with Programs*, v.23, p.90.

Costain, J. K., Domoracki, W. J., and Çoruh, C., 1992, Enhancement of crustal reflection seismic data by binning (sorting) along tectonic strike: An example from the Northern Appalachians, *EOS Trans. Am. Geoph. Union*, v.70, p.556-557.

Daniels, D. L., and Leo, G. W., 1985, Geologic interpretation of basement rocks of the Atlantic Coastal Plain, USGS Open-File Report 85-655, 45 p.

de Boer, J. Z., McHone, J. G., Puffer, J. H., Ragland, P. C., 1988, Mesozoic and Cenozoic magmatism, *in* Sheridan, R.E., and Grow, J.A., eds., **The Atlantic Continental Margin**, The Geology of North America Volume I-2, Geological Society of America, Boulder, Colorado, p.217-242.

Dean, S. L., Kulander, B. R., and Skinner, J. M., 1988, Structural chronology of the Alleghanian orogeny in southeastern West Virginia, *GSA Bulletin*, v.100, p.299-310.

Debiglia, N., and Corpel, J., 1997, Automatic 3-D interpretation of potential field data using analytic signal derivatives, *Geophysics*, v.62, p.87-96.

DEKORP Research Group, 1990, Comparitive investigations of continental reflectivity, *Tectonophysics*, v.173, p.199-206.

Diecchio, R. J., 1985, Post-Martinsburg Ordovician stratigraphy of Virginia and West Virginia, Publication 57, Virginia Division of Mineral Resources, 77p.

Domoracki, W. J., 1995, A geophysical investigation of geologic structure and regional tectonic setting at the Savannah River Site, South Carolina, unpubl. PhD Dissertation, VPI&SU, Blacksburg, Virginia, 236 p.

Edsall, R. W., 1974, A seismic reflection study over the Bane anticline, M.S. thesis, Virginia Polytechnic Institute and State University, Blacksburg, Virginia, 109p.

Edwards, D. J., Lyatsky, H. V., and Brown, R. J., 1996, Interpretation of gravity and magnetic data using the horizontal-gradient vector method in the Western Canada Basin, *First Break*, v.14, p.231-246.

Evans, M. A., 1989, The structural geometry and evolution of foreland thrust systems, northern Virginia, *GSA Bulletin*, v101, p.339-354.

Evans, M. A., 1994, Joints and decollement zones in the Middle Devonian shales: Evidence for multiple deformatin evnets in the central Appalachian Plateau, *GSA Bulletin.* v.106, p.447-460.

Faure, S., Tremblay, A., and Angelier, J., 1996, Alleghanian paleostress reconstruction in the northern Appalachians: Intraplate deformation between Laurentia and Gondwana, *GSA Bulletin*, v.108, p.1467-1480.

Ferrill, D. A., and Dunne, W. M., 1989, Cover deformation above a blind duplex: An example from West Virginia, U.S.A., J. *Struc. Geol.*, v.11, p.421-431.

Ferrill, D. A., and Thomas, W. A., 1988, Acadian dextral transpression and synorogenic sedimentary successions in the Appalachians, *Geology*, v.16, p.604-608.

Fountain, D. M., Hurich, C. A., and Smithson, S. B., 1984, Seismic reflectivity of mylonitic zones in the crust, *Geology*, v.12, n.4, p.195-198.

Frey, M. G., 1973, Influence of Salina Salt on structure in New York - Pennsylvania, *AAPG Bulletin*, v.57, p.1027-1037.

Fyfe, W. S., 1986, Fluids in the deep continental crust, *in* Barazangi, M., and Brown, L.D., eds., **Reflection Seismology, The Continental Crust**, AGU Geodynamics Series Volume 14, Washington, D.C., p.33-39.

Gates, A. E., 1987, Transpressinal dome formatin in the southwest Virginia Piedmont, *Am. J. Science*, v.287, p.927-949.

Gates, A. E., 1997, Multiple reactivations of accreted terrane boundaries: An example from the Carolina terrane, Brookneal, Virginia, *in* Glover, L., III, and Gates, A.E., eds., **Central and Southern Appalachian Sutures: Results from the EDGE Project and Related Studies**, GSA Special Paper 314, Geological Society of America, Boulder, Colorado, p.49-63.

Gates, A. E., Speer, J. A., and Pratt, T. L., 1988, The Alleghanian southern Appalachian Piedmont: A transpressional model, *Tectonics*, v.7, p.1307-1324.

Gathright, T. M., III, 1976, Geology of the Shenandoah National Park, Virginia, Bulletin 86, Virginia Division of Mineral Resources, Charlottesville, Virginia, 93p., 3 plates.

Glover, L.G., III, 1992, A new tectonic model of for the central and southern Appalachians, *in* Glover, L.G., III, Çoruh, C, Costain, J.K, and Bollinger, G.A., Piedmont Seismic Reflection Study: A Program Integrated with Tectonics to Probe the Cause of Eastern Seismicity, NUREG/CR-5731, U.S. Nuclear Regulatory Commission, Washington, D.C., p.1-53.

Glover, L., III, Poland, F. B., Tucker, R. D., and Bourland, W. C., 1980, Diachronous Paleozoic mylonites and structural heredity of Triassic-Jurassic basins in Virginia, *GSA Abstracts w/Programs*, v.12, p.178.

Glover, L., III, Sheridan, R. E., Holbrook, W. S., Ewing, J., Talwani, M., Hawman, R. B., and Wang, P., 1997, Paleozoic collisions, Mesozoic rifting, and structure of the Middle Atlantic states continental margin: An 'EDGE' project report, *in* Glover, L., III, and Gates, A.E., eds., **Central and Southern Appalachian Sutures: Results from the EDGE Project and Related Studies**, GSA Special Paper 314, Geological Society of America, Boulder, Colorado, p.107-135.

Glover, L., III, Speer, J. A., Russell, G. S., and Farrar, S. S., 1983, Ages of regional metamorphism and ductile deformation in the central and southern Appalachians, *Lithos*, v.16, p.223-245.

Gohn, G. S., 1988, Late Mesozoic and early Cenozoic geology of the Atlantic Coastal Plain: North Carolina to Florida, *in* Sheridan, R.E., and Grow, J.A., eds., **The Atlantic Continental Margin**, The Geology of North America Volume I-2, Geological Society of America, Boulder, Colorado, p.107-130.

Goodwin, E. B., and Thompson, G. A., 1988, The seismically reflective crust beneath highly extented terranes: Evidence for its origin in extension, *GSA Bulletin*, v.100, p.1616-1626.

Grauch, V. J. S., and Cordell, L., 1987, Limitations of determining gravity or magnetic boundaries from the horizontal gradient of gravity or pseudogravity data, *Geophysics*, v.52, p.118-121.

Grow, J. A., and Sheridan, R. E., 1988, U. S. Atlantic continental margin; A typical Atlantic-type or passive continental margin, *in* Sheridan, R.E., and Grow, J.A., eds., **The Atlantic Continental Margin**, The Geolgy of North America Volume I-2, Geological Society of America, Boulder, Colorado, p.1-8.

Gunn, P. J., 1975, Linear transformations of gravity and magnetic fields: *Geophysical Prospecting*, v.23, p. 300-312.

Gwinn, V. E., 1964, Thin-skinned tectonics in the plateau and northwestern Valley and Ridge provinces of the central Appalachians, *GSA Bulletin*, v.75, p.863-900.

Hanson, H. J., and Edwards, J., Jr., 1986, The lithology and distribution of pre-Cretaceous basement rocks beneath the Maryland Coastal Plain, Maryland Geological Survey Report of Investigations 44, 27p.

Harris, L. D., and Bayer, K. C., 1979, Sequential development of the Appalachian orogen above a master decollement − A hypothesis, *Geology*, v.7, p.568-572.

Harris, L. D., de Witt, W., Jr., and Bayer, K. C., 1982, Interpretive seismic profile along interstate I-64 from the Valley and Ridge to the coastal plain in central Virginia, USGS Oil and Gas Investigations Chart OC-0123.

Harris, L. D., and Milici, R. C., 1977, Characteristics of a thin-skinned style of deformation in the southern Appalachians, and potential hydrocarbon traps, USGS Professional Paper 1018, 40p.

Harry, D. L., Oldow, J. S., and Sawyer, D. S., 1995, The growth of orogenic belts and the role of crustal heterogeneities in decollement tectonics, *GSA Bulletin*, v.107, p.1411-1426.

Hatcher, R. D., Jr., 1986, Interpretation of seismic reflection data in complexly deformed terranes: A geologist's perspective, *in* Barazangi, M., and Brown, L. D., eds., **Reflection Seismology, The Continental Crust**, AGU Geodynamics Series Volume 14, Washington, D.C., p.9-12.

Hatcher, R. D., Jr., 1989, Tectonic synthesis of the U. S. Appalachians, *in* Hatcher, R.D., Jr., Thomas, W. A., and Viele, G. E., eds., **The Appalachian-Ouachita Orogen in the United States**, The Geology of North America Volume F-2, Geological Society of America, Boulder, Colorado, p.511-535.

Hatcher, R. D., Jr., Howell, D. F., and Talwani, P., 1977, Eastern Piedmont fault system: Speculations on its extent, *Geology*, v.5, p.636-640.

Hatcher, R. D, Jr., Thomas, W. A., Geiser, P. A., Snoke, A. W., Mosher, S., and Wiltschko, D. V., 1989, Alleghanian Orogen, *in* Hatcher, R. D., Jr., Thomas, W. A., and Viele, G. W., eds., **The Appalachian-Ouachita Orogen in the United States**, The Geology of North America Volume F-2, Geological Society of America, Boulder, Colorado, p.233-318.

Heck, F. R., 1989, Mesozoic extension in the southern Appalachians, *Geology*, v.17, p.711-714.

Hittleman, A. M., Dater, D. J., Buhman, R. W., and Racey, S. D., 1994, **Gravity CD-ROM**, National Geophysical Data Center, NOAA, Boulder, CO.

Holbrook, W. S., Catchings, R. D., Jarchow, C. M., 1991, Origin of deep crustal reflections: implications of coincident seismic refraction and reflection data in Nevada, *Geology*, v.19, p.175-179.

Hsu, S.-K., Sibuet, J.-C, and Shyu, C.-T., 1996, High-resolution detection of geologic boundaries from potential-field anomalies: An enhanced analytic signal technique, *Geophysics*, v.61, p.373-386.

Hubbard, D. A., Jr., Rader, E. K., and Berquist, C. R., 1978, Basement wells in the Coastal Plain of Virginia, *Virginia Minerals*, v.24, n.2, p.16-18.

Hubbard, S. S., Çoruh, C., and Costain, J. K., 1991, Paleozoic and Grenvillian structures in the southern Appalachians: Extended interpretation from seismic reflection data, Tectonics, v. 10, p. 141-170.

Hurich, C. A., Smithson, S. B., Fountain, D. M., and Humphrey, M. C., 1985, Seismic evidence of mylonite reflectivity and deep structure in the Kettle Dome metamorphic core complex, Washington, *Geology*, v.13, p.577-580.

Hutchinson, D. R., Klitgord, K. D., Lee, M. W., Trehu, A. M., 1988, U. S. Geological Survey deep seismic reflection profile across the Gulf of Maine, *GSA Bulletin*, v.100, p.172-184.

Jacobeen, F., Jr., and Kanes, W. H., 1974, Structure of the Broadtop synclinorium and its implications for Appalachian structural style, *AAPG Bulletin*, v.58, p.362-375.

Jacobeen, F., Jr., and Kanes, W. H., 1975, Structure of the Broadtop synclinorium, Wills Mountain anticlinorium, and Allegheny frontal zone, *AAPG Bulletin*, v.59, p.1136-1150.

Johnson, S. S., 1965, Geologic Log of W-1432, Virginia Division of Mineral Resources, 18p.

Jones, T., and Nur, A., 1984, The nature of reflections from deep crustal fault zones, *J. Geoph. Res.*, v.89, p.3153-3171.

Keen, C. E., Kay, W. A., Keppie, J. D., Marillier, F., Pe-Piper, G., and Waldron, J. W. F., 1991, Deep seismic reflection data from the Bay of Fundy and Gulf of Maine: Tectonic implications, *Can. J. Earth Sci.*, v.28, p.1096-1111.

Klemperer, S. L., 1987, A relation between heat flow and the seismic reflectivity of the lower crust, *J. Geophys.*, v.61, p.1-11.

Kolich, T. M., 1974, Seismic reflection and refraction studies in the folded Valley and Ridge province at Price Mountain, Montgomery County, Virginia, M.S. thesis, Virginia Polytechnic Institute and State University, Blacksburg, Virginia, 138p.

Kong, S. M., Phinney, R. A., and Chowdhury, K. R., 1985, A nonlinear signal detector for enhancement of noisy seismic record sections, Geophysics, v. 50, p. 539-550.

Kulander, B. R., and Dean, S. L., 1978, **Gravity, Magnetics, and Structure of the Allegheny Plateau/Western Valley and Ridge in West Virginia and Adjacent States**, Report of Investigations 27, West Virginia Geological and Economic Survey, Morgantown, WV, 91 p.

Kulander, B. R., and Dean, S. L., 1986, Structure and tectonics of central and southern Appalachian Valley and Ridge and Plateau Provinces, West Virginia and Virginia, *AAPG Bulletin*, v.70, p.1674-1684.

Kulander, B. R., Dean, S. L., and Lessing, P., 1986, The Browns Mountain anticlinorium, West Virginia, *in* **The Geological Society of America Centennial Field Guide – Southeastern Section**, Geological Society of America, Boulder, Colorado, p.101-104.

Lampshire, L. D., 1992, Crustal structures and the eastern extent of the Lower Paleozoic shelf strata within the central Appalachians: A seismic relfection interpretation, M.S. thesis, Virginia Polytechnic Institute and State University, Blacksburg, Virginia, 84p.

Lampshire, L. D., Çoruh, C., and Costain, J. K., 1994, Crustal structures and the eastern extent of the lower Paleozoic shelf strata within the central Appalachians: A seismic reflection interpretation, *GSA Bulletin*, v. 106, p. 1-18.

Law, A., and Snyder, D. B., 1997, Reflections from a mylonitized zone in central Sweeden, *J. Geoph. Res.*, v.102, p.8411-8425.

Levin, F. K., 1983, The effects of streamer feathering on stacking, *Geophysics*, v.48, p.1165-1171.

Levin, F. K., 1984, The effects of binning on data from a feathered streamer, *Geophysics*, v.49, p.1386-1387.

Lynn, H. B., and Deregowski, S., 1981, Dip limitations on migrated sections as a function of line length and recording time, *Geophysics*, v.46, p.1392-1397.

Maher, H. D., Jr., Dallmeyer, R. D., Secor, D. T., Jr., and Sacks, P. E., 1994, $^{40}Ar/^{39}Ar$ Constraints on chronology of Augusta fault zone movement and Late Alleghanian extension, southern Appalachian Piedmont, South Carolina and Georgia, *Am. J. Science*, v.294, p.428-448.

Manspeizer, W., and Cousminer, H. L., 1988, Late Triassic-Early Jurassic synrift basins of the U.S. Atlantic margin, *in* Sheridan, R. E., and Grow, J. A., eds., **The Atlantic Continental Margin**, The Geology of North America Volume I-2, Geological Society of America, Boulder, Colorado, p.197-216.

Manspeizer, W., deBoer, J., Costain, J. K., Froelich, A. J., Çoruh, C., Olsen, P. E., McHone, G. J., Puffer, J. H., and Prowell, D. C., 1989, *in* Hatcher, R. D. Jr., Thomas, W. A, and Viele, G. W., eds., **The Appalachian-Ouachita Orogen in the United States**, The Geology of North America Volume F-2, Geological Society of America, Boulder, Colorado, p. 319-374.

McBride, J. H., and Nelson, K. D., 1991, Deep seismic reflection constraints on Paleozoic crustal structure and definition of the Moho in the buried southern Appalachian orogen, *in* Meissner, R., Brown, L. D., Durbaum, H-J., Franke, W., Fuchs, K., and Seifert, F., eds., **The Continental Lithosphere: Deep Seismic Reflections**, Geodynamics Series V.22, American Geophysical Union, Washington, D.C., p.9-22.

McCarthy, J., and Thompson, G. A., 1988, Seismic imaging of extended crust with emphasis on the western United States, *GSA Bulletin*, v.100, p.1361-1374.

Meissner, R., and Kusznir, N., 1987, Crustal viscosity and the reflectivity of the lower crust, *Ann. Geophys.*, v.5B, p.364-374.

Meissner, R., and Wever, T., 1986, Nature and development of the crust according to deep reflection data from the German Variscides, *in* Barazangi, M., and Brown, L.D., **Reflection Seismology: A Global Perspective**, AGU Geodynamics Series Volume 13, Washington, D.C., p.31-42.

Mesko, A., 1984, **Digital Filtering: Applications in Geophysical Exploration for Oil**, John Wiley & Sons, New York, 636 p.

Miller, H. G., and Singh, V., 1994, Potential field tilt -- a new concept for location of potential field sources, *J. of Applied Geoph.*, v.32, p.213-217.

Miller, J. D., and Kent, D. V., 1988, Regional trends in the timing of Alleghanian remagnetization in the Appalachians, *Geology*, v.16, p.588-591.

Mixon, R. B., and Newell, W. L., 1977, Stafford fault system: Structures documenting Cretaceous and Tertiary deformation along the Fall Line in northeastern Virginia, *Geology*, v.5, p.437-440.

Nabighian, M. N., 1972, The analytic signal of two-dimensional magnetic bodies with polygonal cross-section: Its properties and use for automated anomaly interpretation, *Geophysics*, v. 37, p.507-517.

Nabighian, M. N., 1984, Toward a three-dimensional automatic interpretation of potential field data via generalized Hilbert transforms - fundamental relations: *Geophysics*, v. 49, p.780-786.

Nelson, K. D., Arnow, J. A., McBride, J. H., Willemin, J. H., Huang, J., Zheng, L., Oliver, J. E., Brown, L. D., and Kaufman, S., 1985, New COCORP profiling in the southeastern United States.Part I: Late Paleozoic suture and Mesozoic rift basin: Geology, v. 13, p. 714-717.

Nettleton, L. L., 1940, **Geophysical Prospecting for Oil**, McGraw-Hill, New York, 444 p.

Ogawa, Y., Jones, A.G., Unsworth, M.J., Booker, J.R., Lu, X., Craven, J., Roberts, B., Parmalee, J., and Farquharson, C., 1996, Deep electrical conductivity structures of the Appalachian Orogen in the Southeastern U.S., *Geoph. Res. Letters*, v.23, p.1597-1600.

Okay, A. F., 1986, High-pressure / low-temperature metamophic rocks of Turkey, *in* Evans, B.W., and Brown, E.H., **Blueschists and Eclogites**, GSA Memoir 164, p.333-347.

Okaya, D. A., and Jarchow, C. M., 1989, Extraction of deep crustal reflections from shallow vibroseis data using extended correlation, *Geophysics*, v.54, p.555-562.

Oldow, J. S., Bally, A. W., Ave Lallemant, H. G., 1990, Transpression, orogenic float and lithospheric balance, Geology, v.18, p.991-994.

Olsen, P. E., McCune, A. R., and Thomson, K. S., 1982, Correlation of the early Mesozoic Newark Supergroup by vertebrates, principally fishes, *Am. J. Science*, v.282, p.1-44.

Olsen, P. E., and Schlische, R. W., 1990, Transtensional arm of the early Mesozoic Fundy rift basin: Penecontemporaneous faulting and sedimentation, *Geology*, v.18, p.695-698.

Olsson, R. K., Gibson, T. G., Hansen, H. J., and Owens, J. P., 1988, Geology of the northern Atlantic coastal plain: Long Island to Virginia, *in* Sheridan, R. E., and Grow, J. A., eds., **The Atlantic Continental Margin**, The Geology of North America Volume I-2, Geological Society of America, Boulder, Colorado, p.87-106.

Perry, W. J., Jr., 1978, Sequential deformation in the central Appalachians, *Am. J. Science*, v.278, p.518-542.

Peterson, T.A., Brown, L.D., Cook, F.A., Kaufman, S., and Oliver, J.E., 1984, Structure of the Riddleville Basin from COCORP seismic data and implications for reactivation tectonics, *J. of Geology*, v.92, p.261-271.

Pratt, T. L., 1982, A geophysical investigation of a concealed granitoid beneath Lumberton, North Carolina, M.S. thesis, Virginia Polytechnic Institute and State University, Blacksburg, Virginia, 55p.

Pratt, T. L., 1986, A geophysical study of the Earth's crust in central Virginia with implications for lower crustal reflections and Appalachian crustal structure, PhD dissertation, VPI&SU, Blacksburg, Virginia, 69p.

Pratt, T. L, Çoruh, C., and Costain, J. K., 1987, Lower crustal reflections in central Virginia, USA, *Geoph. J. Royal Astr. Soc.*, v89, p.163-170.

Pratt, T. L., Çoruh, C., Costain, J. K., and Glover, III, L., 1988, A geophysical study of the Earth's crust in central Virginia and its implications for Appalachian crustal structure: Journal of Geophysical Research, v. 93, p. 6649-6667.

Prowell, D. C., 1983, Index of faults of Cretaceous and Cenozoic age in the eastern United States, USGS Miscellaneous Field Studies Map MF-1269.

Prowell, D. C., 1988, Cretaceous and Cenozoic tectonism on the Atlantic coastal magrin, *in* Sheridan, R. E., and Grow, J. A., eds., **The Atlantic Continental Margin**, The Geology of North America Volume I-2, Geological Society of America, Boulder, Colorado, p.681-684.

Quinlan, G., Beaumont, C., and Hall, J., 1993, Tectonic model for crustal seismic reflectivity patterns in compressional orogens, *Geology*, v.21, p.663-666.

Rader, E. K., and Biggs, T. H., 1976, Geology of the Strasburg and Toms Brook quadrangles, Virginia, Report of Investigations 45, Virginia Division of Mineral Resources, Charlottesville, Virginia, 104p., 4 plates.

Ragland, P. C., Hatcher, R. D., Jr., and Whittington, D., 1983, Juxtaposed Mesozoic diabase dike sets from the Carolinas: A preliminary assessment, *Geology*, v.11, p.394-399.

Ratcliffe, N. M., and Burton, W. C., 1985, Fault reactivation models for origin of the Newark Basin and studies related to eastern U.S. seismicity, *in* Robinson, G. R., Jr., and Froelich, A. J., eds., **Proceedings of the Second U.S. Geological Survey Workshop on the Early Mesozoic Basins of the Eastern United States**, USGS Circular 946, p.36-44.

Ratcliffe, N. M., Burton, W. C., D'Angelo, R. M., and Costain, J. K., 1986, Low-angle extensional faulting, reactivated mylonites, and seismic reflection geometry of the Newark Basin margin in eastern Pennsylvania, *Geology*, v.14, p.766-770.

Reinhardt, J., Prowell, D. C., and Christopher, R. A., 1984, Evidence for Cenozoic tectonism in the southwest Georgia Piedmont, *GSA Bulletin*, v.95, p.1176-1187.

Renick, H., Jr., 1974, Some implications of simple geometric analysis of marine cable feathering in seismic exploration, *Geophysical Prospecting*, v.22, p.54-67.

Reston, T. J., 1990, Shear in the lower crust during extension: Not so pure and simple, *Tectonophysics*, v.173, p.175-183.

Rodgers, J., 1970, **The Tectonics of the Appalachians**, Wiley-Interscience, New York, 271p.

Roest, W. R., Verhoef, J., and Pilkington, M., 1992, Magnetic interpretation using the 3-D analytic signal, *Geophysics*, v.57, p.116-125.

Sacks, P. E., and Secor, D. T., 1990, Kinematics of Late Paleozoic continental collision between Laurentia and Gondwana, *Science*, v.250, p.1702-1705.

Schorr, G. T., 1986, Study of seismic reflection data over Virginia Mesozoic basins, unpub. M.S. Thesis, VPI&SU, Blacksburg, Virginia, 78p.

Sengbush, R. L, Lawrence, P. L., and McDonal, F. J., 1961, Interpretation of synthetic seismograms, *Geophysics*, v.26, p.138-157.

Serpa, L., and de Voogd, B., 1987, Deep seismic reflection evidence for the role of extension in the evolution of continental crust, *Geoph. J. Royal Astr. Soc.*, v.89, p.55-60.

Sheridan, R. E., Musser, D. L., Glover, L., III, Talwani, M., Ewing, J. I., Holbrook, W. S., Purdy, G. M., Hawman, R., and Smithson, S., 1993, Deep sesimic reflection data of EDGE U.S. Mid-Atlantic continental margin experiment: Implications for Appalachian sutures and Mesozoic rifting and magmatic underplating, *Geology*, v.21, p.563-567.

Shumaker, R. C., 1974, Influence of Salina Salt on structure in New York - Pennsylvania: Discussion, *AAPG Bulletin*, v.58, p.543-544.

Stamatakos, J., Hirt, A. M., and Lowrie, W., 1996, The age and timing of folding in the central Appalachians from paleomagnetic results, *GSA Bulletin*, v.108, p.815-829.

Swanson, M. T., 1986, Preexisting fault control for Mesozoic basin formation in eastern North America, *Geology*, v.14, p.419-422.

Taner, M. T., Koehler, F., and R. E. Sheriff, 1979, Complex seismic trace analysis, *Geophysics*, v.44, p.1041-1063.

Taylor, S. R., 1989, Geophysical framework of the Appalachians and adjacent Grenville Province, *in* Prakiser, L. C., and Mooney, W. D., eds., **Geophysical Framework of the Continental United States**, GSA Memoir 172,Boulder, Co., p. 317-347.

Thomas, W. A., 1991, The Appalachian-Ouacita rifted margin of southeastern North America, *GSA Bulletin*, v.103, p.415-431.

Thomas, W. A., 1993, Low-angle detachment geometry of the late Precambrian-Cambrian Appalachian-Ouachita rifted margin of southeastern North America, *Geology*, v.21, p.921-924.

Vacquier, V., Steenland, N. C., Henderson, R. G., and Zietz, I., 1953, **Interpretation of Aeromagnetic Maps**, Geological Society of America Memoir 47, New York, 151 p.

Valentino, D. W., Gates, A. E., and Glover, L., III, 1994, Late Paleozoic transcurrent tectonic assembly of the central Appalachians, *Tectonics*, v. 13, p.110-126.

Valentino, D. W., Valentino, R. W., and Hill, M. L., 1995, Paleozoic transcurrent conjugate shearzones in the central Appalachian Piedmont of southeastern Pennsylvania, *Journal of Geodynamics*, v. 19, p.303-324.

Virginia Division of Mineral Resources, 1993, Geologic Map of Virginia, Virginia Division of Mineral Resources, scale 1:500000.

West Virginia Geologic and Economic Survey, 1986, Geologic Map of West Virginia, West Virginia Geologic and Economic Survey, scale 1:250000, 2 sheets.

Wever, T., Trappe, H., and Meissner, R., 1987, Possible relations between crustal reflectivity, crustal age, heat flow, and viscosity of the continents, *Ann. Geophys.*, v.5B, p.255-266.

Wilkes, G. P., Johnson, S. S., and Milici, R. C., 1989, Exposed and inferred early Mesozoic basins onshore and offshore, Virginia, Virginia Division of Mineral Resources Publication 94, 2 plates.

Williams, R. T., Hatcher, R. D., Jr., Çoruh, C., Costain, J. K., Zoback, M. D., Anderson, R. N., Diebold, J. B., and Phinney, R. A., 1987, The Southern Appalachian Ultradeep Scientific

Drill Hole: Progress of site location investigations and other recent developments, *in* Behr, H. J, Stehli, F. G., and Vidal, H., eds., **Observation of the Continental Crust Through Drilling, II: Proceedings of the International Symposium**, Springer-Verlag, Berlin, p.44-55.

Wilson, T. H., 1989, Geophysical studies of a large blind thrust, Valley and Ridge Province, central Appalachians, *AAPG Bulletin*, v.73, p.276-288.

Wilson, T. H., and Shumaker, R. C., 1988, Three-dimensional structural interrelationships within Cambrian-Ordovician lithotectonic unit of central Appalachians, *AAPG Bulletin*, v.72, p.600-614.

Wilson, T. H., and Shumaker, R. C., 1992, Broad Top Thrust Sheet: An extensive blind thrust in the central Appalachians, *AAPG Bulletin*, v.76, p.1310-1324.

Withjack, M. O., Olsen, P. E., Schlische, R. W., 1995, Tectonic evolution of the Fundy rift basin, Canada: Evidence of extension and shortening during passive margin development, *Tectonics*, v.14, p.390-405.

Wu, J., 1996, Potential pitfalls of crooked-line seismic reflection surveys, *Geophysics*, v.61, p.277-281.

Wu, J., Milkereit, B., and Boerner, D. E., 1995, Seismic imaging of the enigmatic Sudbury Structure, *J. Geoph. Res*., v.100, no.B3, p.4117-4130.

Yilmaz, O., **Seismic Data Processing**, Investigations in Geophysics No. 2, Soc. of Expl. Geoph., Tulsa, 526 p.

Young, R. S., and Rader, E. K., 1974, Geology of the Woodstock, Wolf Gap, Conicville, and Edinburg quadrangles, Virginia, Report of Investigations 35, Virginia Division of Mineral Resources, Charlottesville, Virginia, 69p., 4 plates.

Appendix: Seismic Data Processing

The following flow chart gives the general processing scheme for lines WV1 and WV3. Differences from this scheme are annotated below. Line WV2 was processed in a similar manner by Lampshire (1992).

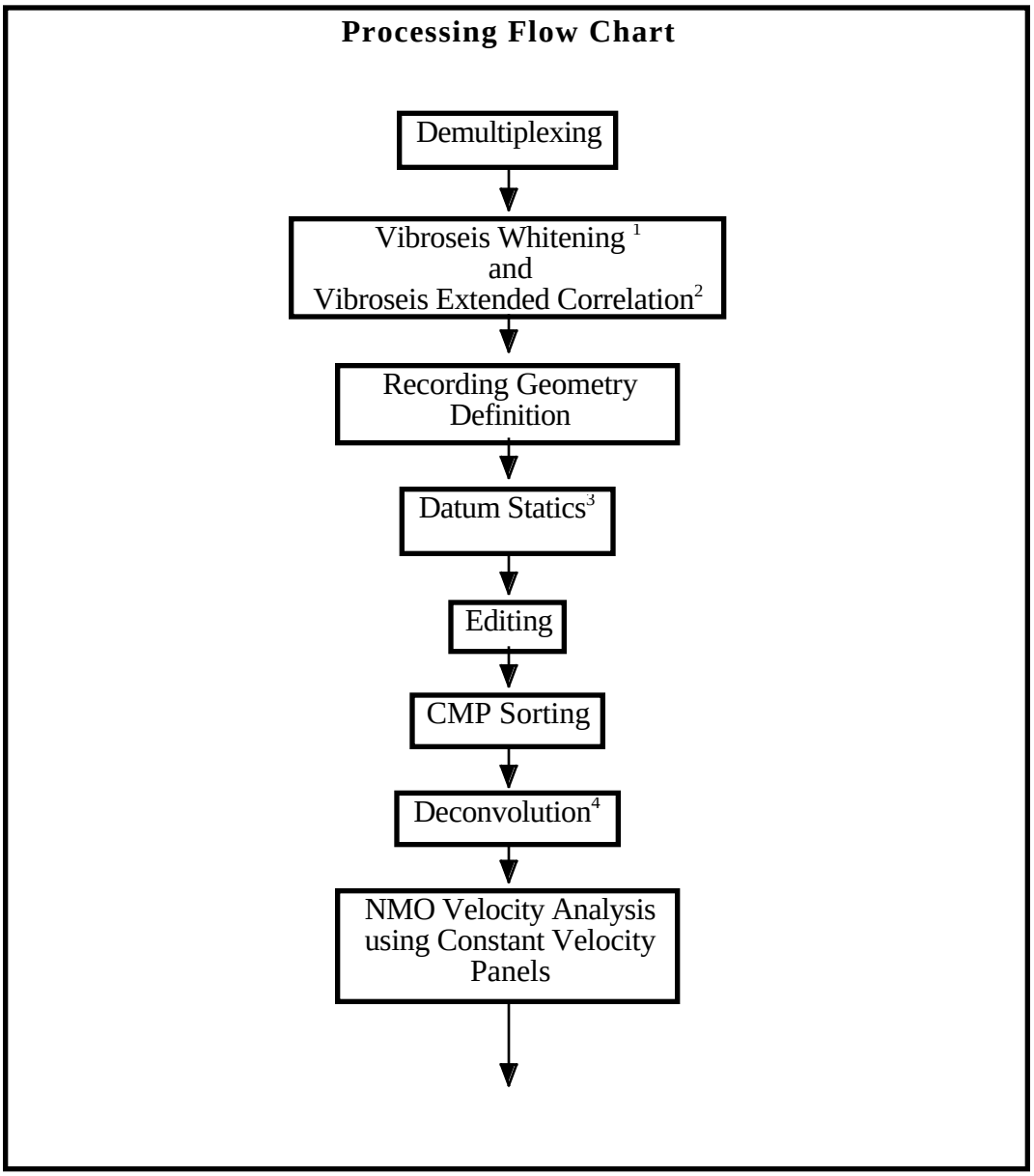

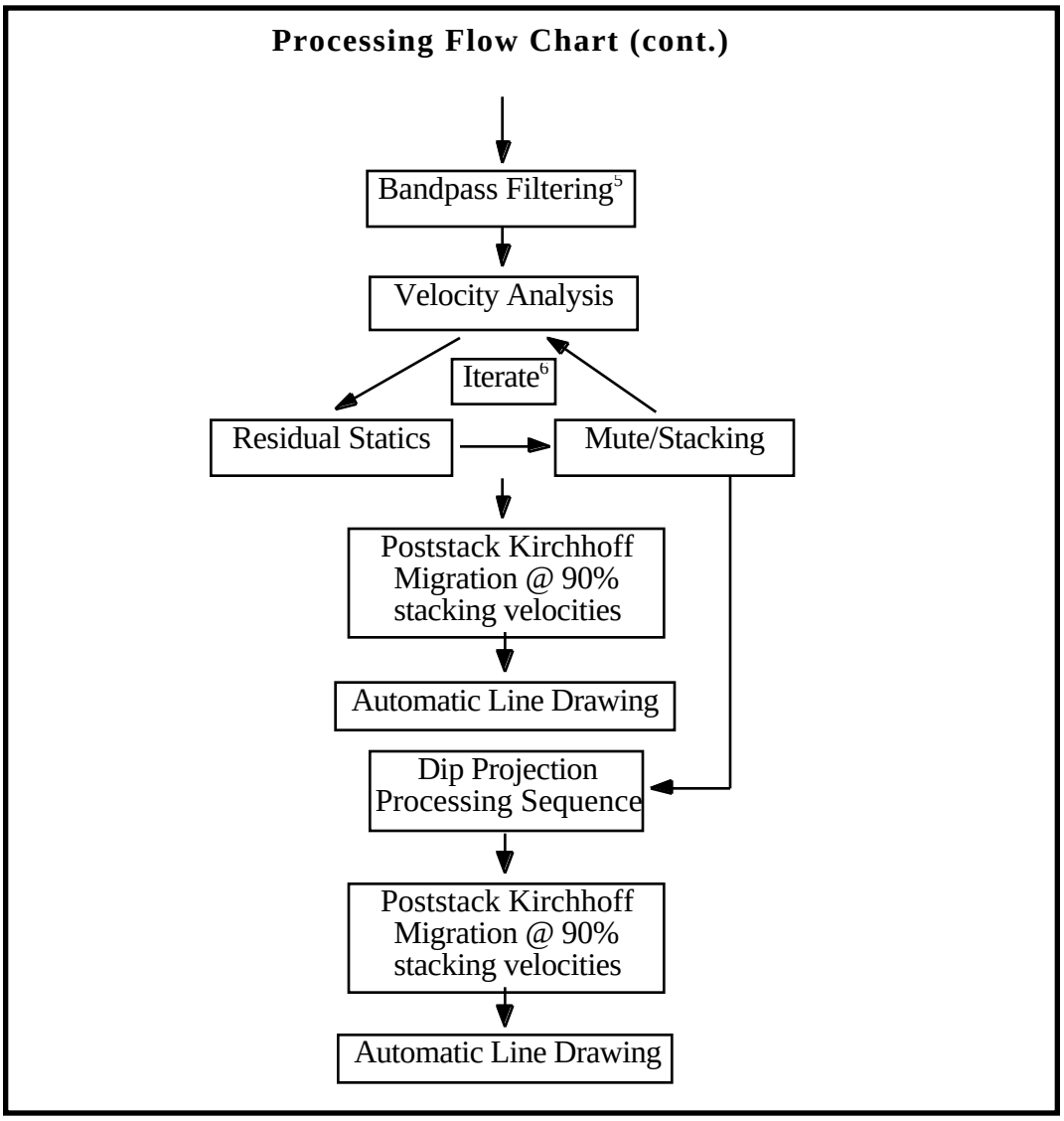

---

[1] Vibroseis Whitening (Çoruh and Costain, 1983) was applied to WV3. The method was tested but not used on WV1.

[2] Extended correlation (Pratt, 1982; Okaya and Jarchow, 1989) applied to all the data. Lines WV1 and WV3 were correlated to 10.4 seconds from a full correlation length of 5 seconds.

[3] Datum statics applied for lines WV1 and WV3 using a sloping datum, west-to-east.
For WV1: Datum Elevations − 720 to 500 m; Velocities − 3220 to 6130 m/s
For WV3: Datum Elevations − 900 to 250 m; Velocities − 3240 to 5280 m/s
A bulk static shift of 200 ms was added to WV1 and WV3 to preserve near surface reflections.

[4] Deconvolution operators were varied spatially to accommodate changes noticed during autocorrelation tests. The operator was also varied temporally for line WV3.

For WV1: Design gates: 520-2500 ms and 900-2880 ms for a 0 to 10400 ms application gate.
Gap: Varied from 20 to 24 ms.

For WV3: Design gates: 400-2150 ms and 750-2500 ms for a 0 to 2500 ms application gate;
2500-5000 ms for a 2501 to 5000 ms application gate.
5000-10000 ms for a 5000 to 10400 ms application gate.
Gap: Varied from 19 to 25 ms for the upper two sections;
26 to 39 ms for the deep section.

[5] Bandpass Filters: WV1 – Trapezoidal filter, 14/17/50/56 Hz frequencies, 125 points.
WV3 – Trapezoidal filter, 14/17/48/56 Hz frequencies, 125 points.

[6] Iteration between velocity analysis, residual statics, and mute/stacking continued until final results were deemed acceptable. In addition, the statics solutions for lines WV1 and WV3 were calculated separately for overlapping individual sections of the line, then merged during the final stacking phase. This process gave the best overall results.

Vita

Samuel Thomas Peavy was born in Mörtch, near Bitburg, Federal Republic of Germany on August 9, 1961. After attending eleven different schools on two continents and five states, he matriculated from Hyatt High School in Fields, Louisiana in 1979 as the top 12.5% of his class (#1 in 8). From there he received a B.S. in Physics (cum laude) from McNeese State University in Lake Charles, Louisiana in 1983. He then traveled to 'The Rock' where he had a good time getting 'Screeched' and earning an M.Sc. in Geophysics at the Memorial University of Newfoundland in 1985. After six years of teaching college-level physics in Louisiana and South Carolina, he came to Blacksburg and 'gradually' earned his Ph.D. in Geophysics in 1997. He will begin what he hopes will be a long and interesting career as a college professor at Rutgers University-Newark this fall as an Assistant Professor of Geophysics.